

FILE COPY  
NO 50



RM No. A7H29

NACA

NASA FILE COPY

Loan expires on last  
date stamped on back cover.

PLEASE RETURN TO

RESEARCH DISTRIBUTION SECTION  
LANGLEY RESEARCH CENTER

NATIONAL AERONAUTICS AND

SPACE ADMINISTRATION

Langley Field, Virginia

# RESEARCH MEMORANDUM

HIGH-SPEED AERODYNAMIC CHARACTERISTICS

OF HORN AND OVERHANG BALANCES

ON A FULL-SCALE ELEVATOR

By

Joseph W. Cleary and Walter J. Krumm

THIS DOCUMENT ON LOAN FROM THE FILES OF

Ames Aeronautical Laboratory

Moffett Field, Calif.

NATIONAL ADVISORY COMMITTEE FOR AERONAUTICS

LANGLEY AERONAUTICAL LABORATORY

LANGLEY FIELD, HAMPTON, VIRGINIA

RETURN TO THE ABOVE ADDRESS.

REQUESTS FOR PUBLICATIONS SHOULD BE ADDRESSED  
AS FOLLOWS:

NATIONAL ADVISORY COMMITTEE FOR AERONAUTICS  
1512 H STREET, N. W.

WASHINGTON 2, D. C.

**NATIONAL ADVISORY COMMITTEE  
FOR AERONAUTICS**

WASHINGTON

February 27, 1948





NATIONAL ADVISORY COMMITTEE FOR AERONAUTICS

RESEARCH MEMORANDUM

HIGH-SPEED AERODYNAMIC CHARACTERISTICS  
OF HORN AND OVERHANG BALANCES  
ON A FULL-SCALE ELEVATOR

By Joseph W. Cleary and Walter J. Krumm

SUMMARY

High-speed wind-tunnel tests have been conducted of horn- and overhang-balance elevators on a full-scale, semispan, horizontal tail. The effects of unshielding the horn and of unsealing the overhang were investigated.

Analysis of the data shows that shielded-horn balances can be used advantageously to give a positive rate of change of hinge-moment coefficient with angle of attack, or when used in conjunction with an overhang balance to limit this quantity to a small value. Although unshielding the horn caused considerable overbalancing and a relatively large positive rate of change of hinge-moment coefficient with angle of attack, these quantities can be regulated by appropriately choosing the horn area and chord. Compressibility caused slight overbalancing with the horn balance shielded. The overhang having a balance chord 33 percent of the elevator chord aft of the hinge line did not overbalance the elevator below a Mach number of 0.825.

Removing the nose seal from the elevator caused a slight reduction in the elevator effectiveness but no important changes in the elevator hinge moments.

In general, the elevator effectiveness decreased and the lift-curve slope increased as the Mach number increased within the limits of the tests.

INTRODUCTION

Various methods have been devised for relieving the excessive control forces experienced in airplanes when maneuvering at high speeds. These methods usually incorporate some form of control-surface balance the main function of which is to reduce the aerodynamic

hinge-moment coefficient and still give a desirable rate of change of hinge-moment coefficient with angle of attack. Many of such balancing devices are subject to the adverse effects of compressibility. These effects can be most accurately evaluated by testing the actual control surface.

A full-scale semispan horizontal tail from a fighter airplane was tested in the Ames 16-foot high-speed wind tunnel to investigate the effectiveness of shielded- and unshielded-horn and overhang balances and to evaluate their effects on the floating characteristics of the elevator at high subsonic Mach numbers.

Lift, drag, pitching moments, and elevator hinge moments were measured. Critical Mach numbers were determined at two stations from measurements of the chordwise pressure distribution.

Large-amplitude vibrations and the resultant structural deterioration limited the maximum Mach number to 0.75 for most of the tests. For tests with a reduced semispan, however, the maximum Mach number was extended to 0.825. The Reynolds number range extended from 6,400,000 to 16,900,000 as shown in figure 1.

#### APPARATUS

The full-scale semispan tail was mounted in the Ames 16-foot high-speed wind tunnel as shown in figure 2. The gap between the tunnel wall and the root of the tail was approximately 0.12 inch. The effects of leakage between the tunnel and the test chamber were minimized by an end plate.

The tail was formed to the NACA 0012-64 airfoil section modified to 10.64-percent thickness by extending the basic chord. Straight lines extended from 63 percent of the chord to the trailing edge, forming a flat-sided elevator having an included angle at the trailing edge of  $11.8^\circ$ .

The various elevator balances tested were modifications of the basic overhang balance. These elevator balances, as illustrated by figure 3, included a plain overhang with and without a shielded tip, a shielded normal-nose horn, unshielded normal- and elliptical-nose horns, and a plain overhang (sealed and unsealed) on a reduced semispan tail. The unshielded elliptical-nose horn and the overhang with the unshielded tip are shown in figure 4 as installed in the wind tunnel.

The overhang balance had a chord of 33 percent of the elevator chord aft of the hinge line. An elevator nose seal extended over

the overhang-balance portion of the elevator unless otherwise noted. The gap between the elevator nose and the stabilizer was 0.75 inch. Table I gives the pertinent dimensions and areas of the various balances. The coordinates of the elevator-balance profiles are presented in table II. These coordinates are plotted in figure 5 to show a comparison of the normal-nose and elliptical-nose horns.

The stabilizer and elevator were fabricated from ribs and spars of aluminum alloy riveted together and covered with a flush-riveted aluminum-alloy skin. The surfaces were smooth but noticeable waviness existed over both the stabilizer and the elevator.

The data were taken with the elevator set at fixed angles. Elevator angles were measured at the root with a protractor mounted on the stabilizer, and were later corrected for the deflection due to air loads. Elevator hinge moments were evaluated by measuring, with a calibrated electric strain gage, the strain imposed on a steel cantilever restraining arm.

Measurements of pressure distribution were made for all balances except the elliptical-nose horn from orifices in chordwise rows on the upper and lower surfaces of the tail at stations 52.6 and 108.0 inches from the root.

Lift, drag, and pitching moments were measured about the trunnion with mechanical balances.

#### COEFFICIENTS AND CORRECTIONS

The coefficients used in this report are defined as follows:

$C_L$  lift coefficient ( $L/qS$ )

$C_D$  drag coefficient ( $D/qS$ )

$C_m$  pitching-moment coefficient ( $M/qS$  M.A.C.)

$C_{he}$  elevator hinge-moment coefficient ( $H_e/q b_e \overline{c_e^2}$ )

$P$  pressure coefficient ( $\frac{P_o - p}{q}$ )

where

$L$  total lift, pounds

$D$  total drag, pounds

M	pitching moment about the 25-percent point of the M.A.C., foot-pounds
$H_e$	elevator hinge moment about the hinge line, foot-pounds
q	free-stream dynamic pressure ( $1/2\rho V^2$ ), pounds per square foot
$\rho$	mass density, slugs per cubic foot
V	free-stream velocity, feet per second
S	total area of the semispan tail, square feet
b	semispan of the horizontal tail, feet
M.A.C.	mean aerodynamic chord, feet
$S_e$	elevator area aft of the hinge line (one elevator), square feet
$\overline{c_e^2}$	mean square chord of elevator aft of the hinge line, square feet
$b_e$	elevator span (one elevator), feet
$p_0$	local static pressure, pounds per square foot
p	free-stream static pressure, pounds per square foot

In addition, the following symbols are used:

A	aspect ratio
$\lambda$	taper ratio
M	free-stream Mach number
$M_{cr}$	critical Mach number (the Mach number at which the flow over the model first reaches the velocity of sound)
R	Reynolds number
$\alpha$	angle of attack of the tail, degrees
$\delta_e$	elevator angle, degrees

$x/c$  fractional part of chord

$C_{L\alpha}$   $(\partial C_L / \partial \alpha)_{\delta_e} = 0, M$

$C_{L\delta_e}$   $(\partial C_L / \partial \delta_e)_\alpha = 0, M$

$C_{m\delta_e}$   $(\partial C_m / \partial \delta_e)_\alpha = 0, M$

$a_{\delta_e}$   $\left( \frac{\partial C_L / \partial \delta_e}{\partial C_L / \partial \alpha} \right) C_L = 0, M$

$C_{h\alpha}$   $(\partial C_{h_e} / \partial \alpha)_{\delta_e} = 0, M$

$C_{h\delta_e}$   $(\partial C_{h_e} / \partial \delta_e)_\alpha = 0, M$

The subscripts outside the parenthesis represent the factors considered constant during the measurement of the parameters.

Corrections for the effects of the tunnel boundary on the aerodynamic characteristics have been made by adding the following:

$$\Delta\alpha = 1.03 C_L \text{ (degrees)}$$

$$\Delta C_D = 0.0180 C_L^2$$

Corrections to the pitching-moment and elevator hinge-moment coefficients are small and have been neglected.

Blockage corrections due to the tail have been applied to the wind-tunnel Mach number and dynamic pressure calibrations.

## DISCUSSION AND RESULTS

### Aerodynamic Characteristics

Overhang balance with shielded and unshielded tip.— Tests were made of the overhang balance to serve as a basis for evaluating the aerodynamic characteristics of the horn balances. The tip of the balance was then unshielded to study the effects of compressibility on unshielded balances. Figures 6 to 9 present the variation of lift, drag, and pitching-moment coefficients with Mach number for the overhang balances with shielded and unshielded tip. Parameters

expressing the variation of the lift-curve slope  $CL_a$ , elevator effectiveness  $\alpha\delta_e$ , and the rate of change of pitching-moment coefficient and lift coefficient with elevator angle  $Cm\delta_e$  and  $CL\delta_e$  are presented in figure 10.

No adverse changes occurred in the variation of lift, drag, and pitching-moment coefficient with Mach number below the limit of 0.75. For the shielded overhang balance,  $CL_a$  increased from 0.68 at 0.30 Mach number to 0.87 at 0.75 Mach number while  $CL\delta_e$  decreased from 0.034 to 0.024. These changes in the lift parameters produced a numerical decrease in  $\alpha\delta_e$  from -0.50 to -0.28 for the same Mach number range. Data presented in reference 1 for a similar elevator balance also show a decrease in  $\alpha\delta_e$  for a similar range of Mach numbers. With the overhang tip unshielded, these effects became more pronounced because of the lower critical Mach number of the unshielded section. Table III presents a summary of the more important parameters which illustrate these effects.

The minimum drag coefficient of the tail with either balance was approximately 0.0095. The perceptible rise in drag coefficient (fig. 8) with the overhang tip unshielded at approximately 0.65 Mach number is attributed to the lower critical Mach number of the unshielded section.

The static longitudinal stability of the tail  $-(\partial C_m / \partial CL)_M$  for both balances was only slightly affected by changes in Mach number within the range of the tests. As a result of unshielding the overhang tip,  $-(\partial C_m / \partial CL)_M$  was altered from a slight negative to a positive value. This change is attributed to a rearward shift of the aerodynamic center.

The hinge-moment coefficients for the two elevator balances are presented in figure 11, while the variation with Mach number of the rate of change of hinge-moment coefficient with angle of attack and elevator angle ( $Ch_a$  and  $Ch\delta_e$ ) are shown in figure 12. Table III presents a summary of values for  $Ch_a$  and  $Ch\delta_e$  for all the balances. From the data presented, it appears that the principal effect of compressibility on the hinge-moment characteristics was a numerical increase in  $Ch\delta_e$  for both the shielded and unshielded overhang balances. Although the balance effectiveness was increased at low Mach numbers by unshielding the tip, no particular advantage was observed at the higher Mach numbers.

Effect of seal on the overhang balance.-- The aerodynamic characteristics of the sealed and unsealed overhang balance are presented in figures 13 to 17. Values of the principal parameters which signify these characteristics are tabulated in table III for

Mach numbers of 0.30 and 0.75. Removing the seal from the overhang balance reduced the lift-curve slope  $CL_a$  slightly at all Mach numbers below 0.78. A reduction in  $CL_{\delta_e}$  of approximately 5 percent occurred for Mach numbers below 0.825. A corresponding reduction in  $\alpha_{\delta_e}$  of approximately 7 percent occurred.

The elevator hinge-moment characteristics, as presented by figures 18 and 19, show a stable variation of  $Ch_{\delta_e}$  at all Mach numbers. With the overhang sealed,  $Ch_{\delta_e}$  increased numerically from -0.0040 at 0.30 Mach number to -0.0058 at 0.825 Mach number, an increase of approximately 45 percent. Unsealing the elevator decreased  $Ch_{\delta_e}$  for a limited range of elevator angles at low Mach numbers but the over-all characteristics were not affected. The parameter  $Ch_a$  had a small negative value with the elevator sealed or unsealed for all Mach numbers.

Effect of horn balances.— A shielded normal-nose horn was added to the overhang to investigate the danger of overbalance with this type of balance at high Mach numbers. The horn was then unshielded to determine what benefits might be gained. In order to alleviate the large pressure peaks anticipated near the nose of the unshielded normal-nose horn, additional tests were made with an elliptical-nose horn. The force, pitching-moment, and elevator hinge-moment characteristics for the horn balances are presented in figures 20 to 28 and a summary of these characteristics is given in table III.

Adding the shielded horn to the overhang did not appreciably affect the lift, drag, or pitching-moment characteristics of the tail. The numerical increases in  $CL_{\delta_e}$  and  $\alpha_{\delta_e}$  are attributed to the increased area of the elevator. Unshielding the normal-nose horn, however, caused a 12-percent increase in  $CL_a$  at 0.70 Mach number. Unshielding the horn lowered the critical Mach number of the horn section, thus activating compressibility effects at a lower Mach number.

These effects of compressibility on the lift characteristics of the unshielded horn caused an appreciable increase in  $-(\partial C_m / \partial C_L)_M$  when the Mach number was increased from 0.20 to 0.75. The aerodynamic center of the tail was shifted rearward. This shift was in addition to that which occurred when the horn was unshielded.

A comparison of figures 11 and 27 shows that the shielded normal-nose horn is a powerful means of creating aerodynamic balance at elevator angles greater than  $\pm 2^\circ$  and less than  $\pm 10^\circ$ . Slight overbalancing occurred for some angles of attack at all Mach numbers. However, within the range of Mach numbers of the tests, the effects of compressibility on the hinge-moment characteristics do not appear too severe. The low value of  $Ch_a$ , as indicated by figure 28, is attributed in part to

the balancing properties of the overhang. Without the overhang as an additional balance, it is possible  $Ch_a$  would assume a significant positive value (reference 2).

It is apparent from the hinge-moment coefficients for the horn balances that additional balance can be gained by unshielding the horn. This additional balance appears to decrease with increasing Mach number. However, the effects of compressibility are not conclusive in view of the limited Mach number range. As will be shown later, large pressure peaks occur over the horn. With the horn unshielded, these peaks are sensitive to changes in either elevator angle or angle of attack. Consequently, a large positive value of  $Ch_a$  (0.0072 at 0.30 Mach number with the normal-nose horn) occurred with the horn unshielded. This condition, as would be expected, becomes more pronounced at the higher Mach numbers. Altering the normal-nose horn to an elliptical section, or effectively decreasing the nose radius, proved to be of little value for changing either  $Ch_a$  or  $Ch\delta_e$ .

Although overbalancing occurred with either unshielded horn, the overhang with the unshielded tip did not overbalance for the Mach numbers of the test. It is apparent, therefore, that by an appropriate selection of unshielded-horn-balance area and chord, overbalancing can be eliminated to a Mach number of at least 0.75 while some choice of  $Ch_a$  and  $Ch\delta_e$  can be retained.

#### Distortions of the Tail

In connection with the aerodynamic characteristics of the tail, the effects of surface distortions and structural failures should be considered. At high Mach numbers, noticeable wrinkling of the surfaces and twisting of the stabilizer and elevator were observed. These distortions appeared most severe with the horn unshielded. It is reasonable to assume, therefore, that the effects of Mach number as presented in the figures are due to a combination of compressibility and tail distortion. Several structural failures of the model may have caused some misalignment and warping of the surfaces. The unsymmetry of part of the data may be a result of these structural failures.

#### Critical Mach Numbers

Figures 29 and 30 present the chordwise pressure distribution over the overhang balance. Pressures over the shielded and unshielded normal-nose horn are presented in figures 31 to 34. Both the overhang and horn balances developed pressure peaks well forward

of the elevator hinge line. These pressure peaks were the source of the large amount of balance developed by the horn balances. It is apparent from the pressure data that the unshielded normal-nose horn was sensitive to changes in either elevator angle or angle of attack. This sensitivity is the reason for the large positive value of  $C_{ha}$  that occurred with the unshielded balances.

The critical Mach numbers of the various balances are shown in figure 35 for  $0^\circ$  angle of attack and several elevator angles. Since the critical Mach numbers were not reached for some balances at elevator angles near  $0^\circ$ , the data have been extrapolated when necessary. The critical Mach number of the shielded horn and overhang balances at  $0^\circ$  elevator angle was approximately 0.79. Deflecting the normal-nose horn balance lowered its critical Mach number at a more rapid rate than for any of the other balances. Unshielding the normal-nose horn reduced its critical Mach number approximately 28 percent at  $0^\circ$  elevator angle. A similar reduction occurred when the overhang tip was unshielded.

No significant changes occurred in the spanwise variation of critical Mach number when the overhang balance was employed. Unsealing the overhang did not alter its critical Mach number appreciably.

#### CONCLUSIONS

The results presented in this report lead to the following conclusions:

1. The overhang balance having a chord equal to 33 percent of the elevator chord aft of the hinge line showed an increase of approximately 45 percent for the numerical rate of change of elevator hinge-moment coefficient with elevator angle  $C_{hs\theta}$  between Mach numbers of 0.30 and 0.825. Removing the seal from this balance reduced the elevator effectiveness  $\alpha\delta_e$  approximately 7 percent at all Mach numbers.
2. Shielded-horn balances can be used advantageously to give a positive value of the rate of change of hinge-moment coefficient with angle of attack  $C_{ha}$  or when used in conjunction with an overhang balance to limit  $C_{ha}$  to a small value. They are a powerful means of developing aerodynamic balance at low and high subsonic Mach numbers.
3. Unshielding the horn caused overbalancing and a large positive value of  $C_{ha}$ . However, overbalancing can be eliminated

by the proper selection of horn balance area and chord with some choice of  $C_{h\alpha}$  being retained.

4. The rate of change of lift coefficient with elevator angle  $C_{L\delta_e}$  and the elevator effectiveness  $\alpha_{\delta_e}$  decreased for both horn and overhang balances as the Mach number was increased.

Ames Aeronautical Laboratory,  
National Advisory Committee for Aeronautics,  
Moffett Field, Calif.

#### REFERENCES

1. Schueller, Carl F., Korycinski, Peter F., and Strass, H. Kurt: Tests of a Full-Scale Horizontal Tail Surface in the Langley 16-Foot High-Speed Tunnel. NACA TN. No. 1074, 1946.
2. Lowry, John G., Maloney, James A., and Garner, I. Elizabeth: Wind-Tunnel Investigation of Shielded Horn Balances and Tabs on a 0.7-Scale Model of XF6F Vertical Tail Surface. NACA ACR No. 4C11, 1944.

TABLE I-DIMENSIONS OF THE FULL-SCALE SEMISPAN HORIZONTAL TAIL

ELEVATOR	DIMENSIONS							
	b, ft	S, sq ft	MAC, ft	A	$\lambda$	$b_\theta$ , ft	$S_\theta$ , sq ft	$\bar{c}_\theta^3$ , sq ft
Overhang balance	9.92	44.4	4.58	4.43	0.521	9.38	11.1	1.40
Overhang balance with unshielded tip	9.92	42.3	4.68	4.65	0.521	9.38	11.1	1.40
Shielded normal-nose horn balance	9.92	44.4	4.58	4.43	0.521	9.38	11.1	1.40
Unshielded normal-nose horn balance	9.92	43.0	4.64	4.57	0.521	9.38	11.1	1.40
Unshielded elliptical-nose horn balance	9.92	43.0	4.64	4.57	0.521	9.38	11.1	1.40
Overhang balance on reduced semispan tail	8.54	39.8	4.76	3.67	0.568	8.05	9.50	1.41

NATIONAL ADVISORY  
COMMITTEE FOR AERONAUTICS

TABLE II.—ELEVATOR COORDINATES IN INCHES FOR THE SEMISPAN HORIZONTAL TAIL AT STATION 108.0 INCHES. SECTIONS ARE SYMMETRICAL ABOUT THE CHORD LINE.

<i>Overhang balance</i>	
<i>Distance from L.E.</i>	<i>Ordinate</i>
0	0
0.238	0.970
.476	1.218
.950	1.490
1.424	1.636
1.900	1.696
2.850	1.690
3.800	1.660
<sup>a</sup> 4.532	1.630
19.00	T.E.R. .094

NATIONAL ADVISORY  
COMMITTEE FOR AERONAUTICS

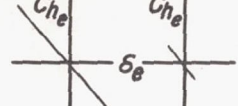
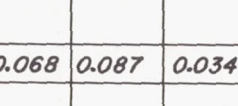
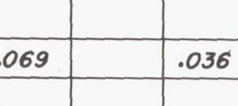
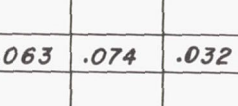
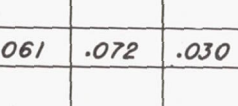
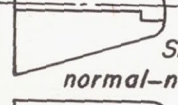
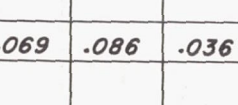
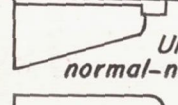
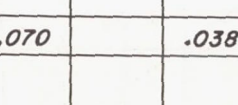
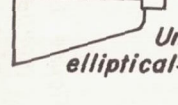
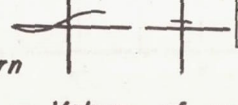
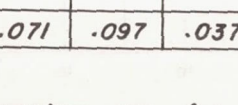
<i>Normal-nose horn balance</i>	
<i>Distance from L.E.</i>	<i>Ordinate</i>
0	0
0.296	1.080
.594	1.378
1.184	1.712
1.776	1.932
2.376	2.006
3.522	2.076
4.740	2.030
8.420	1.748
<sup>b</sup> 9.662	1.630
24.938	T.E.R. .094

<i>Elliptical-nose horn balance</i>	
<i>Distance from L.E.</i>	<i>Ordinate</i>
0	0
0.05	0.246
.55	.802
1.05	1.083
2.05	1.443
4.05	1.815
6.05	1.922
8.05	1.815
8.420	1.748
<sup>b</sup> 9.662	1.630
24.938	T.E.R. .094

<sup>a</sup> Straight lines from station 4.532 inches to trailing edge radius.

<sup>b</sup> Straight lines from station 9.662 inches to trailing edge radius.

TABLE III.—SUMMARY OF THE ELEVATOR CHARACTERISTICS

Balance type	Elevator hinge-moment coefficient $M = 0.30 \quad 0.75$	$C_{L\alpha}$		$C_{L\delta_e}$		$\alpha_{\delta_e}$		$C_{h\alpha}$		$C_{h\delta_e}$			
		0.30	0.75	0.30	0.75	0.30	0.75	0.30	0.75	0.30	0.75		
Overhang				0.068	0.087	0.034	0.024	-0.50	-0.28	-0.0010	-0.0010	-0.0043	-0.0060
Overhang, unshielded tip				.069		.036	.021	-.53		.0003		-0.0027	-0.0062
Overhang, reduced semispan				.063	.074	.032	.024	-.51	-.33	-0.0008	-0.0008	-0.0040	-0.0056
Unsealed overhang, reduced semispan				.061	.072	.030	.023	-.49	-.31	-0.0005	-0.0009	-0.0030	-0.0057
Shielded normal-nose horn				.069	.086	.036	.031	-.52	-.36	.0001	.0005	-0.0028	-0.0034
Unshielded normal-nose horn				.070		.038		-.53		.0072		.0028	
Unshielded elliptical-nose horn				.071	.097	.037	.034	-.52	-.36	.0071	.0099	.0026	-.0003

NATIONAL ADVISORY  
COMMITTEE FOR AERONAUTICSNote — Values of parameters are for  $\alpha$  and  $\delta_e$  of  $0^\circ$ .

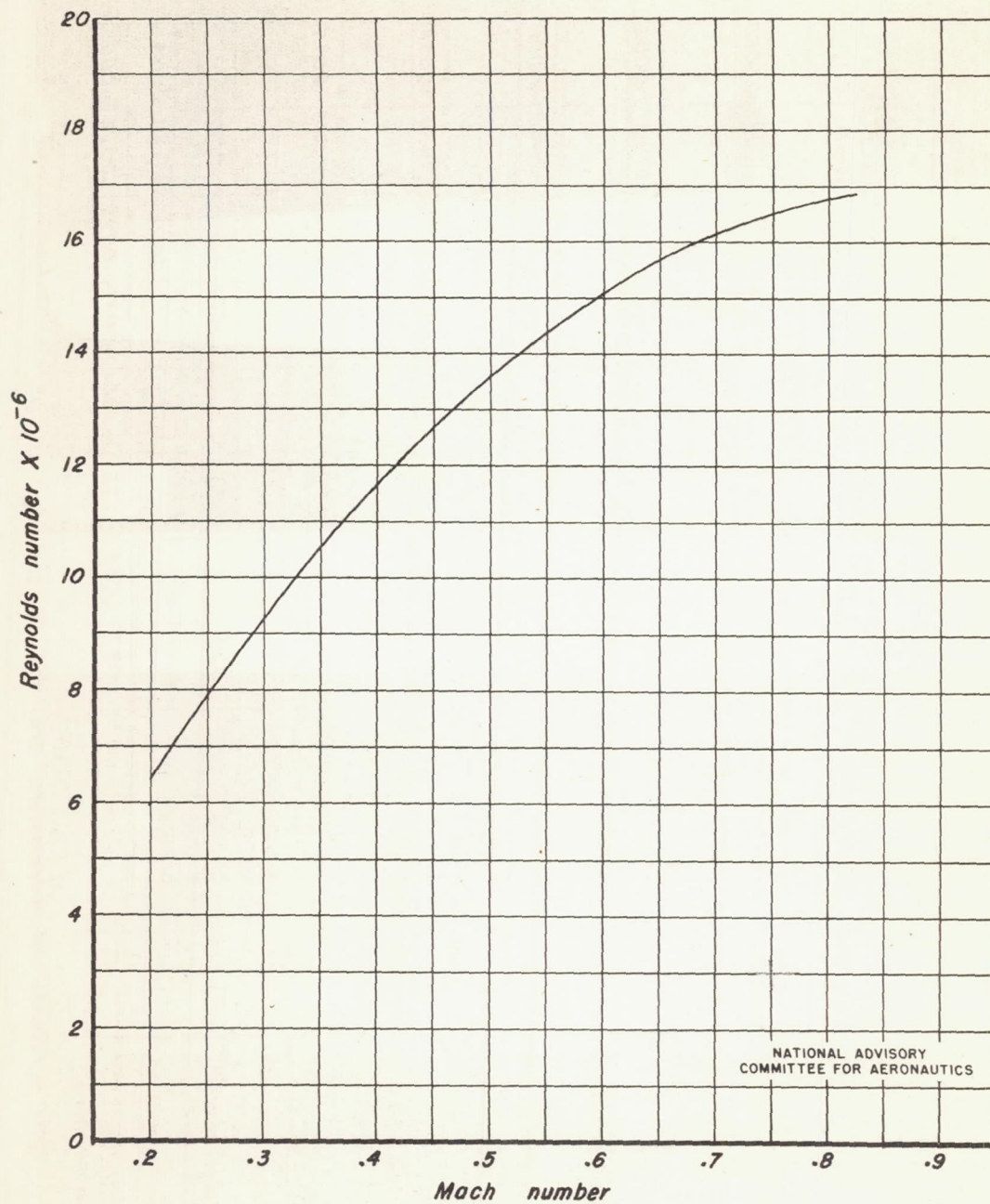
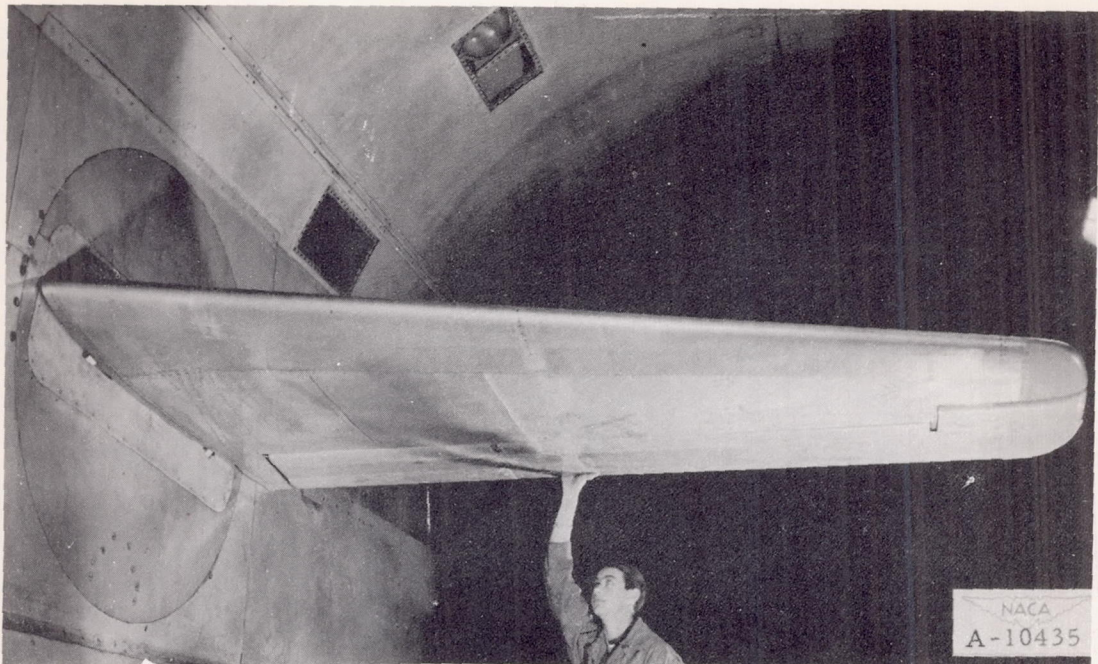


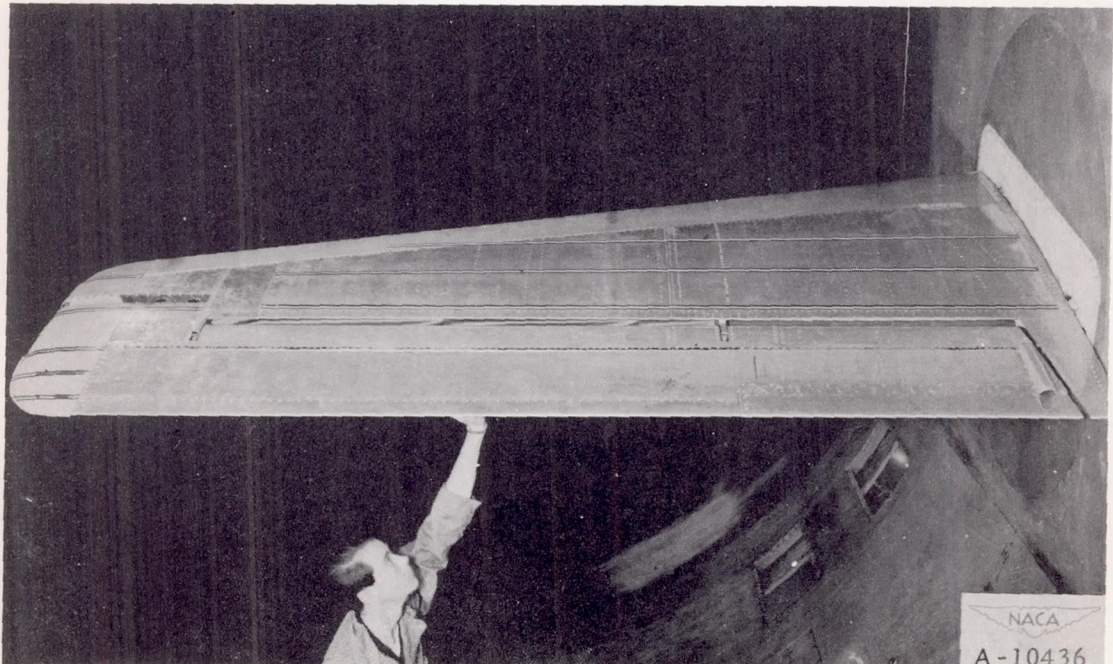
Figure 1.—Approximate variation of test Reynolds number with Mach number for the semispan horizontal tail in the Ames 16-foot high-speed wind tunnel.

NACA RM No. A7H29

Fig. 2

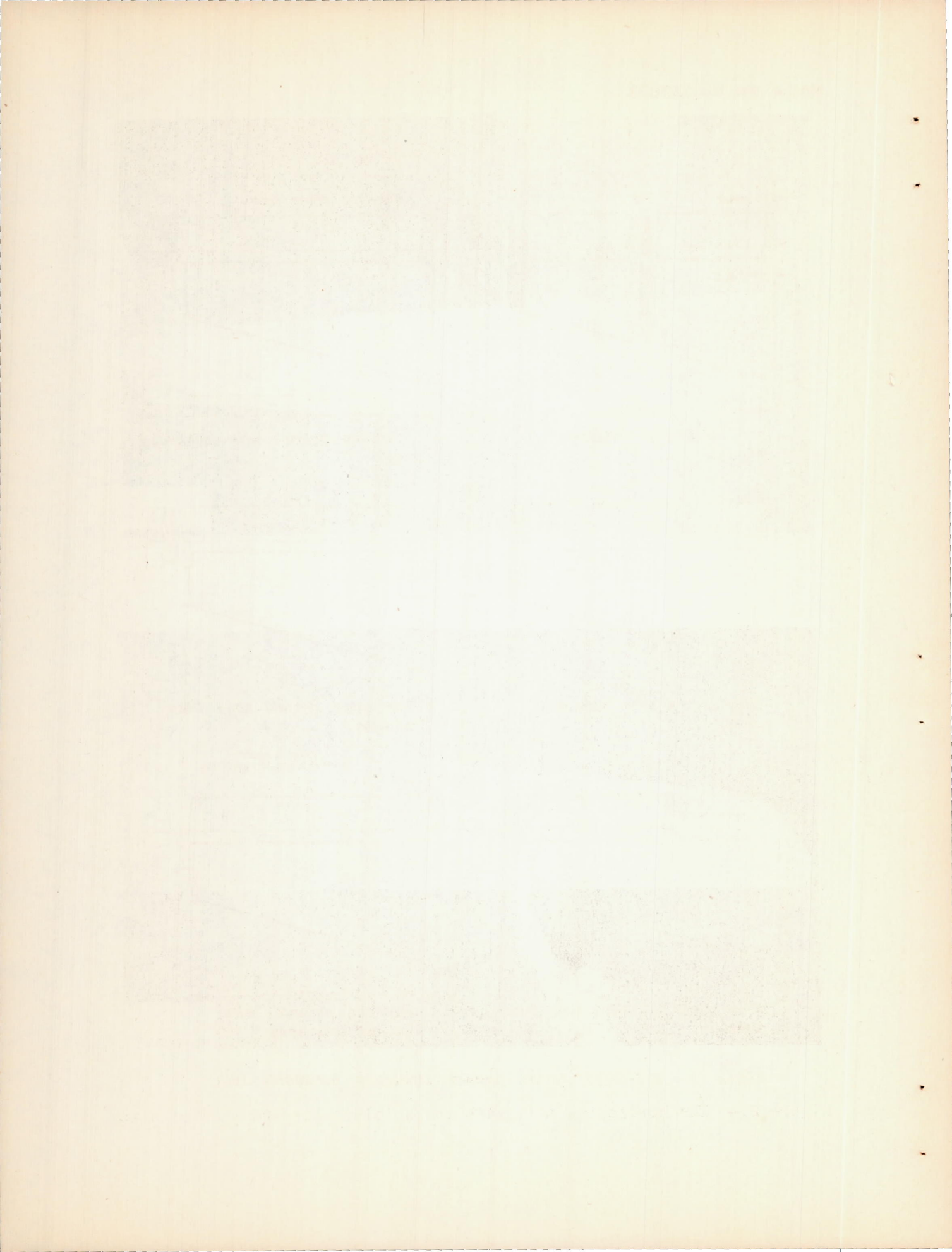


(a) Front view.



(b) Rear view.

Figure 2.— The horizontal tail with the shielded-horn-balance elevator.



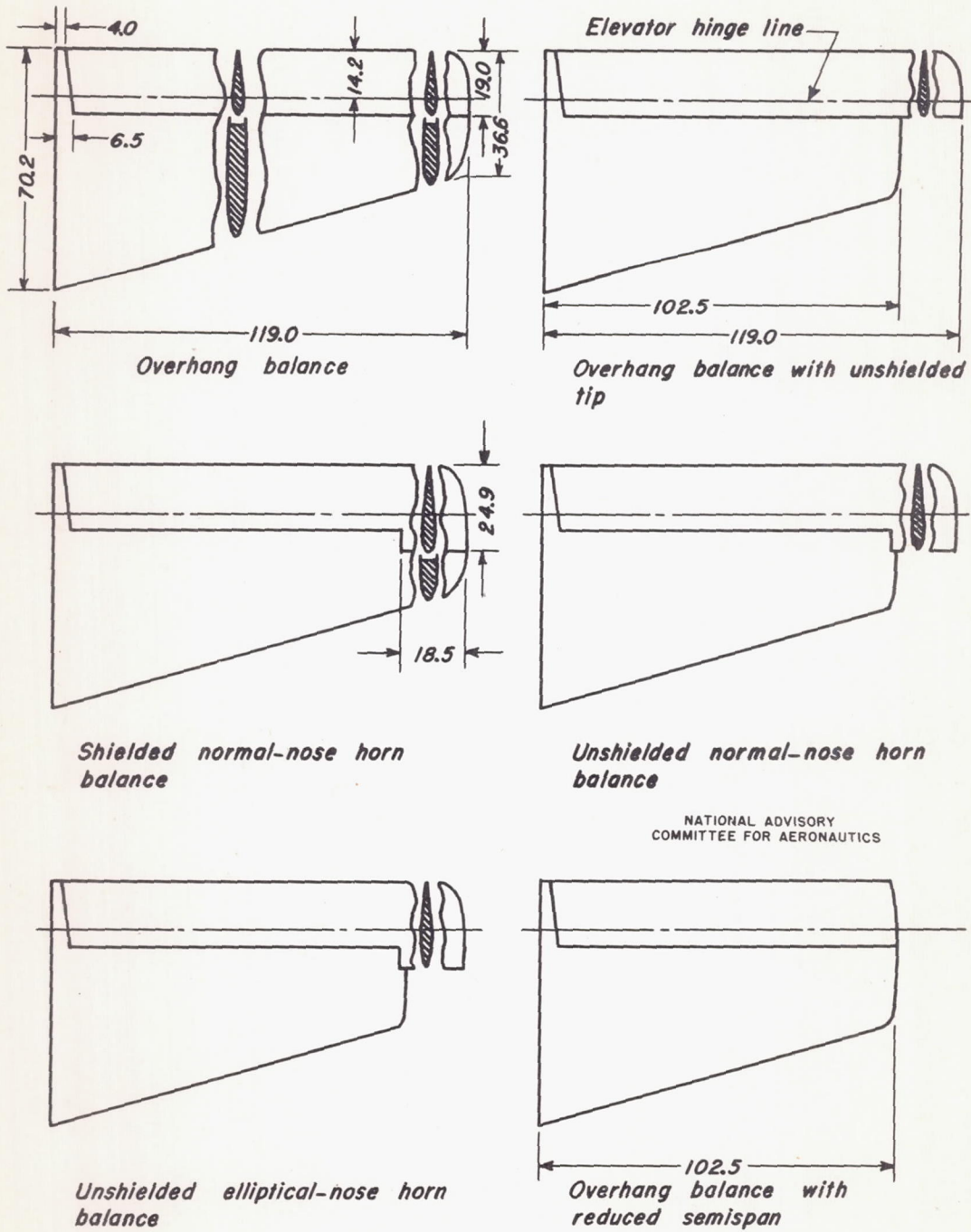
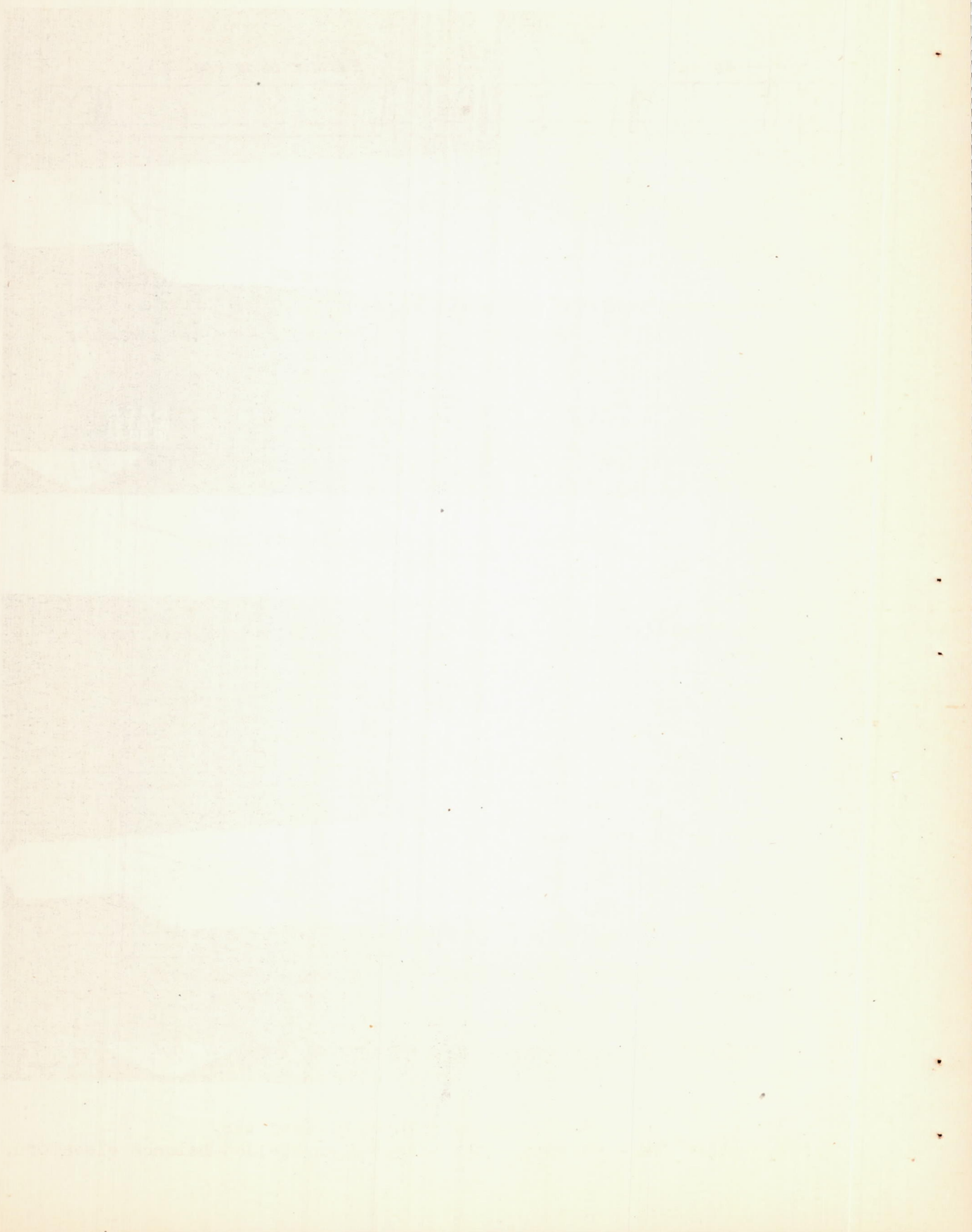
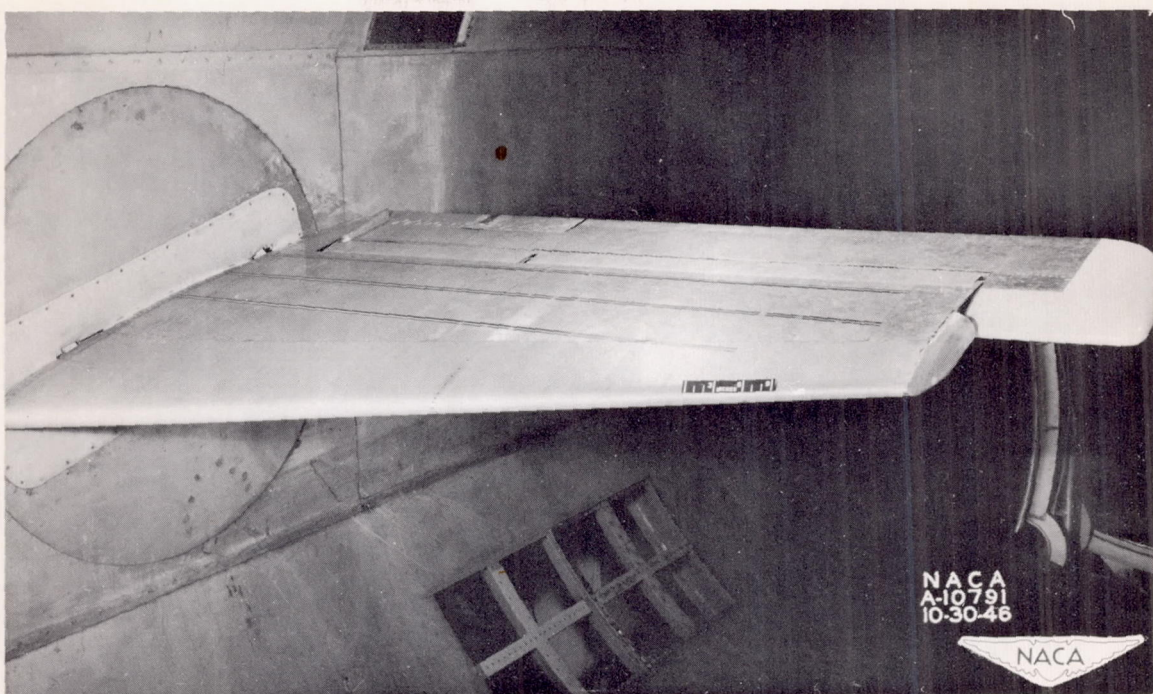
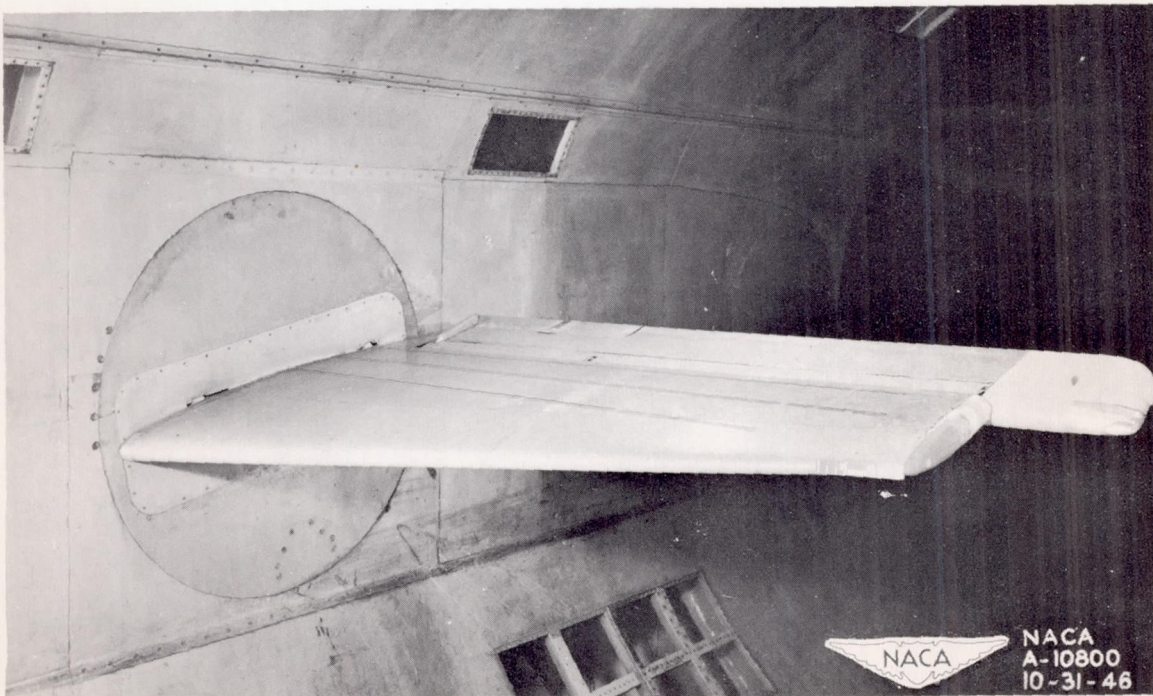


Figure 3.—Elevators tested on the semispan horizontal tail.





(a) Unshielded elliptical-nose horn.

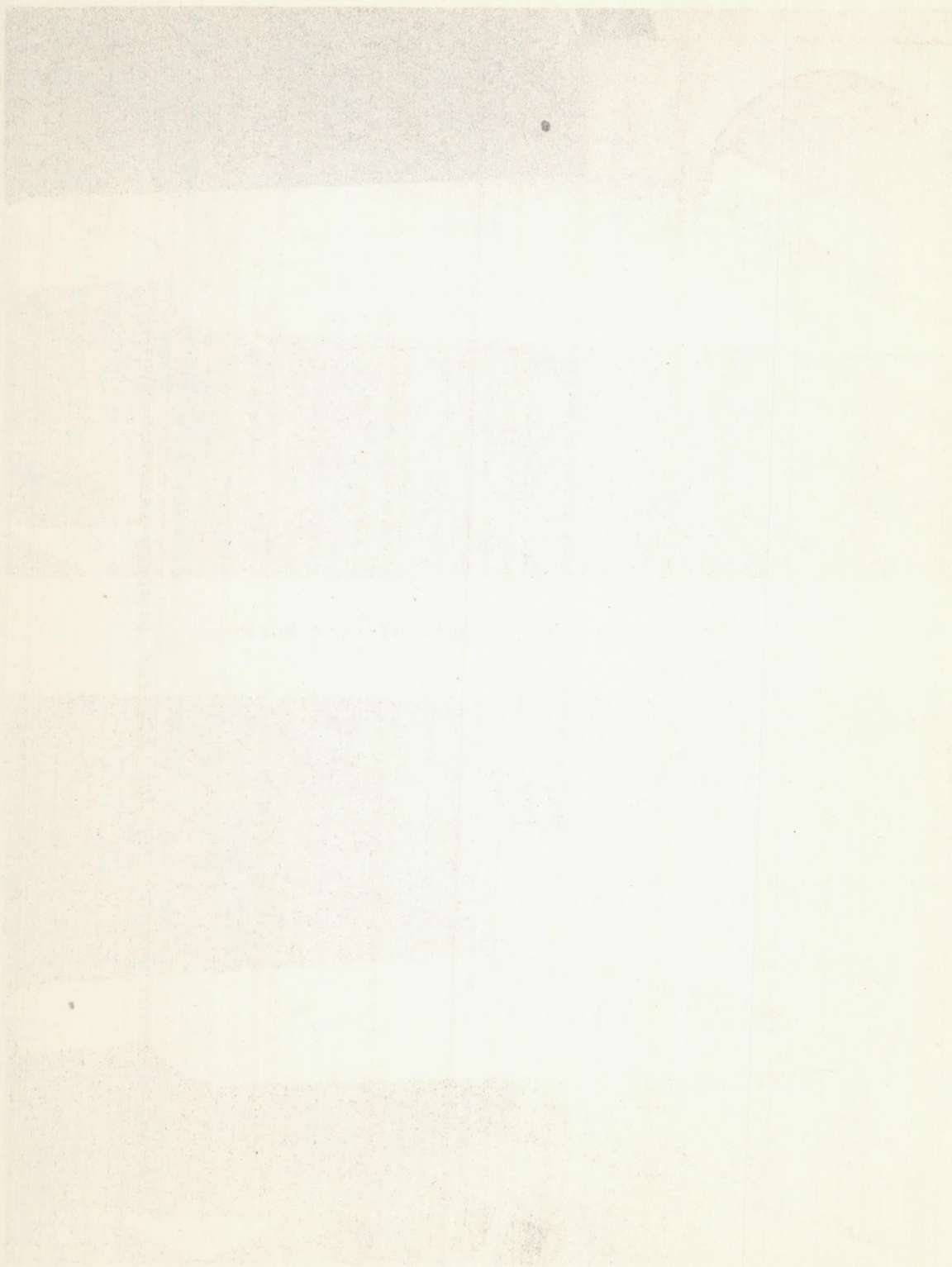


(b) Overhang with unshielded tip.

Figure 4.— The horizontal tail with two unshielded-balance elevators.

45. 5. 1911

РНТА СОИ МЯ АДАИ



Снимок сделан в 1911 году в Баку. (Фото из альбома Адаян)

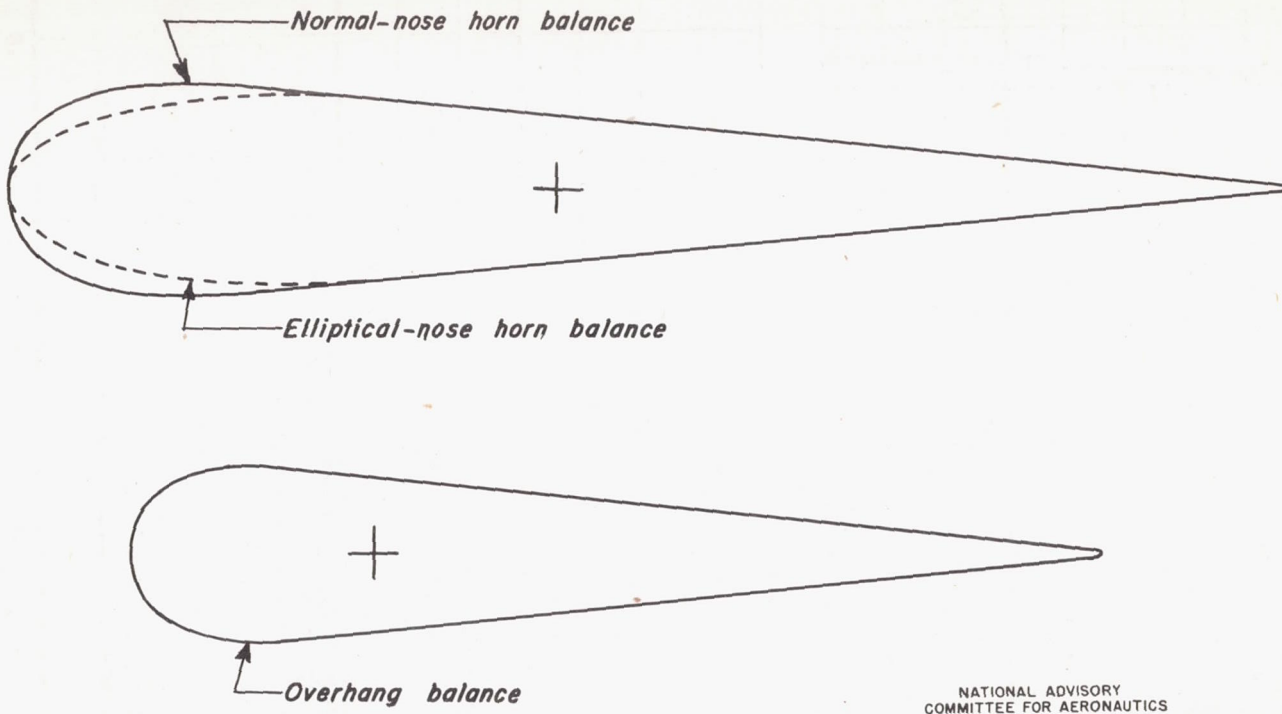


Figure 5.—Elevator profiles for the horn-and overhang-balance elevators.

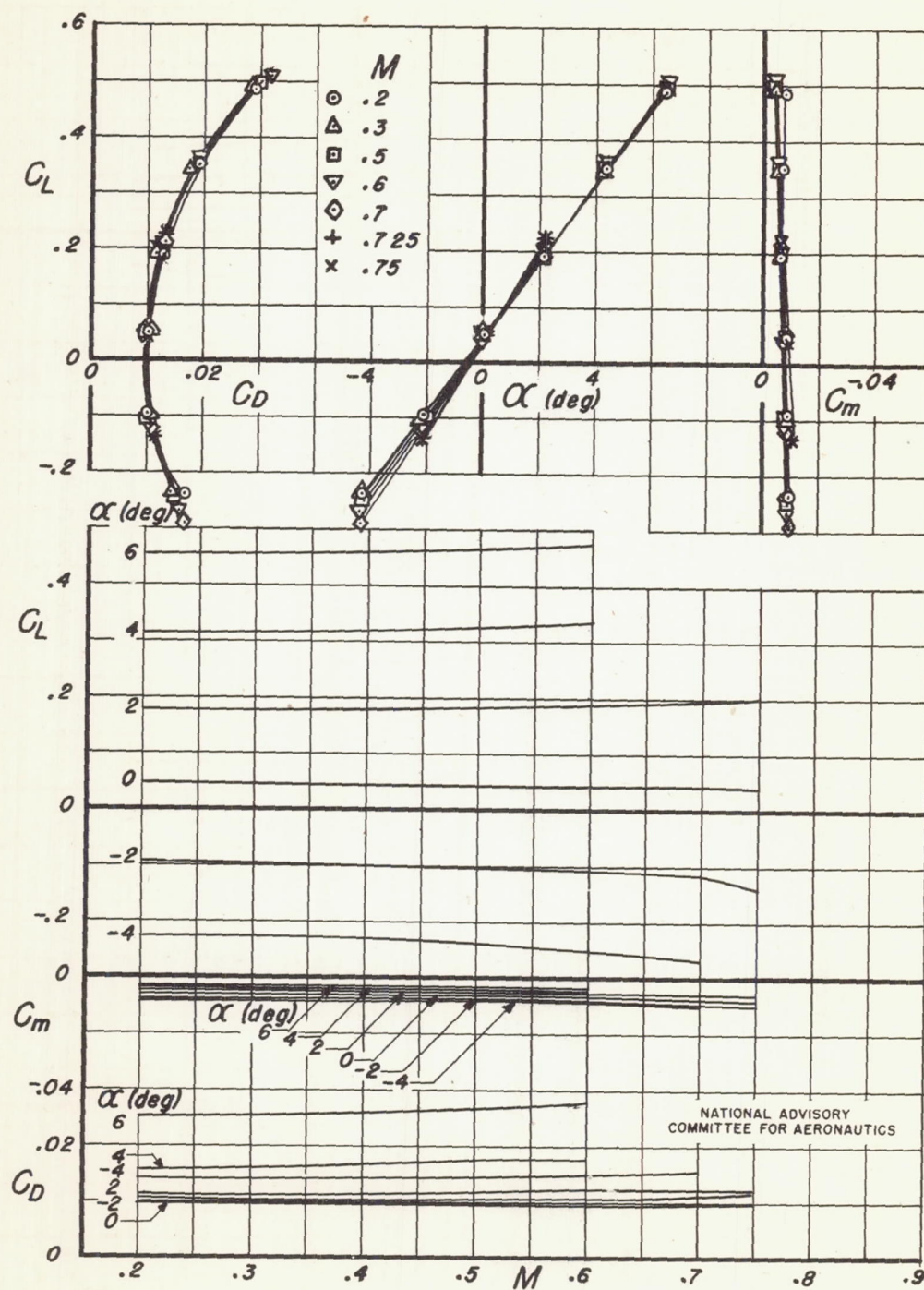


Figure 6.—Lift, drag, and pitching-moment coefficients for the semispan horizontal tail with the overhang-balance elevator.  $\delta_e, 0^\circ$

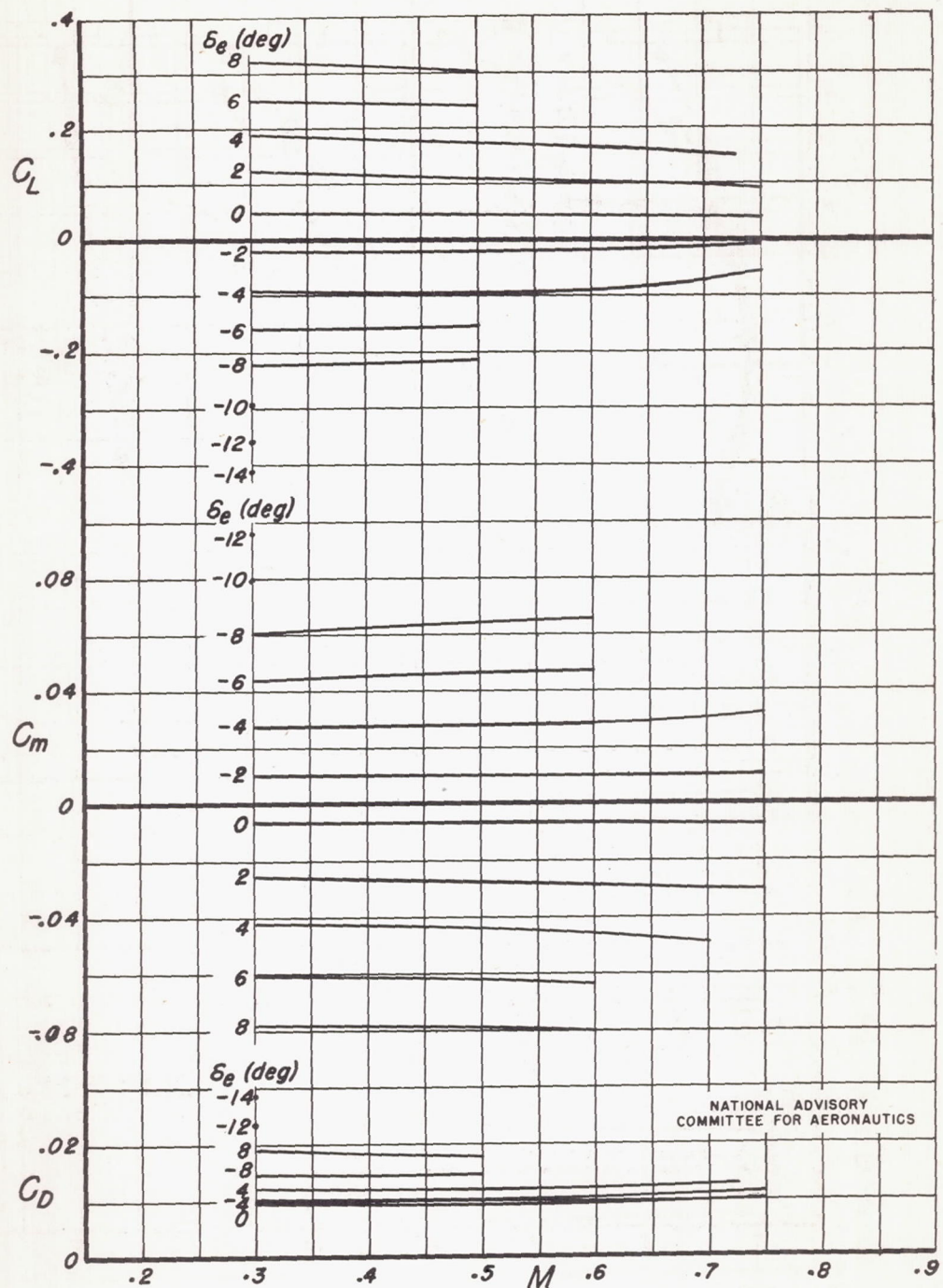


Figure 7.—Lift, drag, and pitching-moment coefficients for the semispan horizontal tail with the overhang-balance elevator.  $\alpha, 0^\circ$

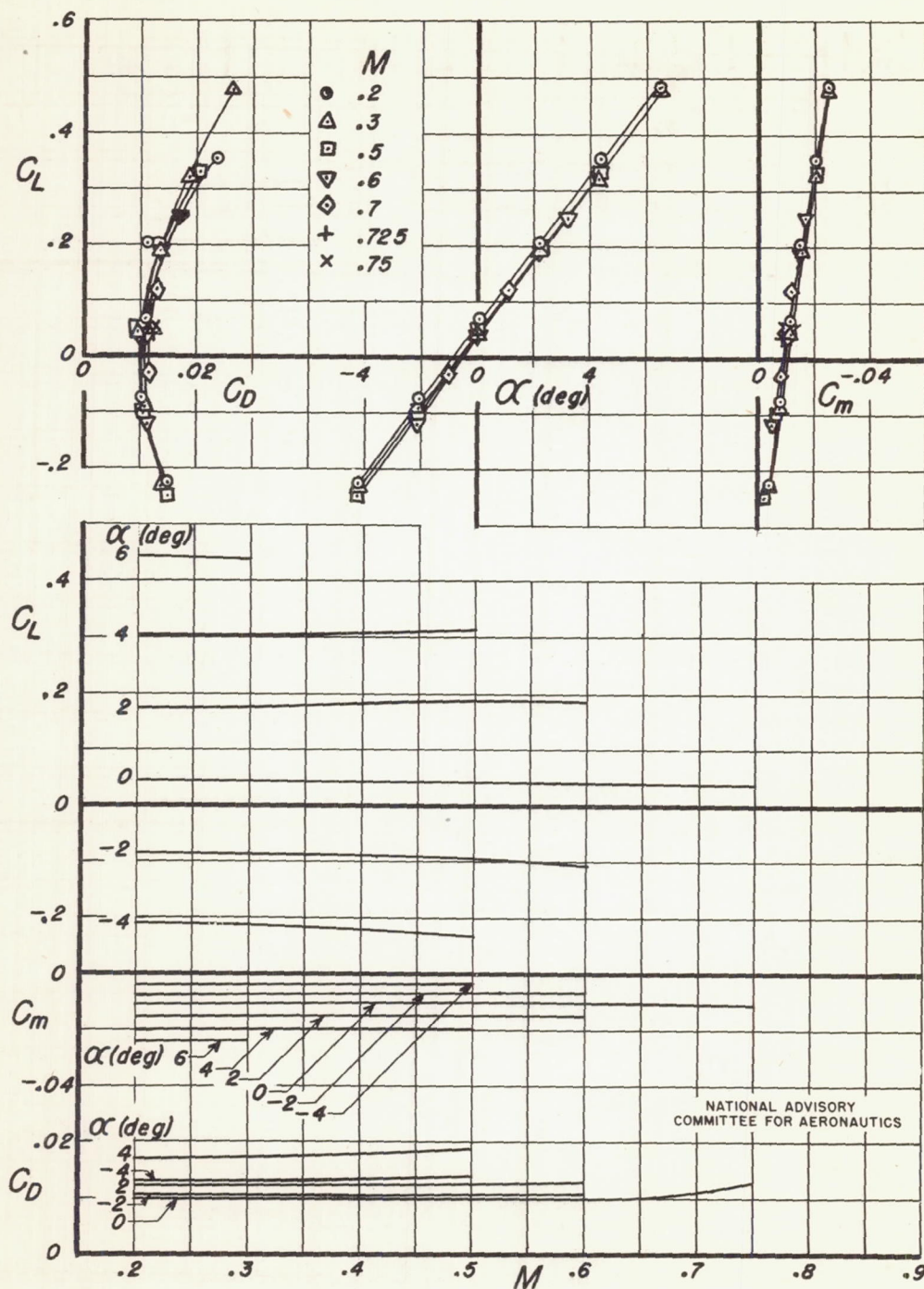


Figure 8. — Lift, drag, and pitching-moment coefficients for the semispan horizontal tail with the overhang-balance elevator having an unshielded tip.  $\delta_e, 0^\circ$

NATIONAL ADVISORY  
COMMITTEE FOR AERONAUTICS

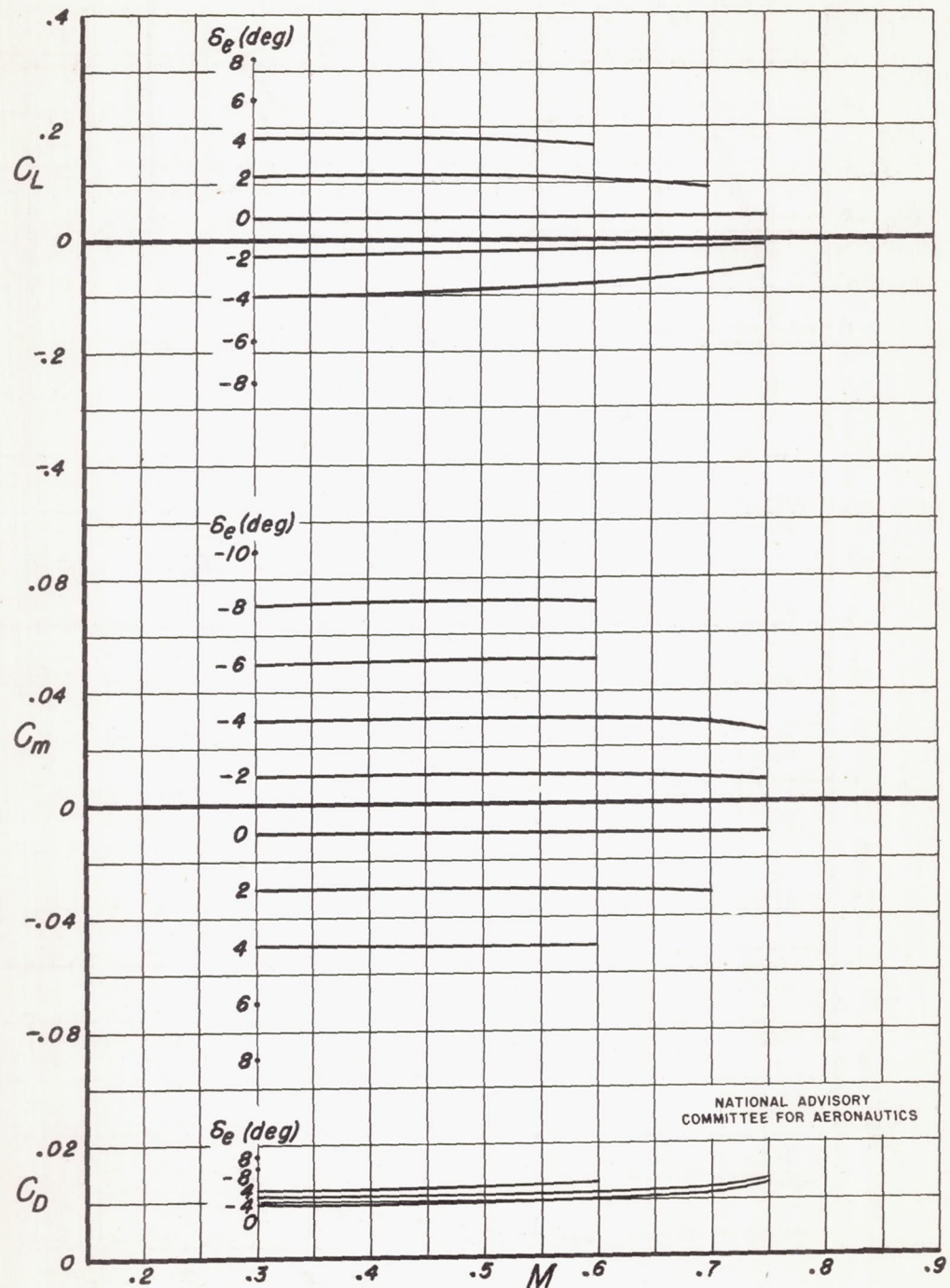


Figure 9. — Lift, drag, and pitching-moment coefficients for the semispan horizontal tail with the overhang-balance elevator having an unshielded tip.  $\alpha, 0^\circ$

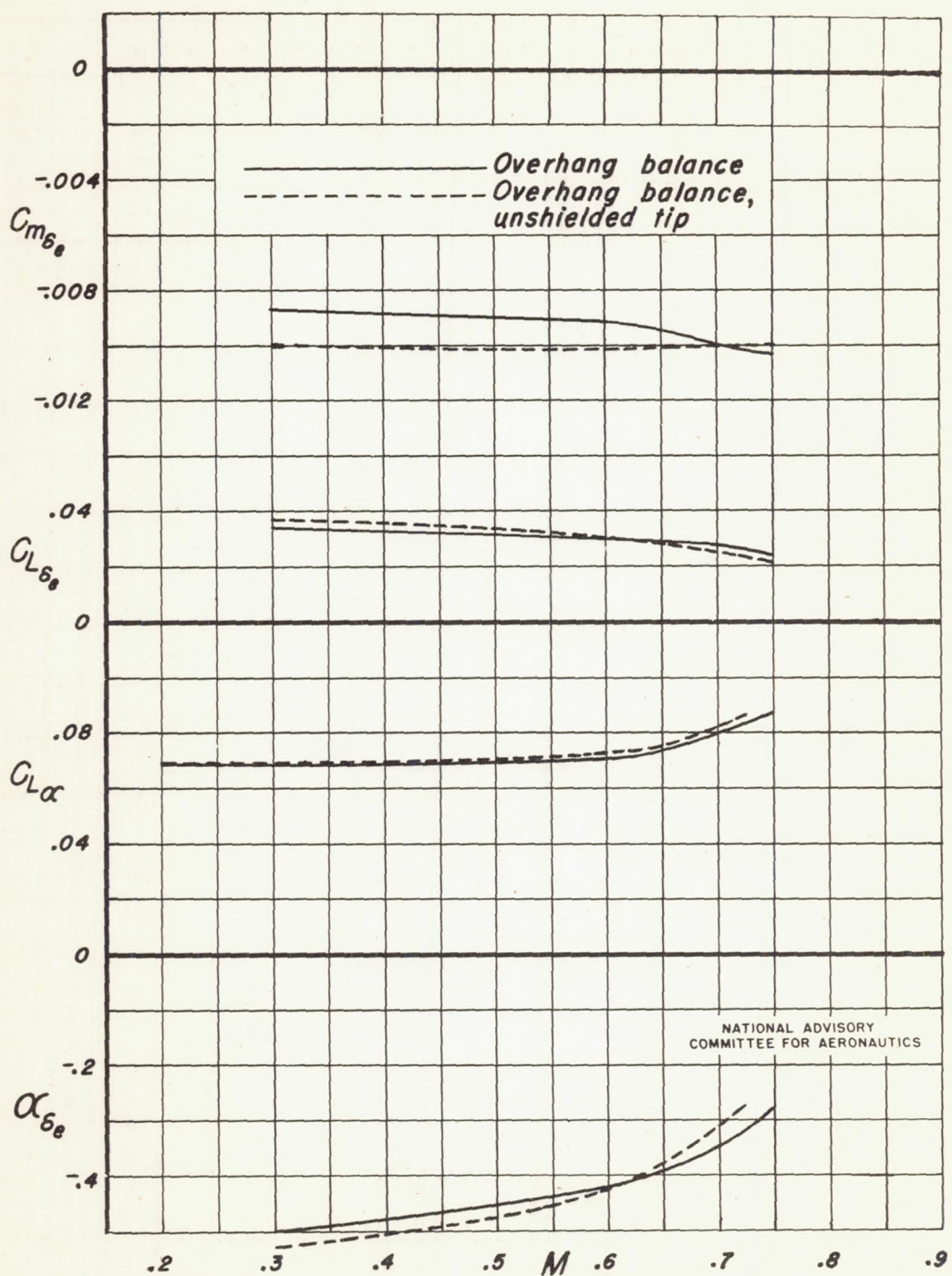


Figure 10.—Variation of pitching moment, lift, and elevator-effectiveness parameters with Mach number for the overhang-balance elevator with and without a shielded tip.

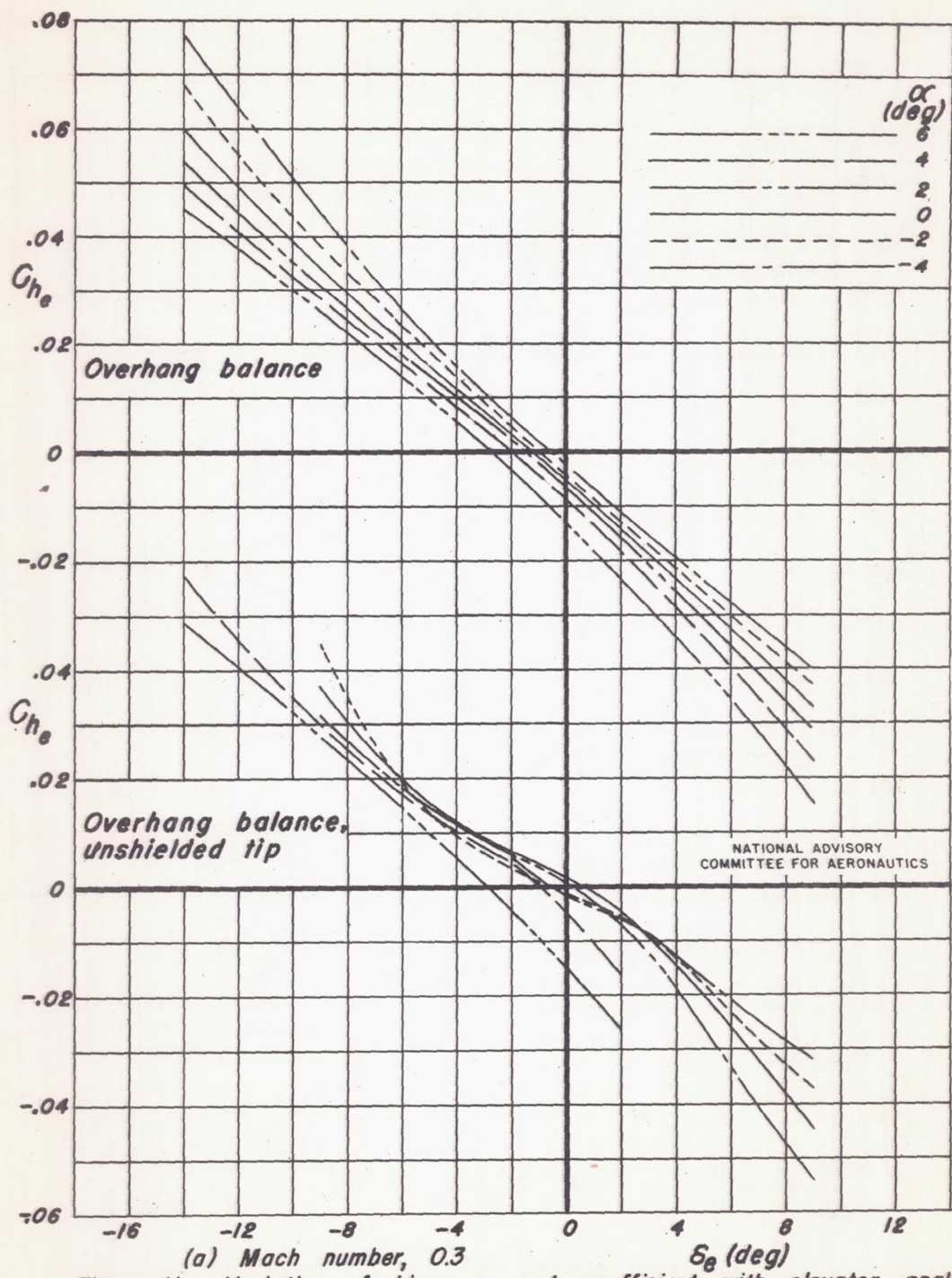
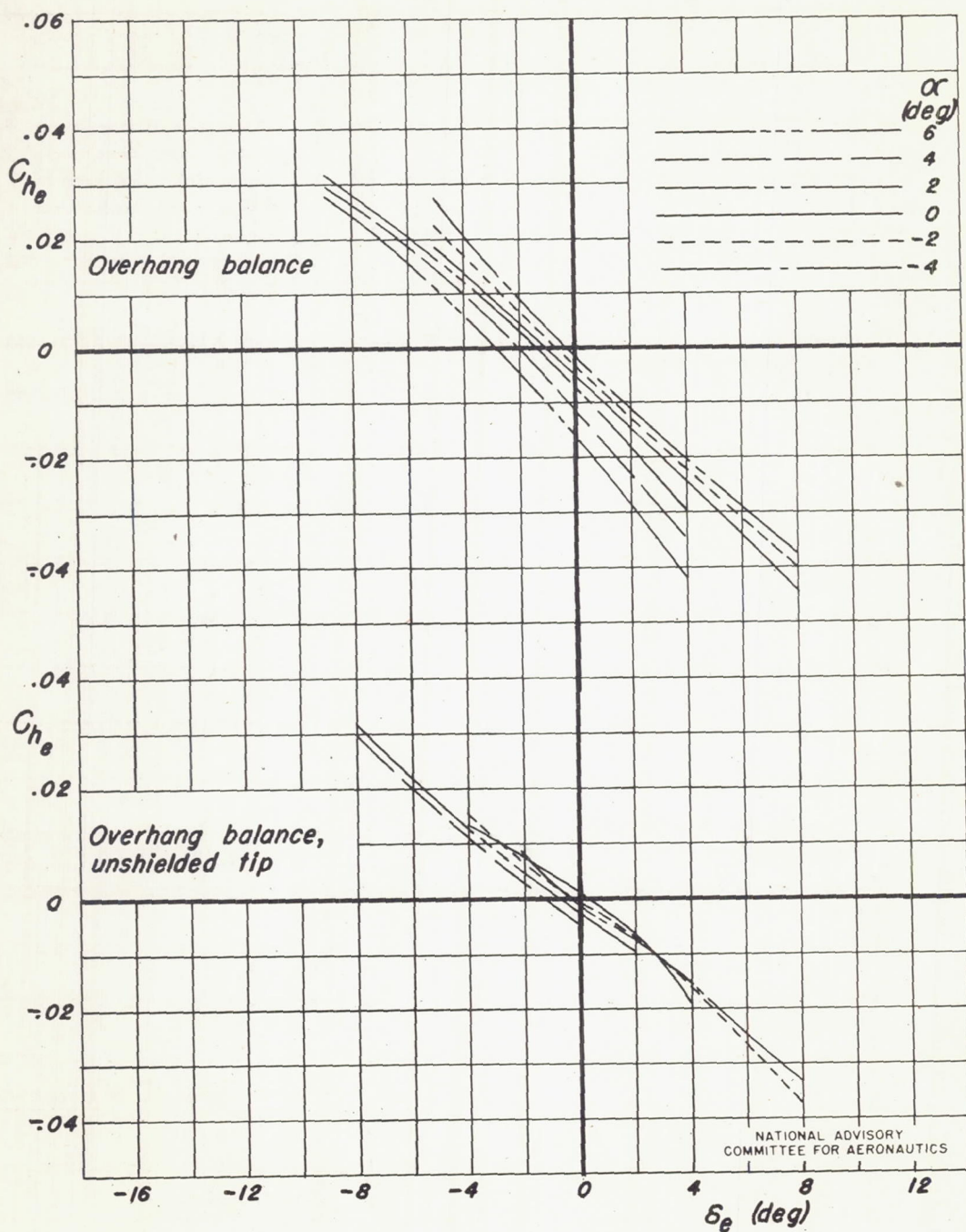
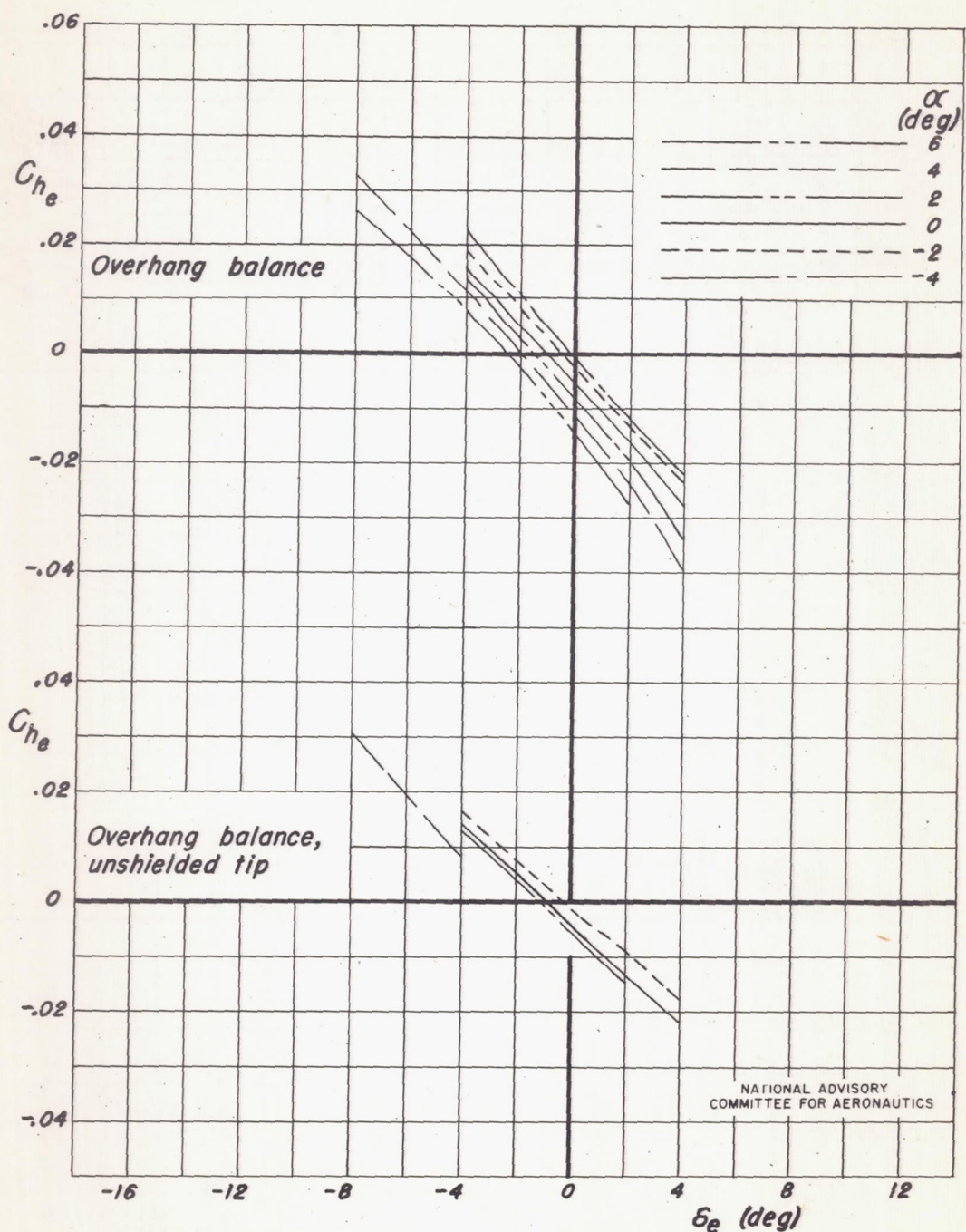


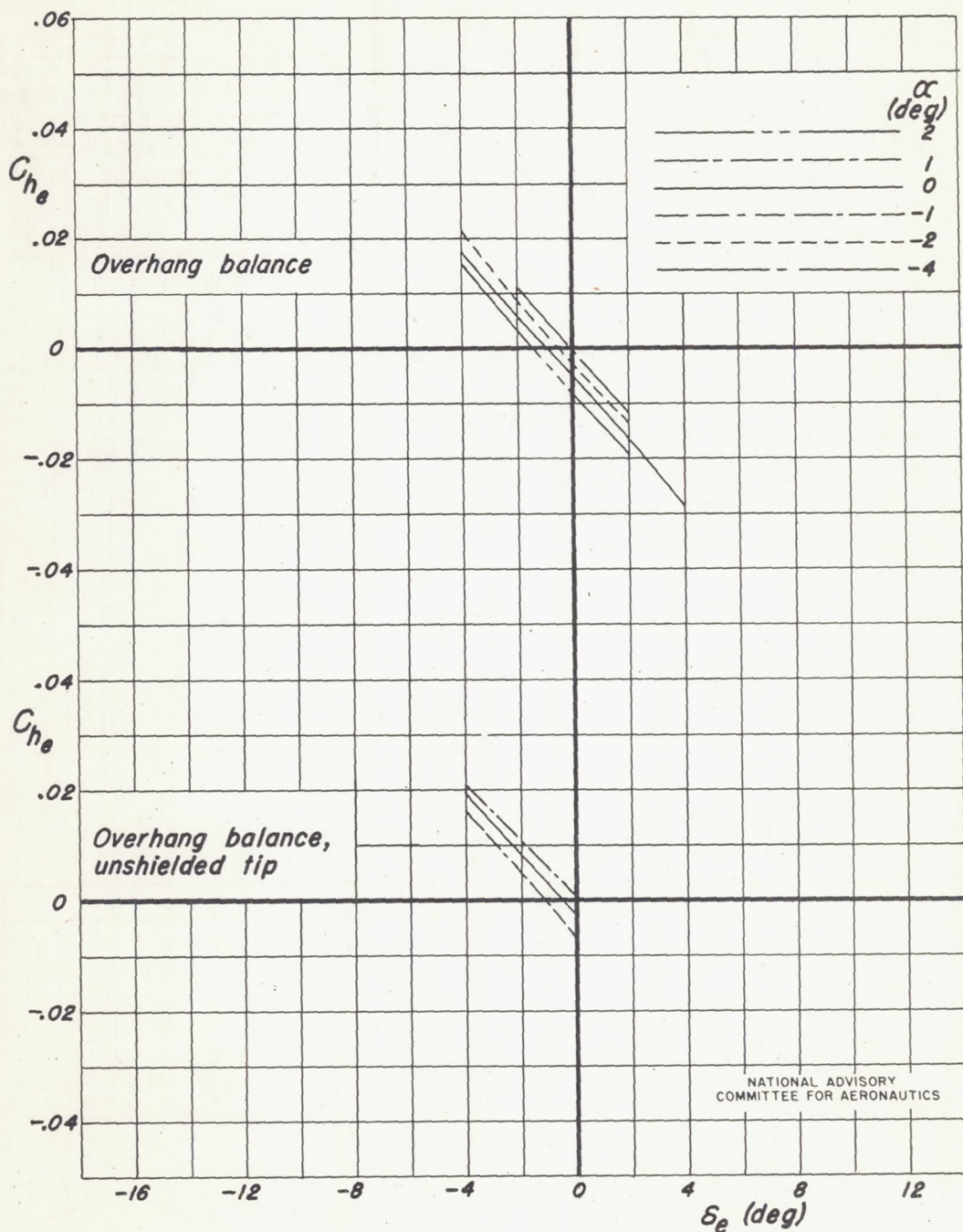
Figure 11. — Variation of hinge-moment coefficient with elevator angle for the overhang-balance elevator with and without a shielded tip.



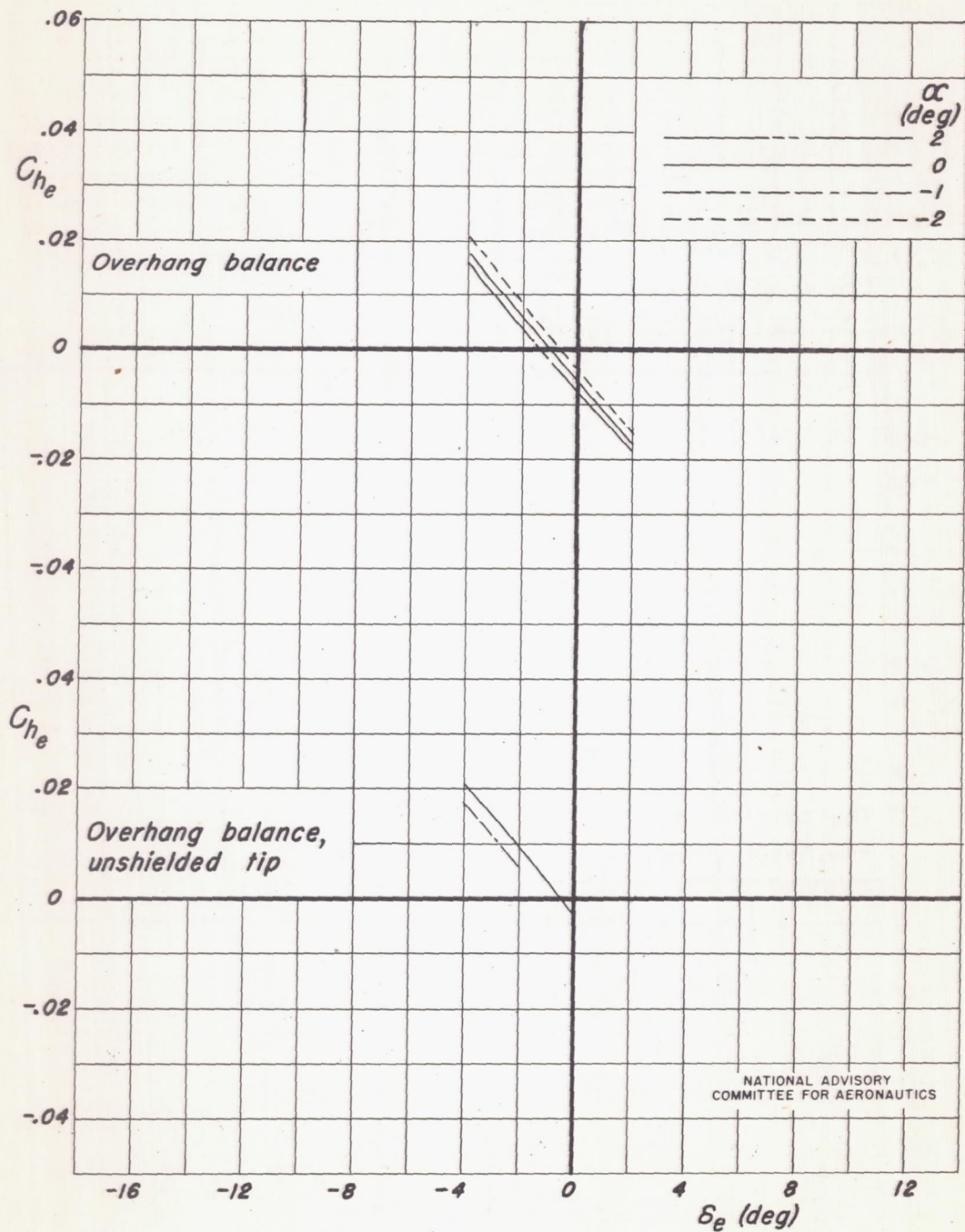
(b) Mach number, 0.5  
Figure 11. — Continued.



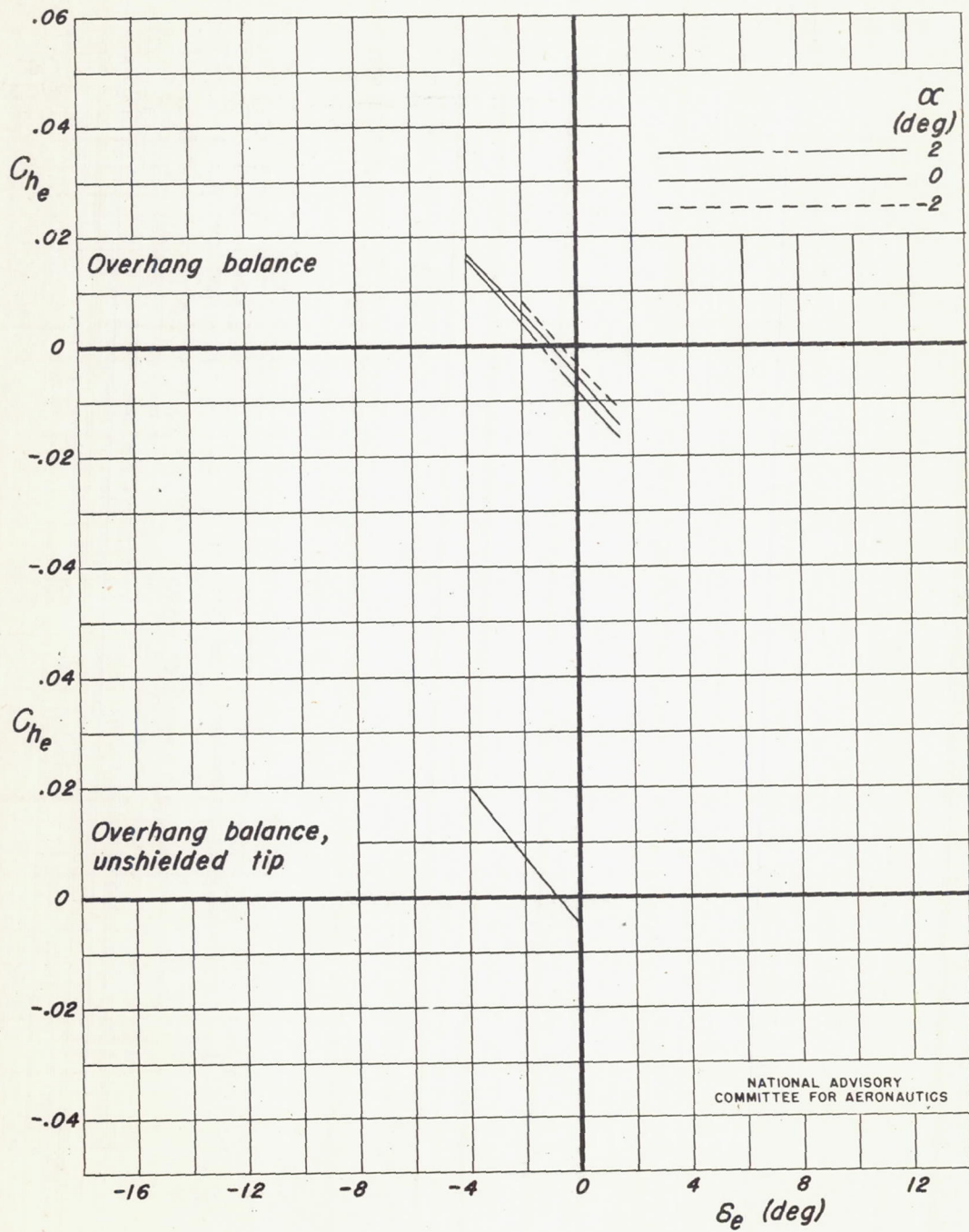
(c) Mach number, 0.6  
Figure 11. — Continued.



(d) Mach number, 0.7  
Figure 11. — Continued.



(e) Mach number, 0.725  
Figure 11. — Continued.



(f) Mach number, 0.75  
Figure 11. — Concluded.

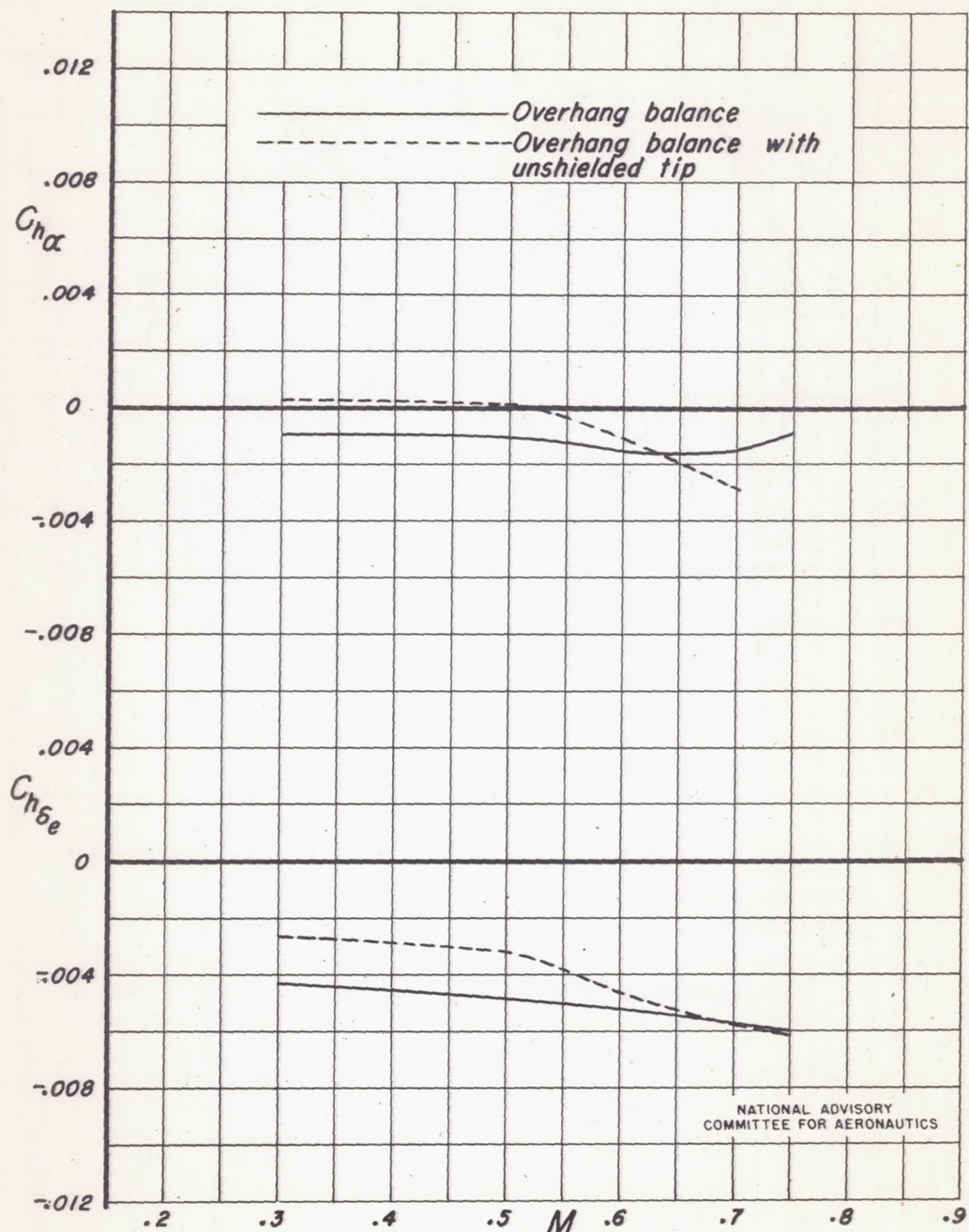


Figure 12.—Variation of elevator hinge-moment parameters with Mach number for the overhang-balance elevator with and without a shielded tip.

NATIONAL ADVISORY  
COMMITTEE FOR AERONAUTICS

Fig. 13

NACA RM No. A7H29

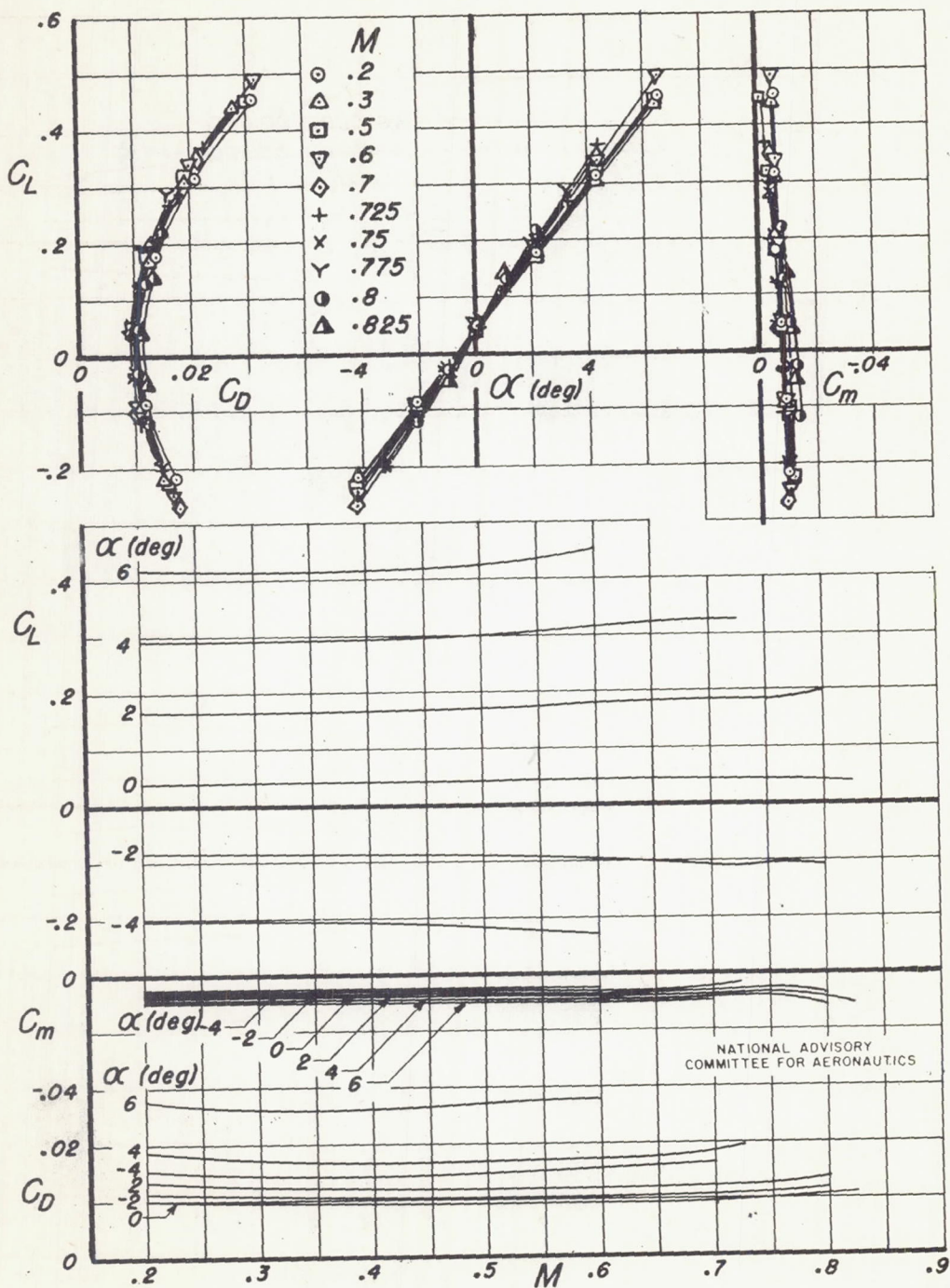


Figure 13.—Lift, drag, and pitching-moment coefficients for the semispan horizontal tail with the sealed overhang-balance elevator having a reduced semispan.  $\delta_e, 0^\circ$

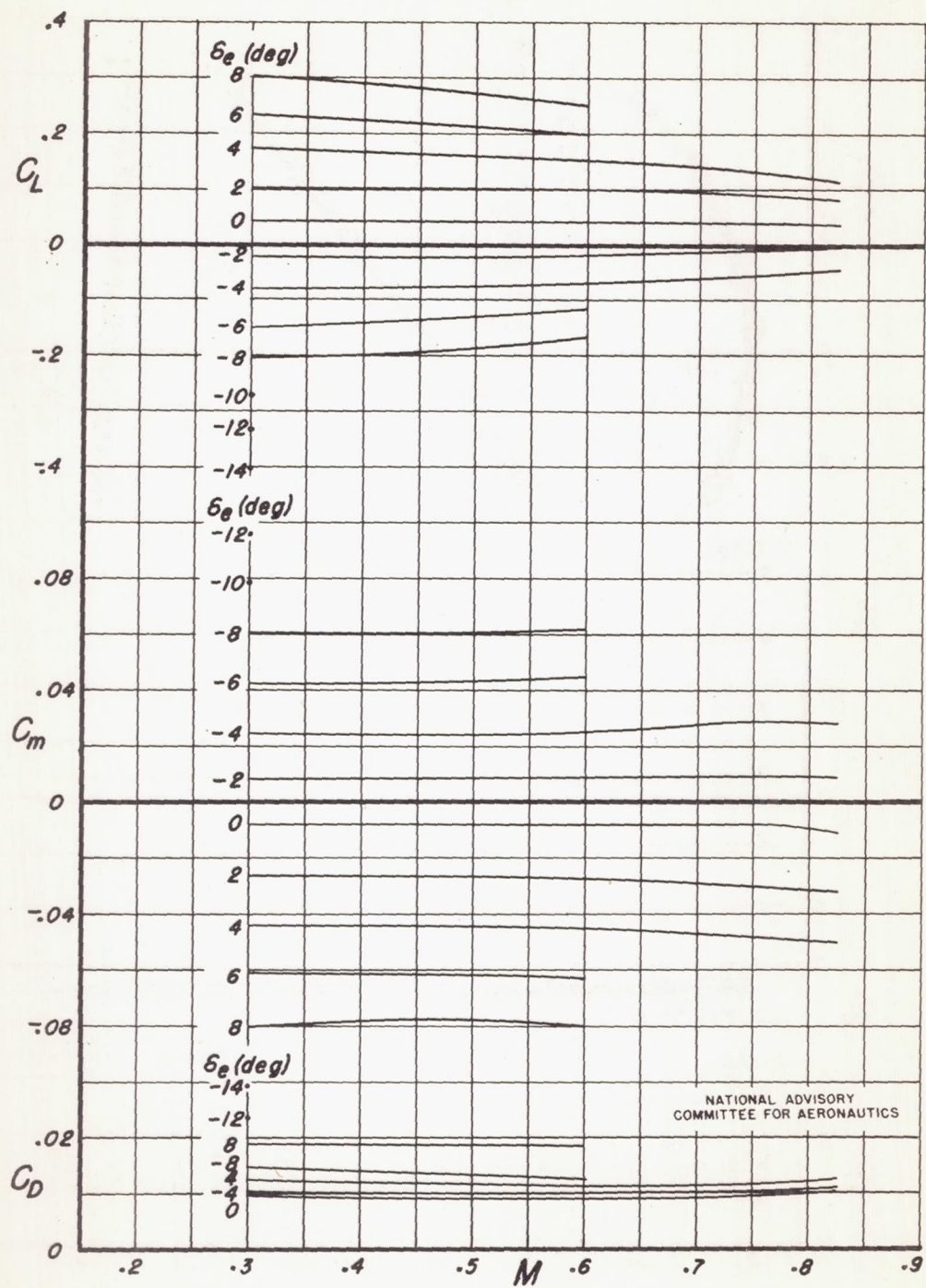


Figure 14.—Lift, drag, and pitching-moment coefficients for the semispan horizontal tail with the sealed overhang-balance elevator having a reduced semispan. Angle of attack, 0°.

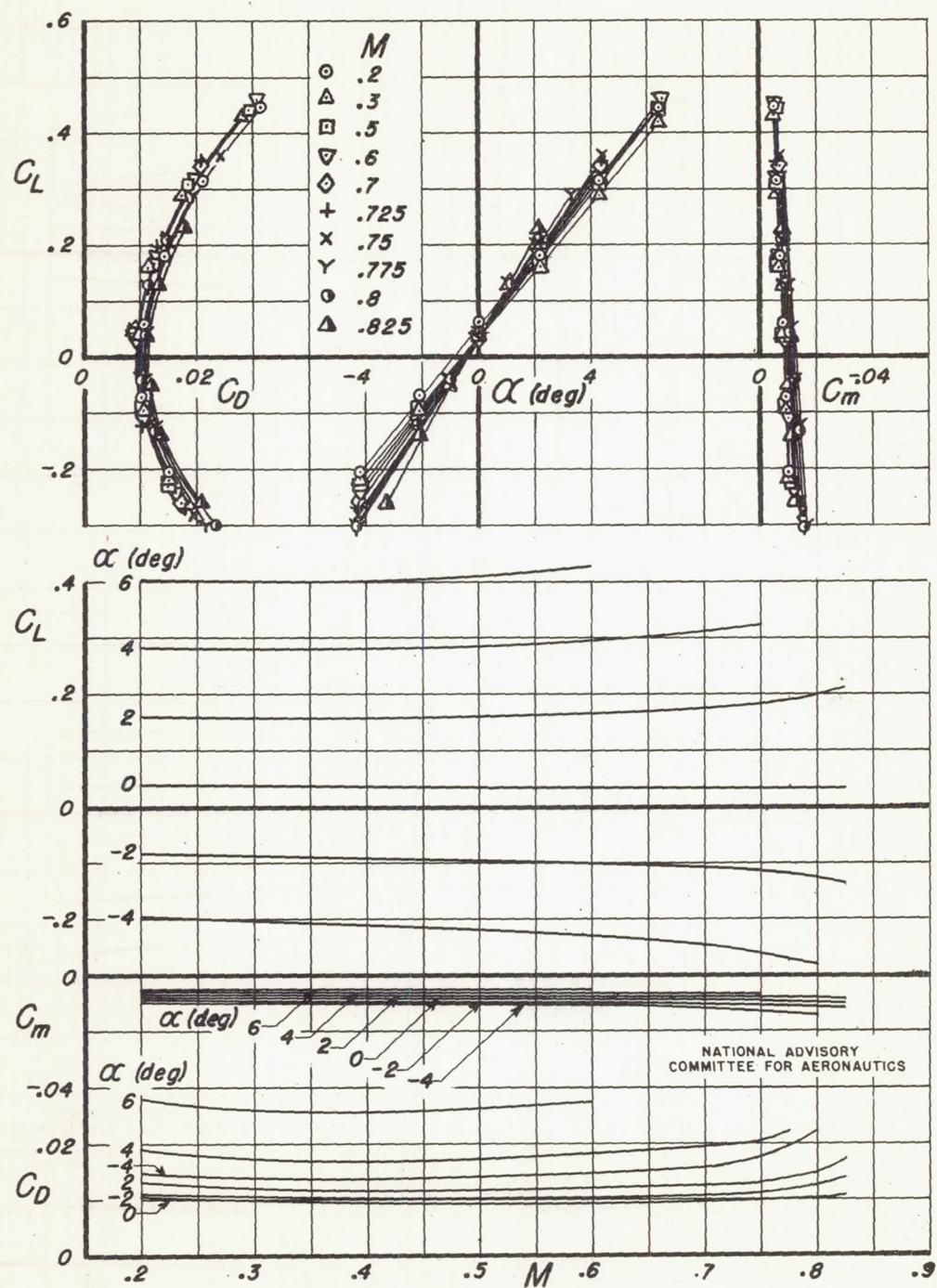


Figure 15.—Lift, drag, and pitching-moment coefficients for the semispan horizontal tail with the unsealed overhang-balance elevator having a reduced semispan.  $\delta_e$ ,  $0^\circ$

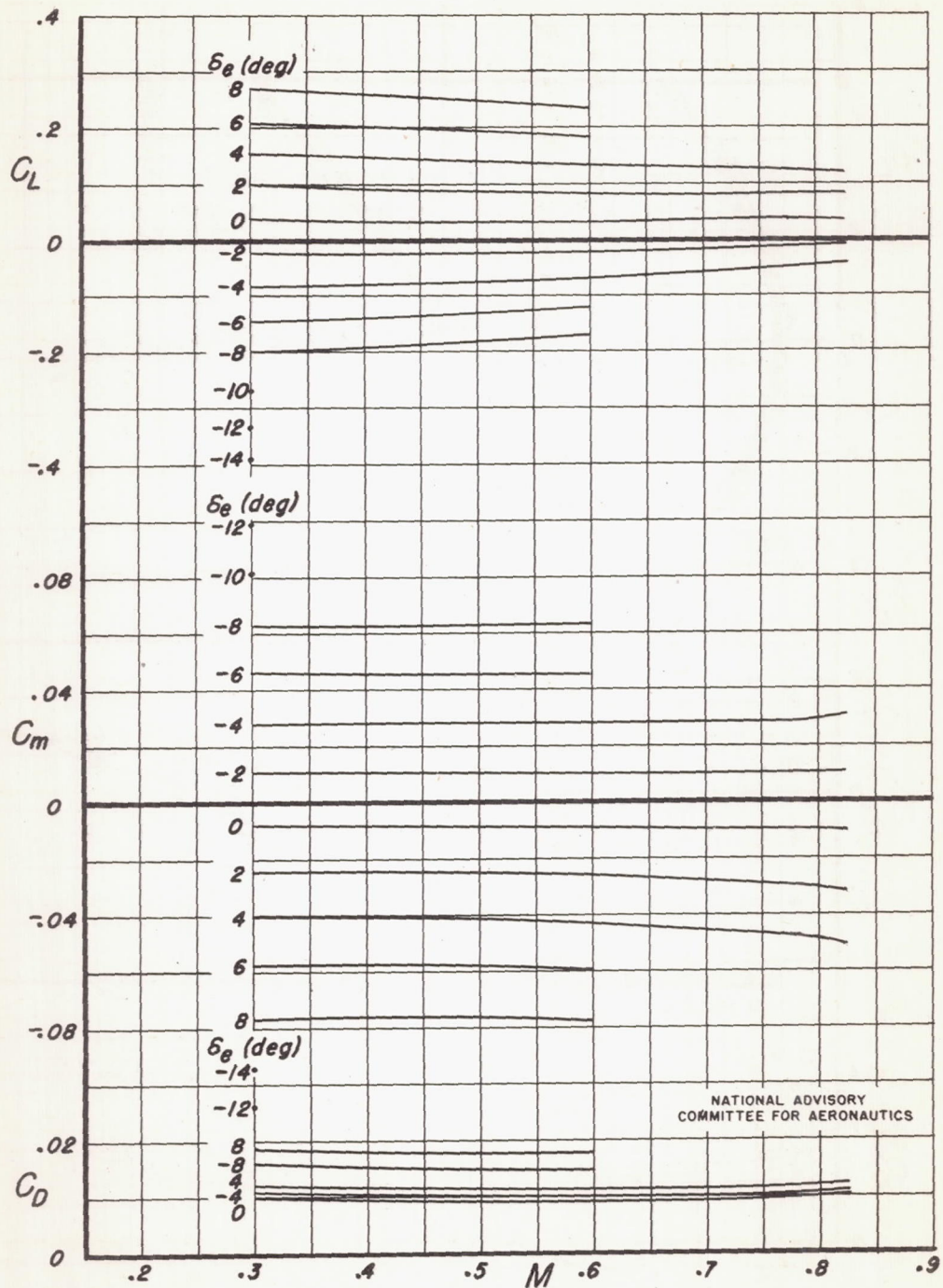


Figure 16.—Lift, drag, and pitching-moment coefficients for the semispan horizontal tail with the unsealed overhang-balance elevator having a reduced semispan.  $\alpha, 0^\circ$

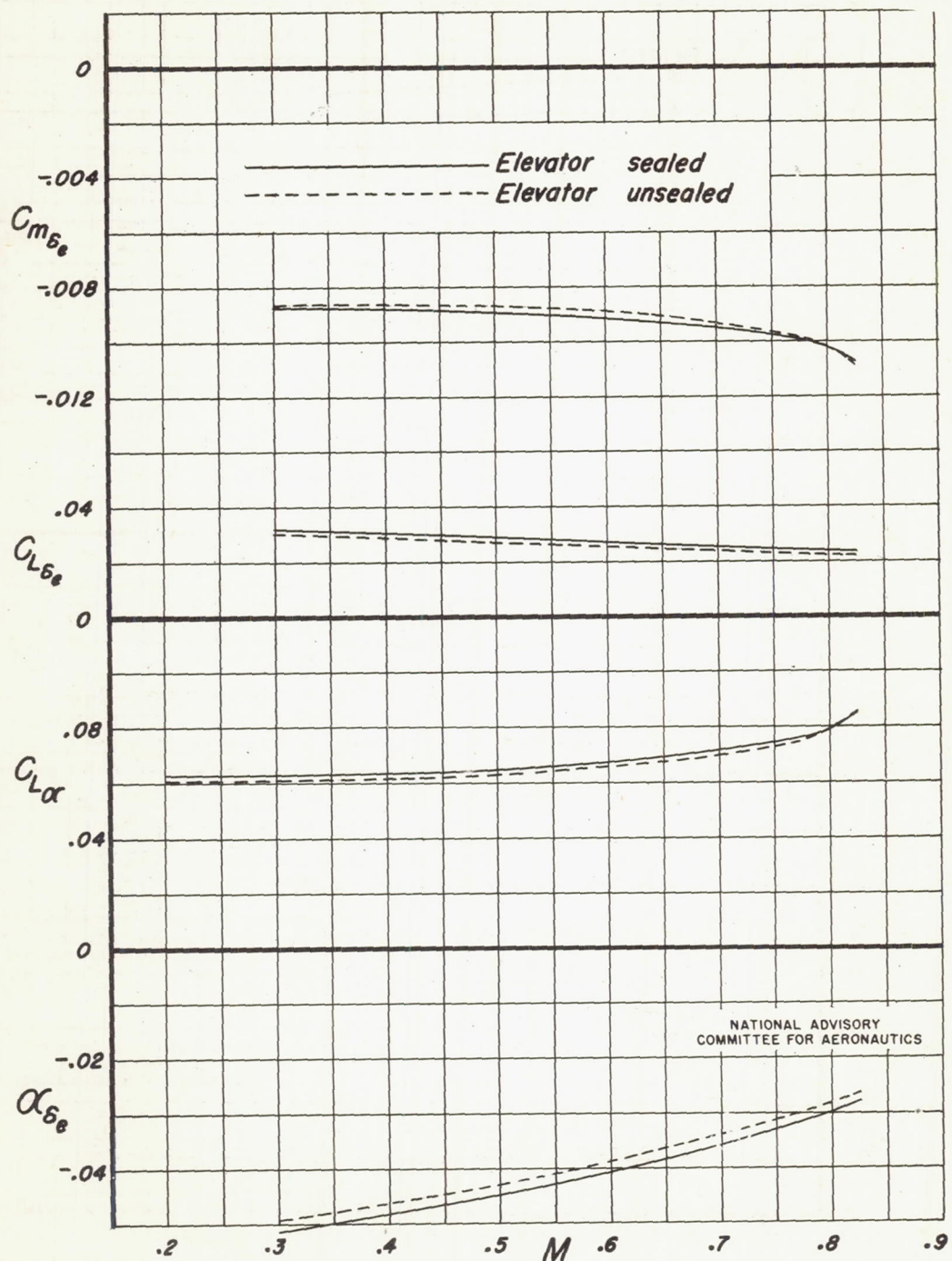


Figure 17.—Variation of pitching-moment, lift, and elevator effectiveness parameters with Mach number for the sealed and unsealed overhang-balance elevator having a reduced semispan.

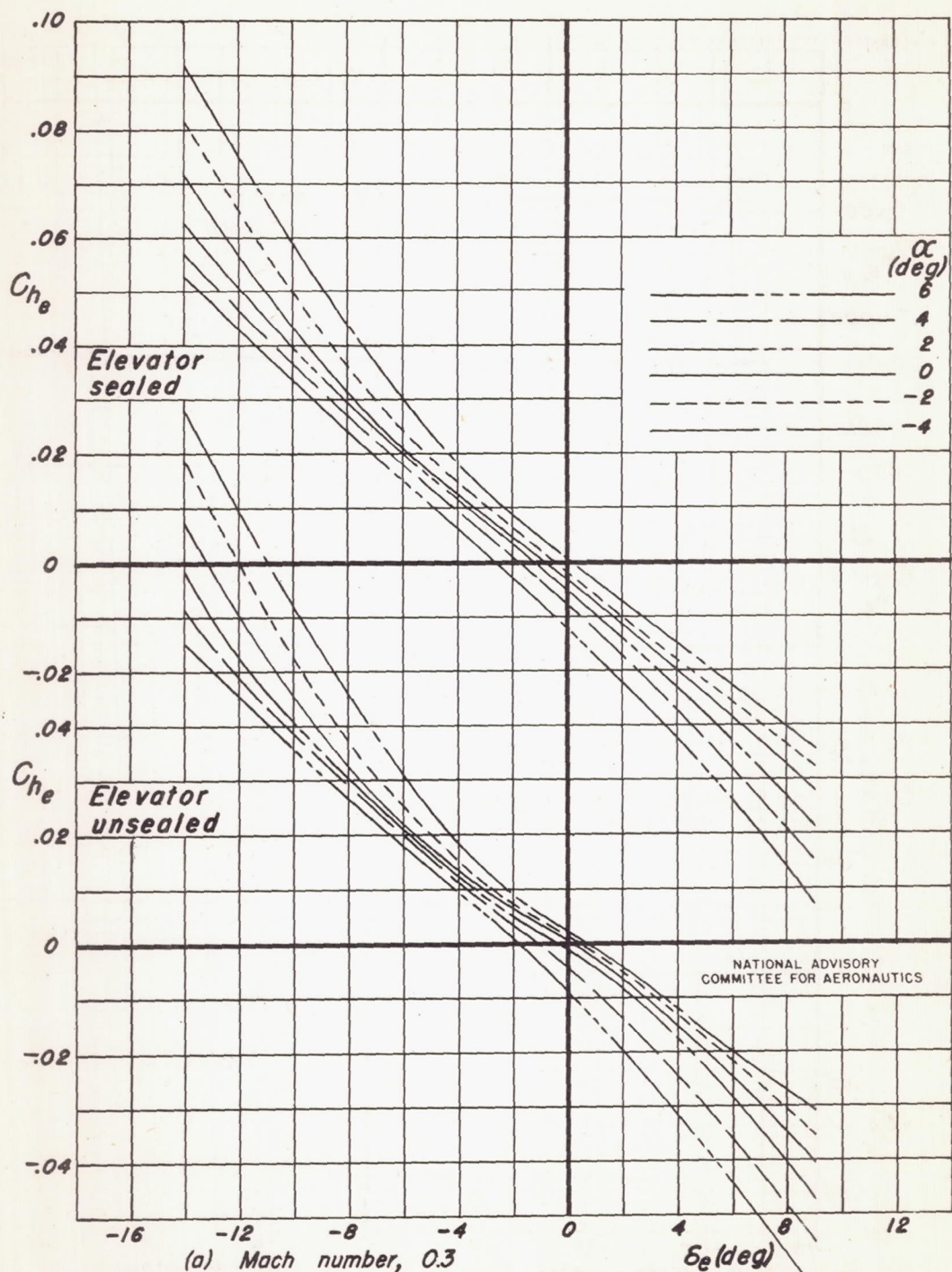


Figure 18.—Variation of hinge-moment coefficient with elevator angle for the sealed and unsealed overhang-balance elevator having a reduced semispan.

Fig. 18 b

NACA RM No. A7H29

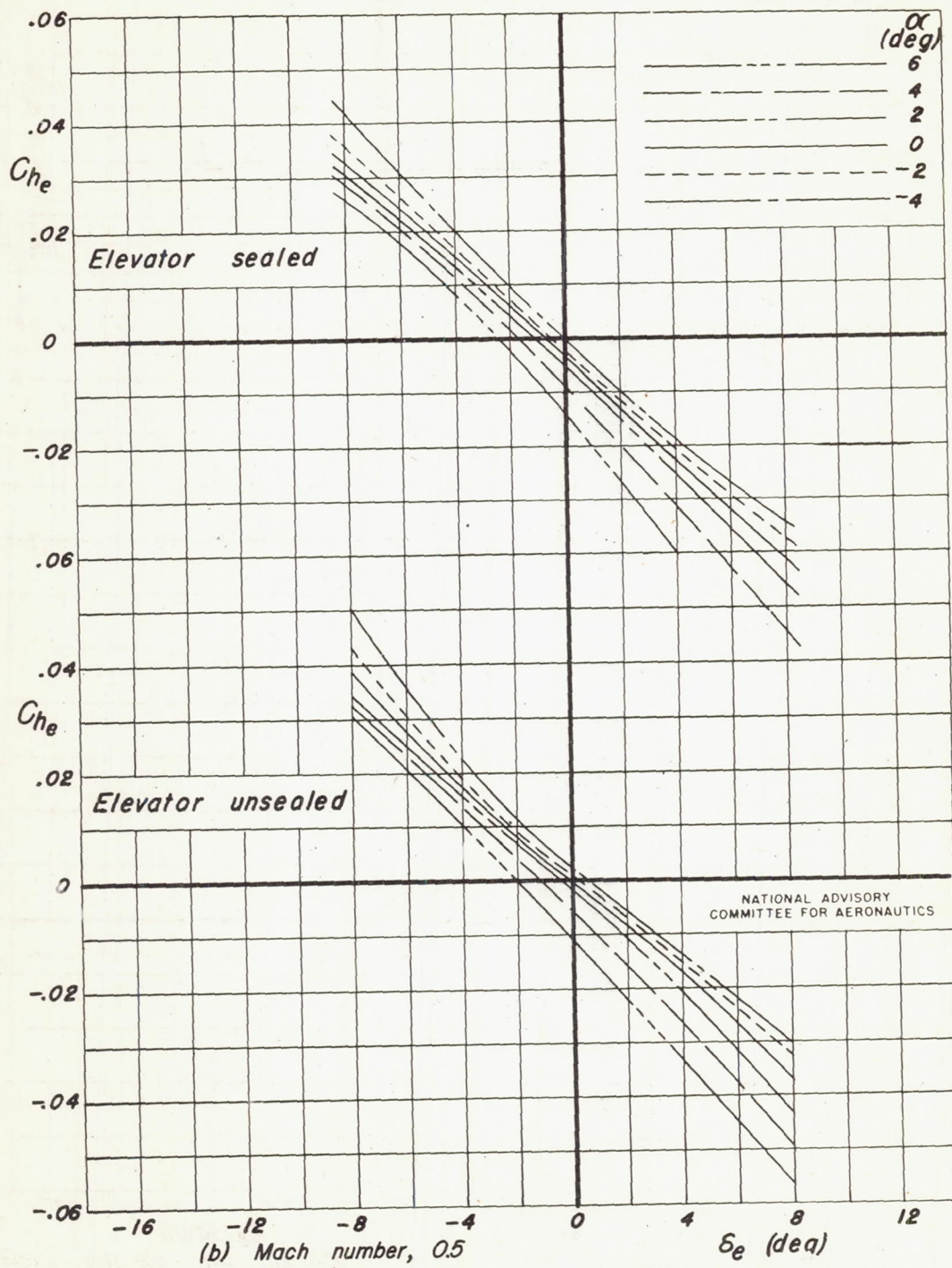
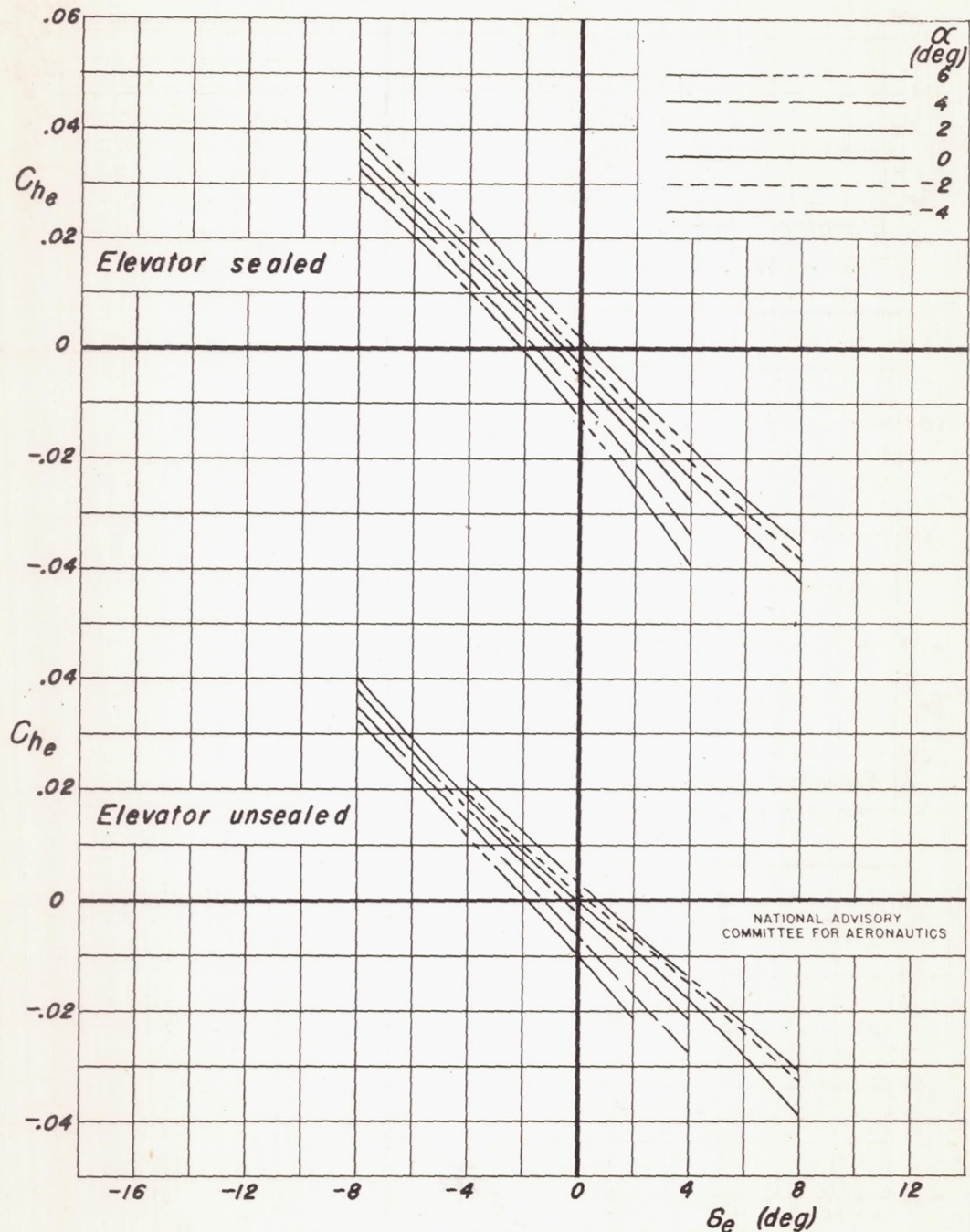
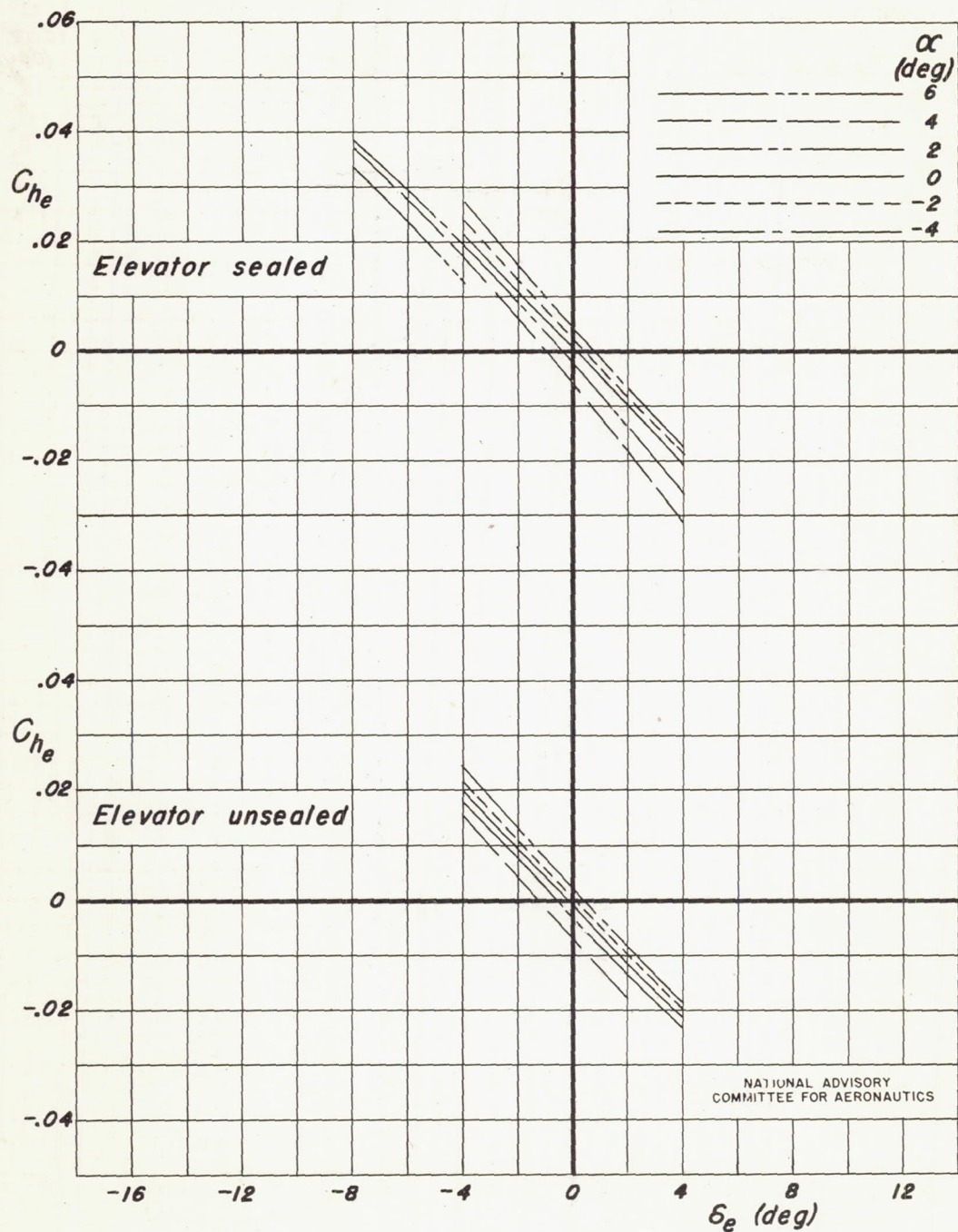
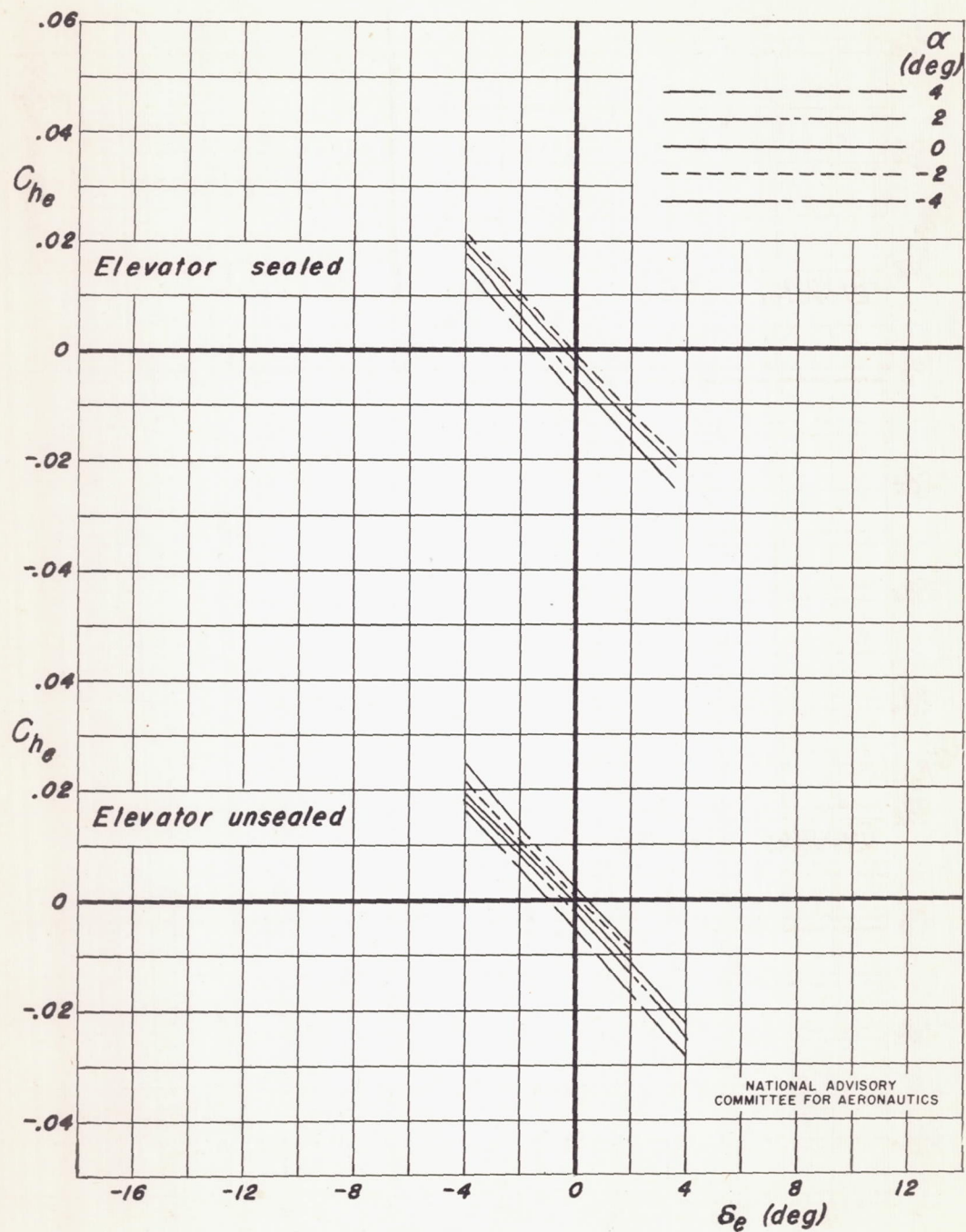


Figure 18.—Continued

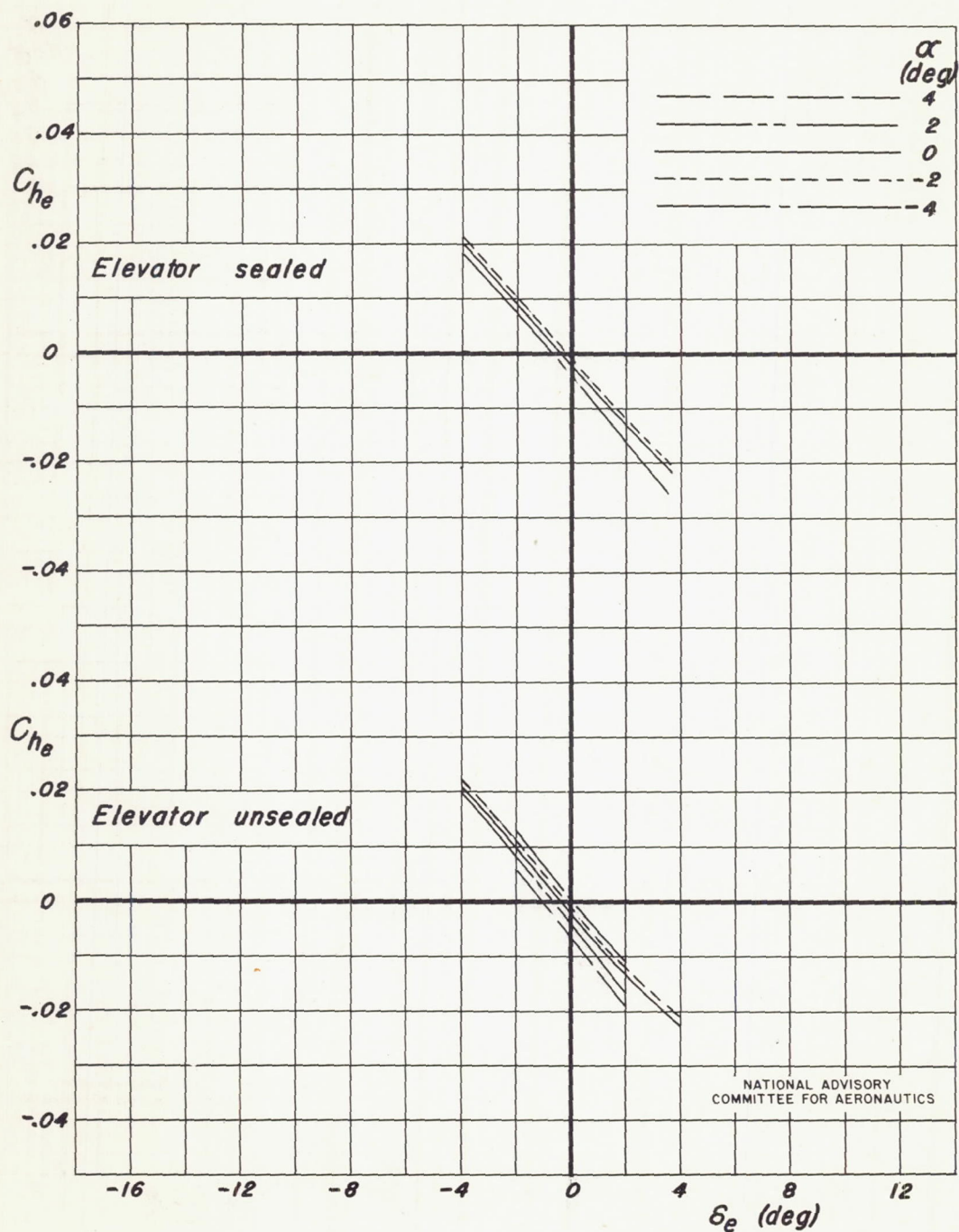
(c) Mach number, 0.6  
Figure 18.—Continued



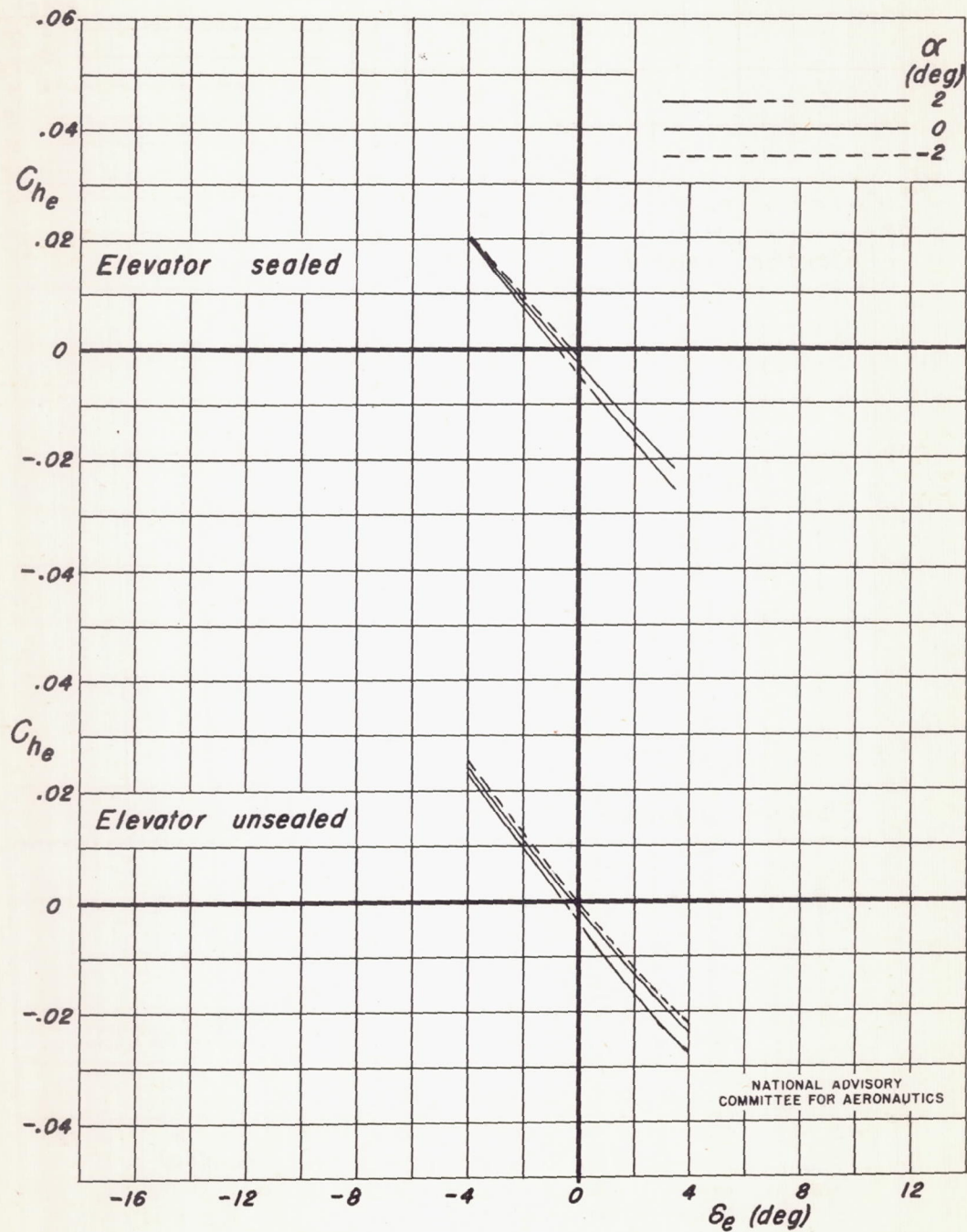
(d) Mach number, 0.7  
Figure 18.-Continued



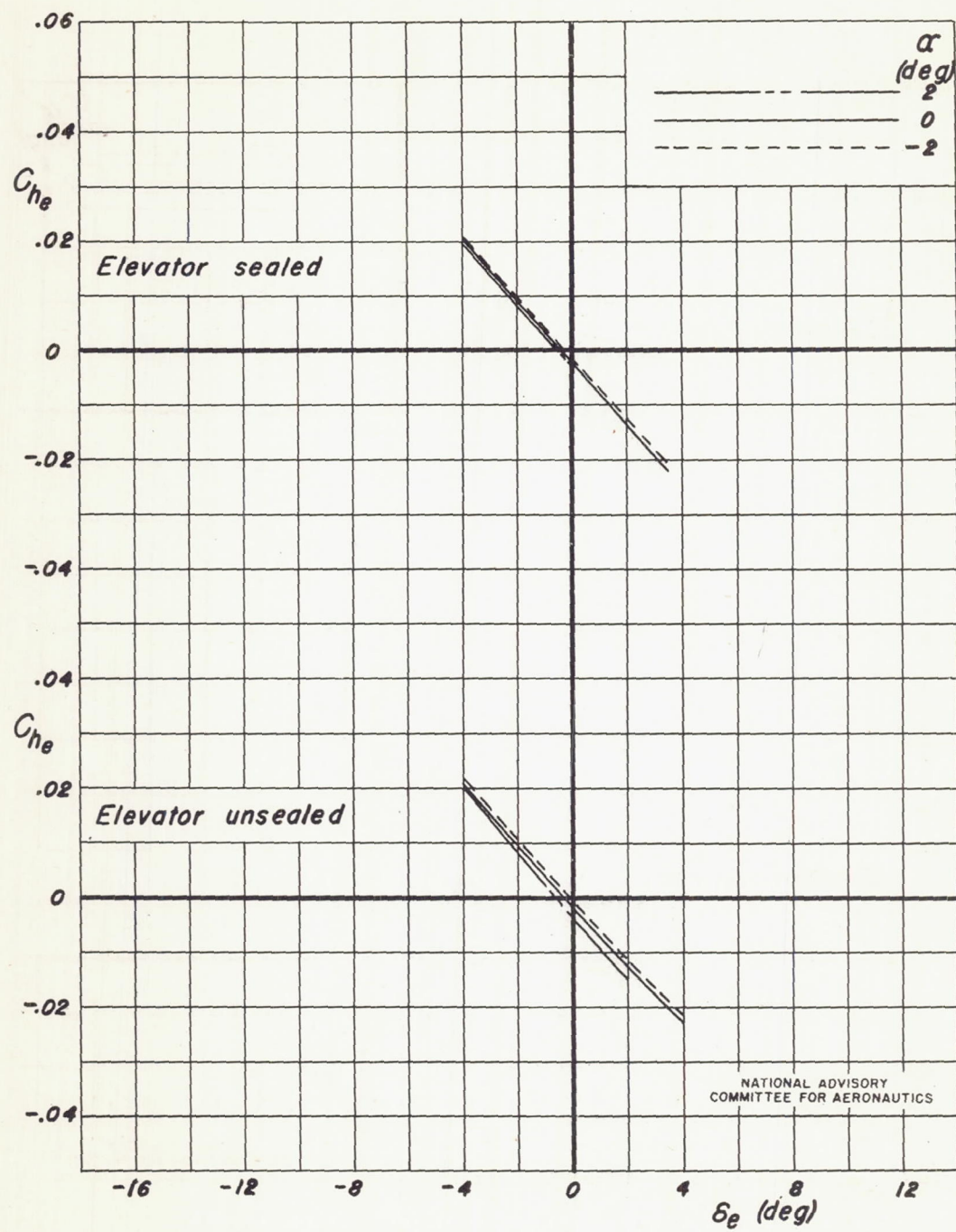
(e) Mach number, 0.725  
Figure 18.—Continued



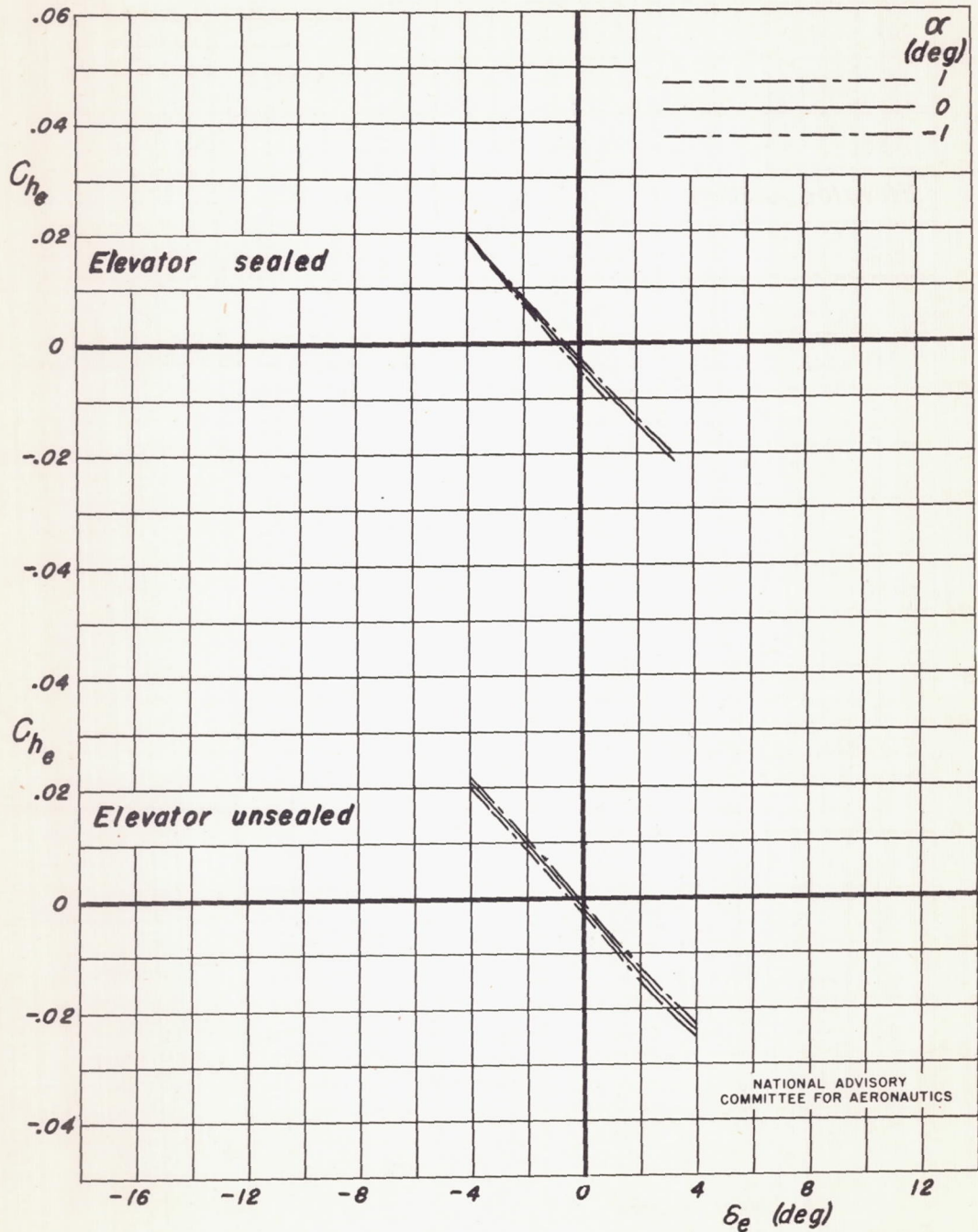
(f) Mach number, 0.75  
Figure 18.—Continued



(g) Mach number, 0.775  
Figure 18.—Continued



(h) Mach number, 0.8  
Figure 18.—Continued



(i) Mach number, 0.825  
Figure 18.—Concluded

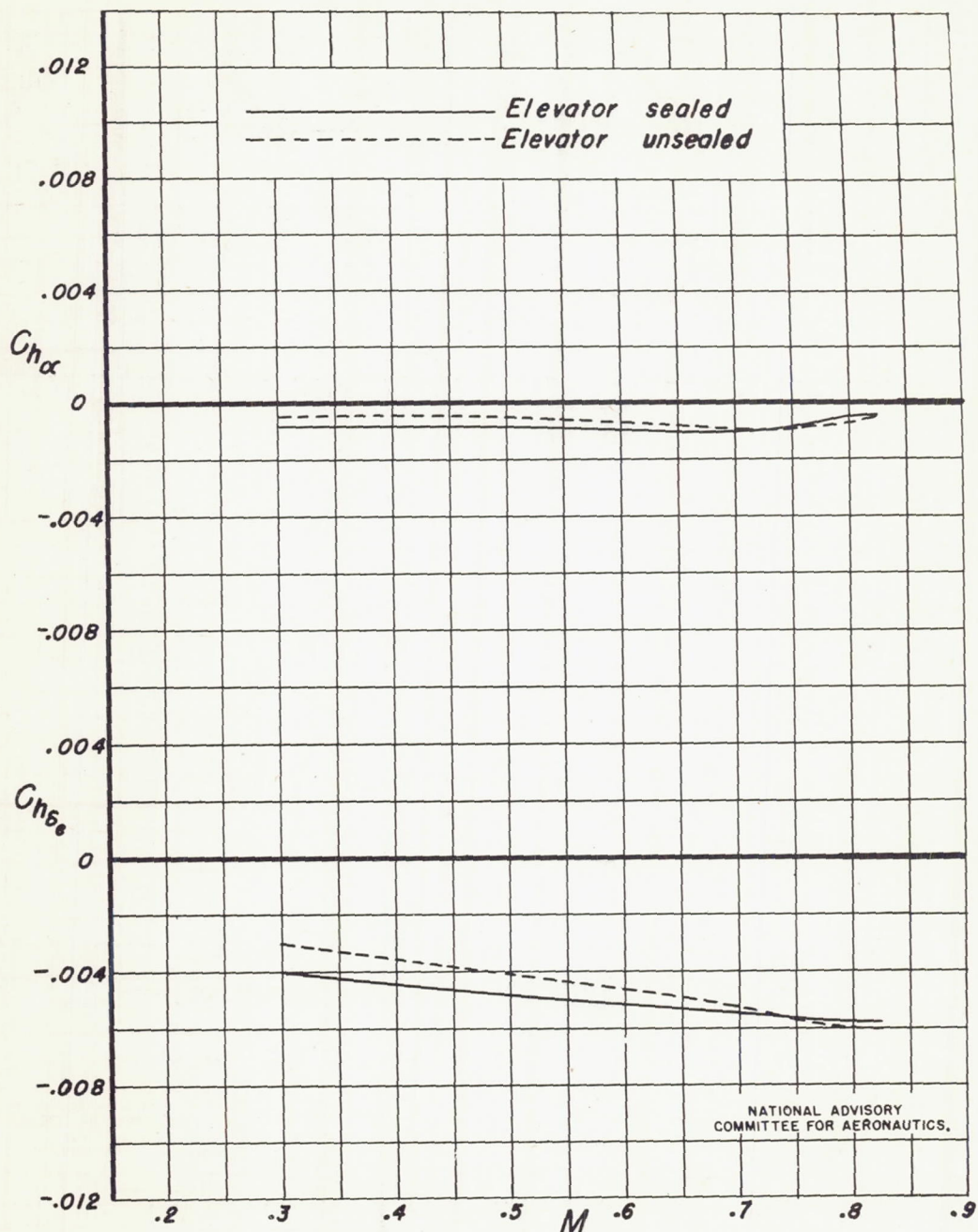


Figure 19.—Variation of elevator hinge-moment parameters with Mach number for the sealed and unsealed overhang-balance elevator having a reduced semispan.

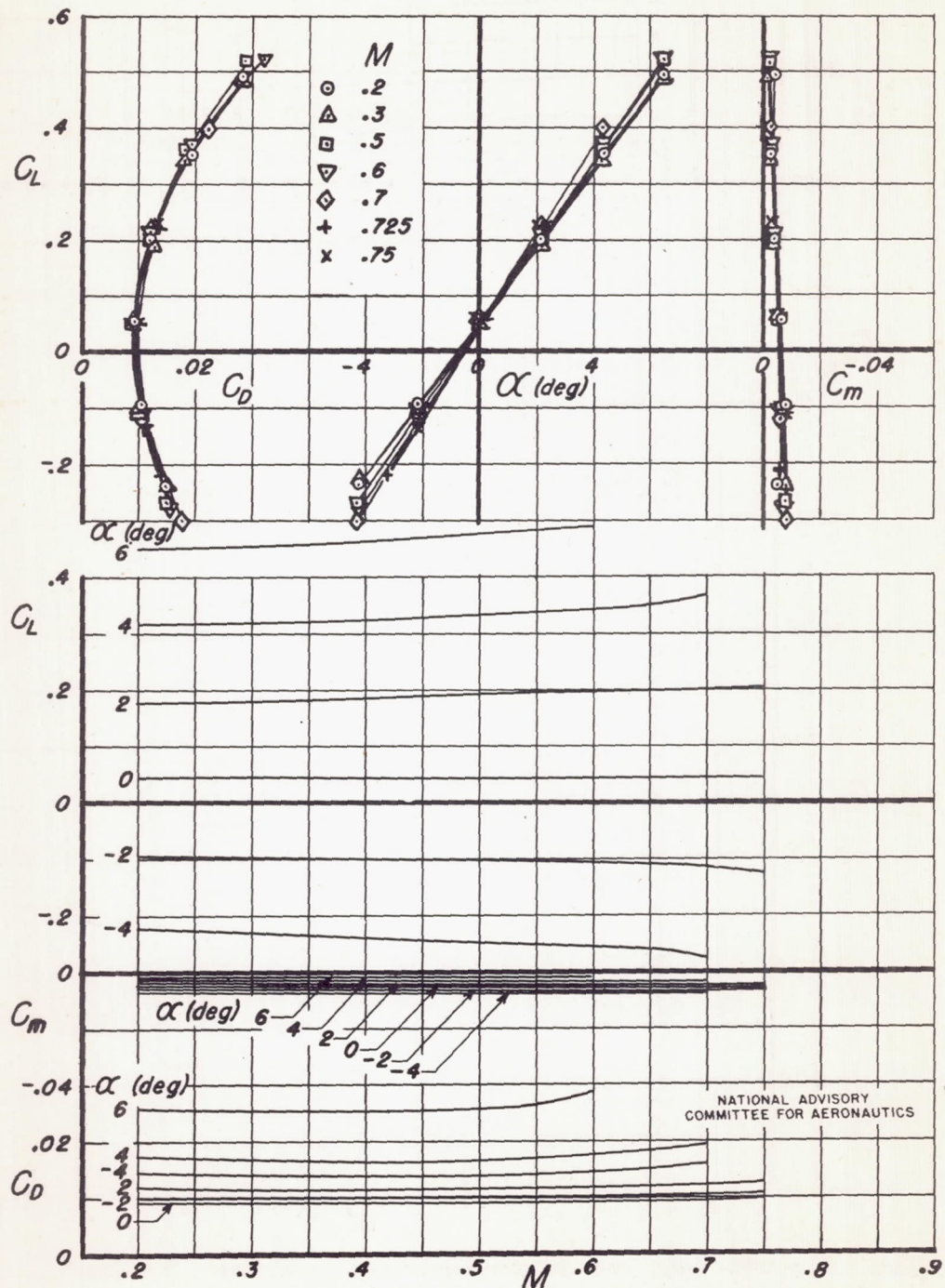


Figure 20.—Lift, drag, and pitching-moment coefficients for the semispan tail with the shielded normal-nose horn-balance elevator.  
 $\delta_e, 0^\circ$

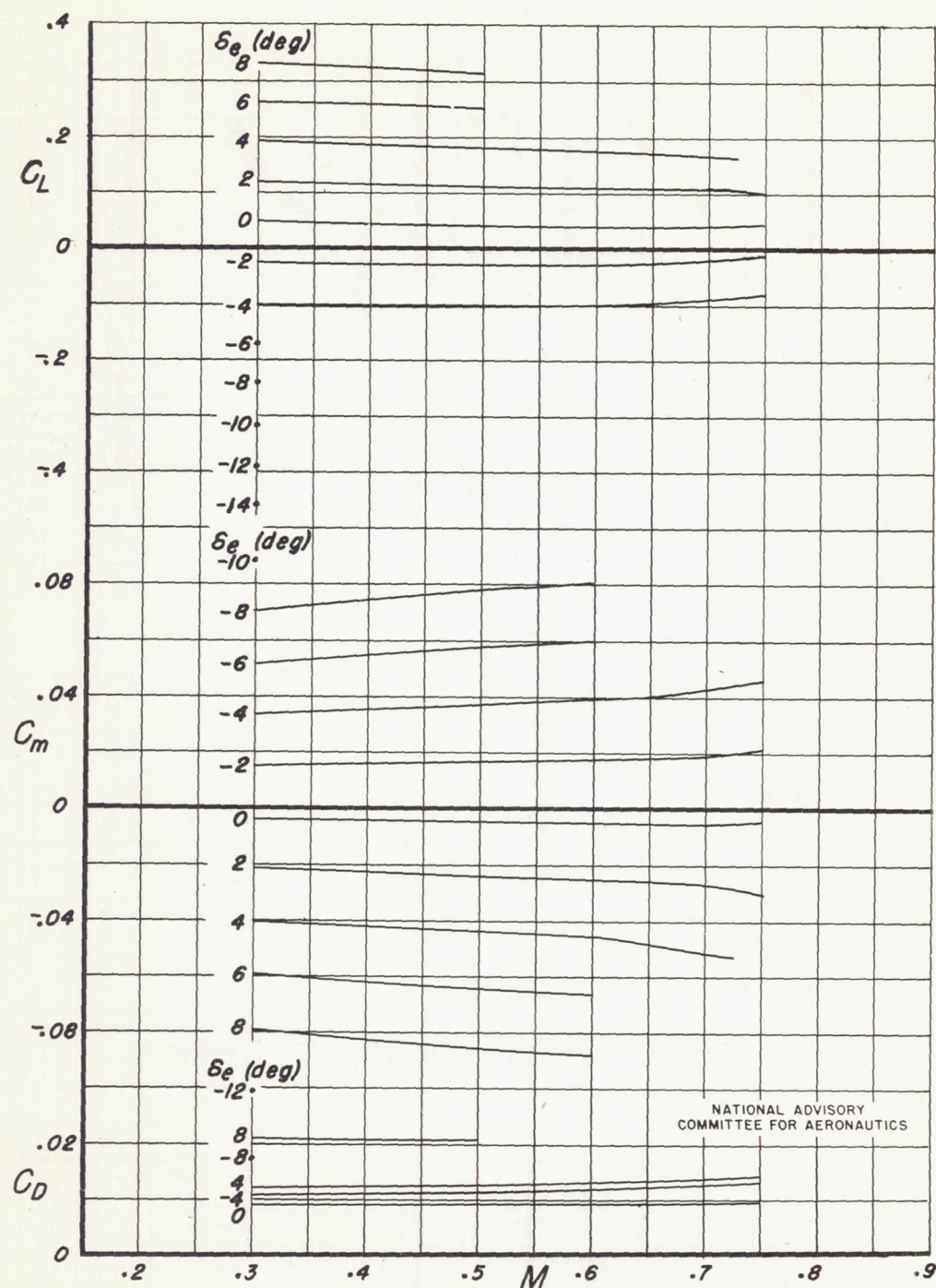


Figure 21.—Lift, drag, and pitching-moment coefficients for the semispan horizontal tail with the shielded normal-nose horn-balance elevator.  $\alpha, 0^\circ$

NATIONAL ADVISORY  
COMMITTEE FOR AERONAUTICS

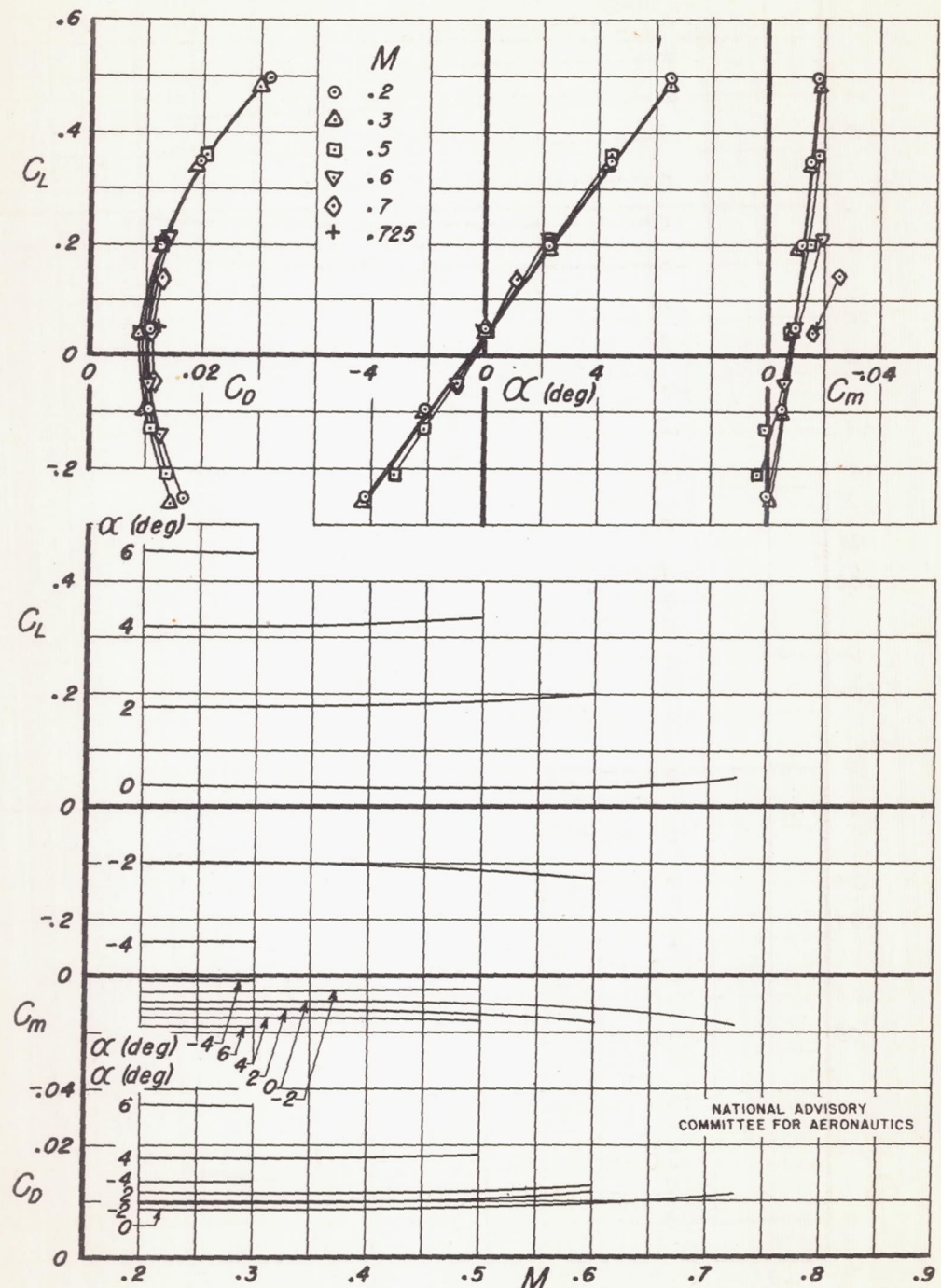


Figure 22.—Lift, drag, and pitching-moment coefficients for the semispan horizontal tail with the unshielded normal-nose horn-balance elevator.  $\delta_e$ ,  $0^\circ$

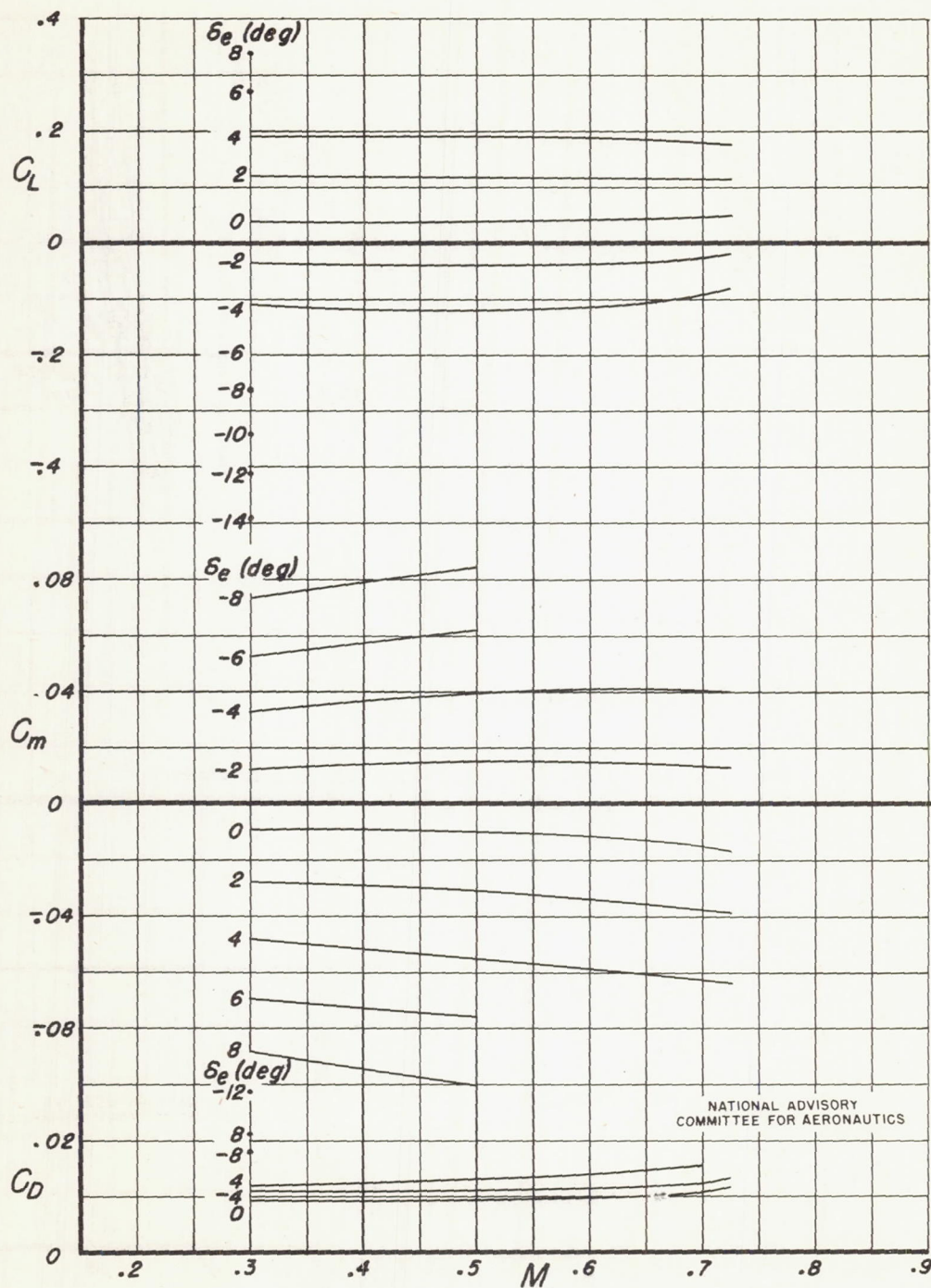


Figure 23.—Lift, drag, and pitching-moment coefficients for the semispan horizontal tail with the unshielded normal-nose horn-balance elevator.  
 $\alpha, 0^\circ$

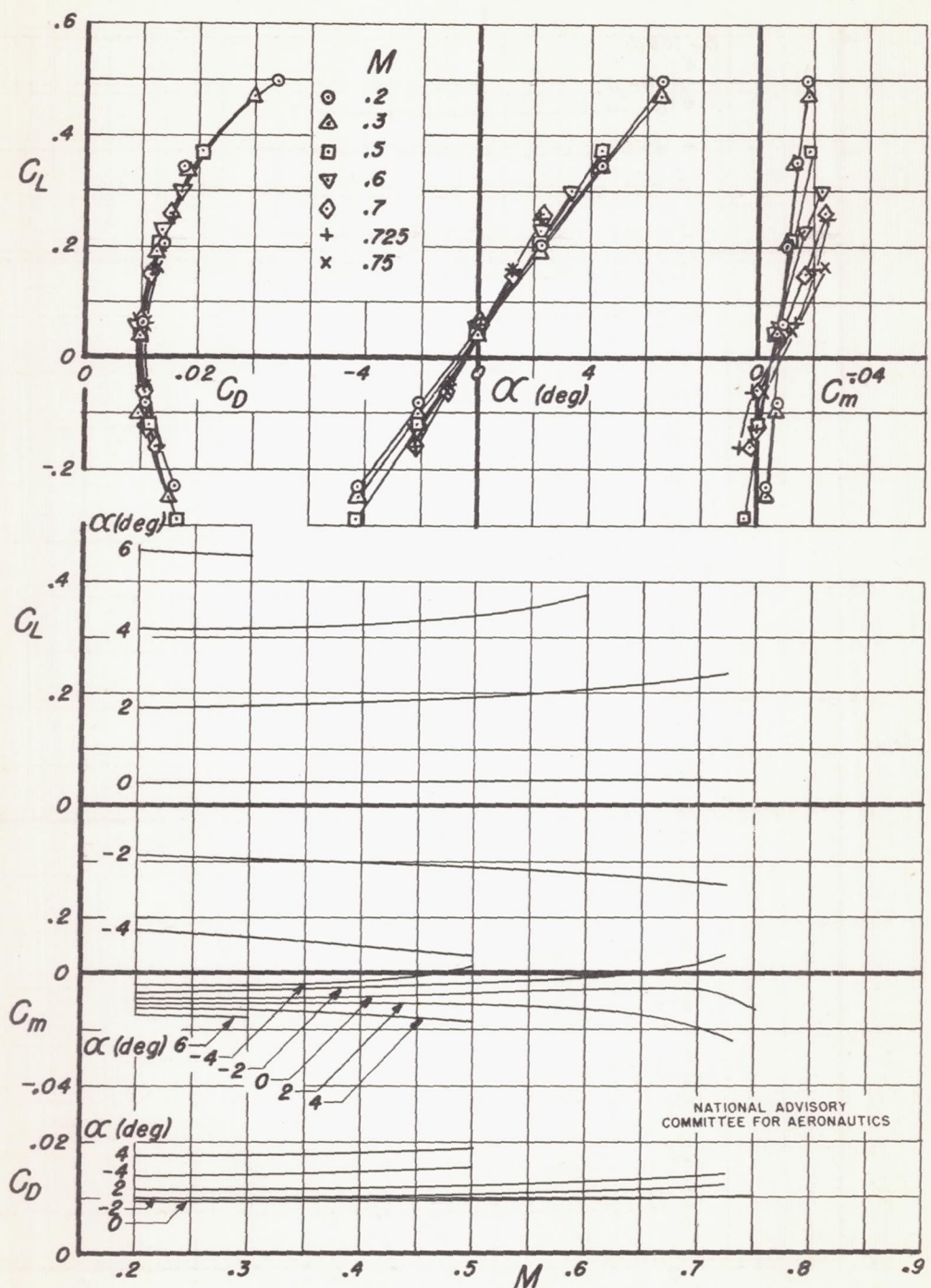


Figure 24.—Lift, drag, and pitching-moment coefficients for the semispan horizontal tail with the unshielded elliptical-nose horn-balance elevator.  $\delta_e, 0^\circ$

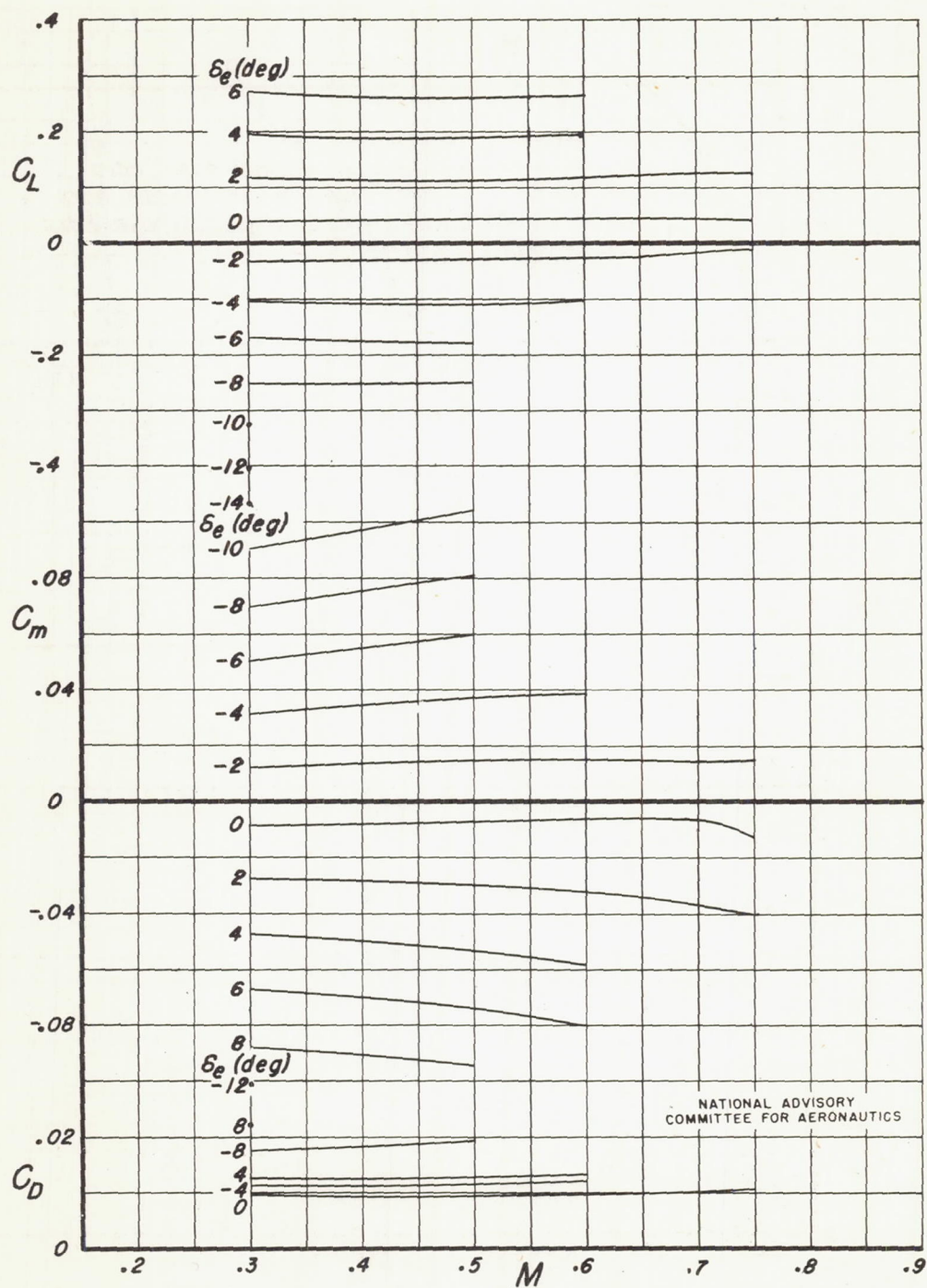


Figure 25.—Lift, drag, and pitching-moment coefficients for the semispan horizontal tail with the unshielded elliptical-nose horn-balance elevator.  
 $\alpha, 0^\circ$

NATIONAL ADVISORY  
 COMMITTEE FOR AERONAUTICS

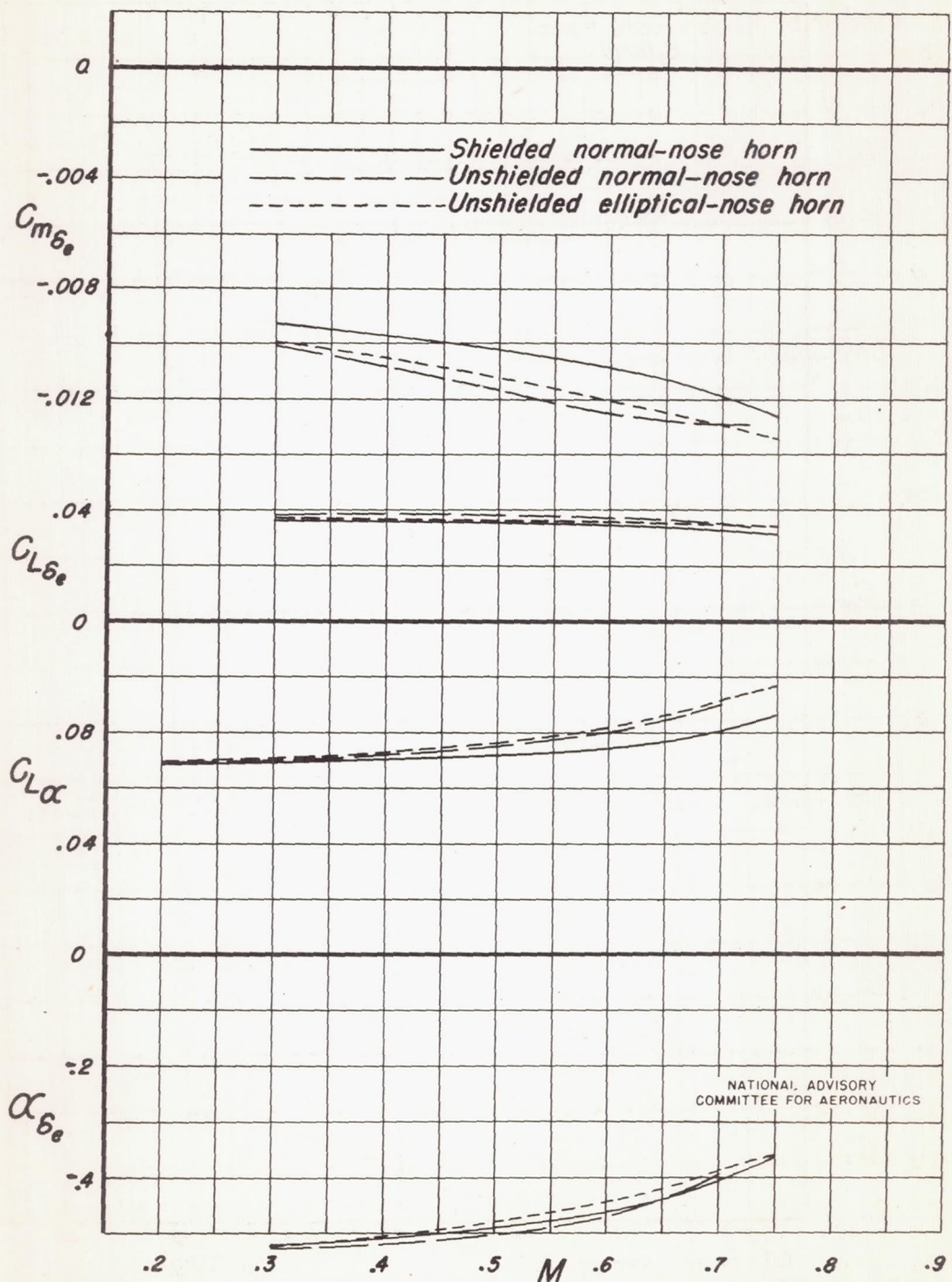


Figure 26.—Variation of pitching-moment, lift, and elevator effectiveness parameters with Mach number for the shielded and unshielded horn-balance elevators.

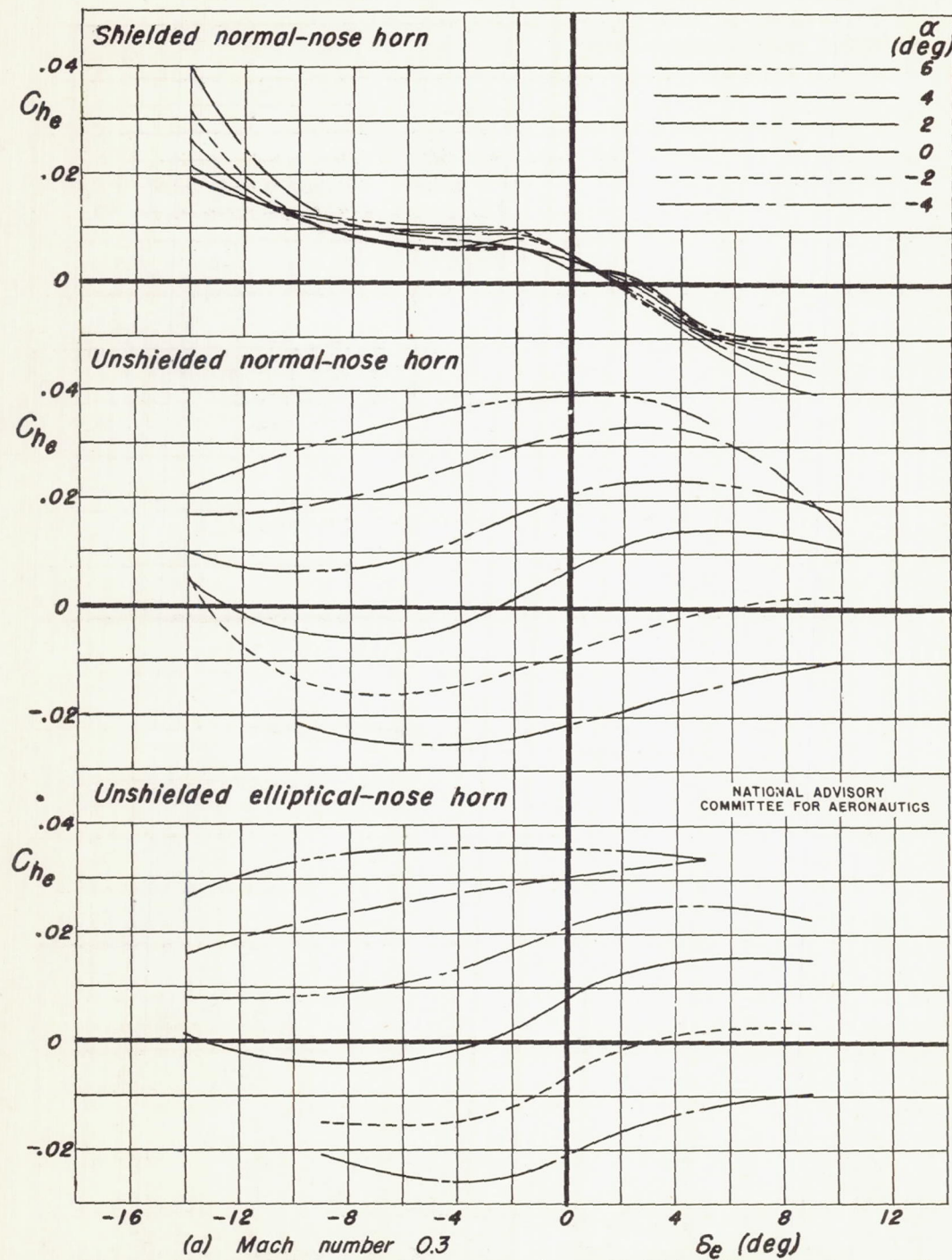


Figure 27.—Variation of hinge-moment coefficient with elevator angle for the shielded and unshielded horn-balance elevators.

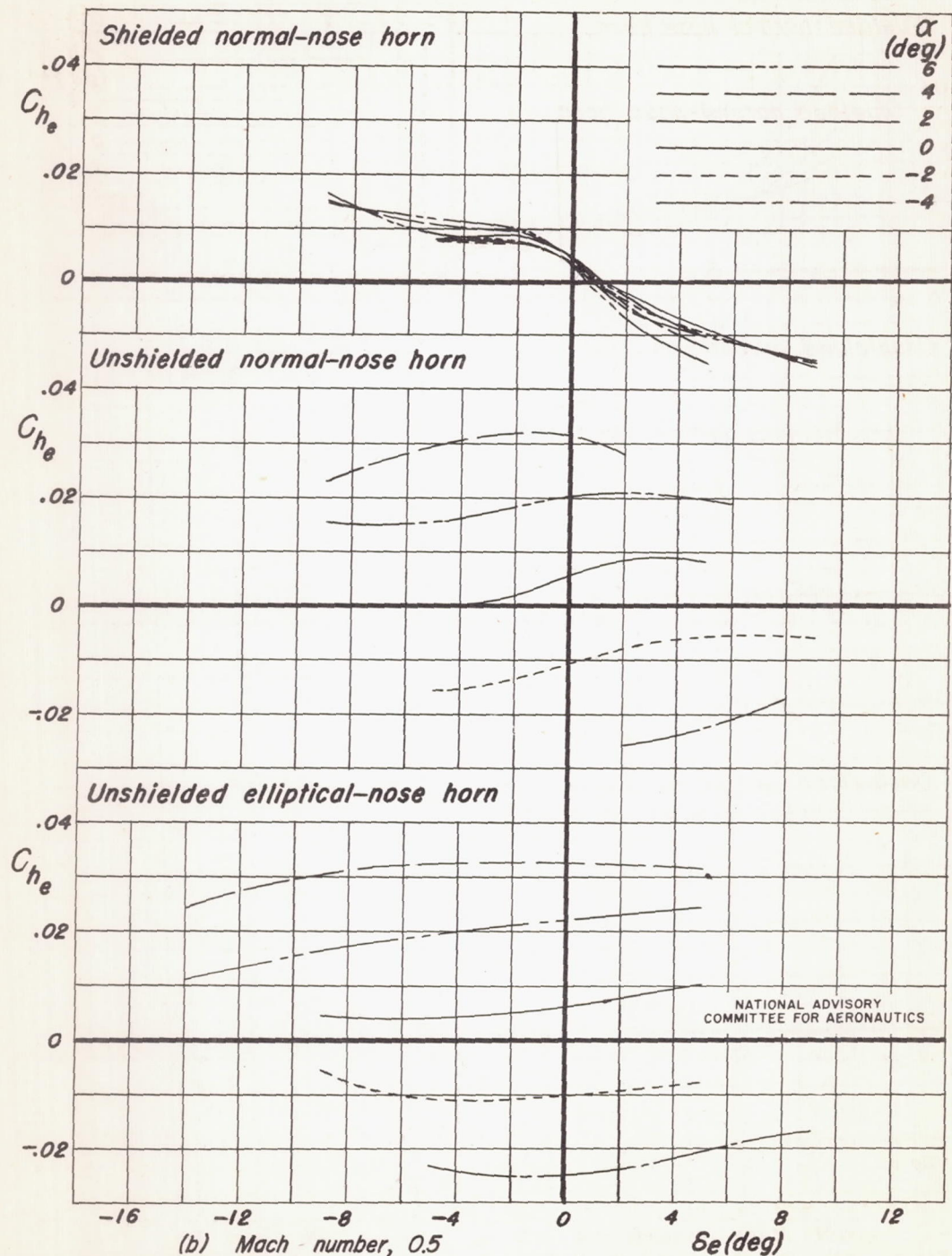


Figure 27. — Continued

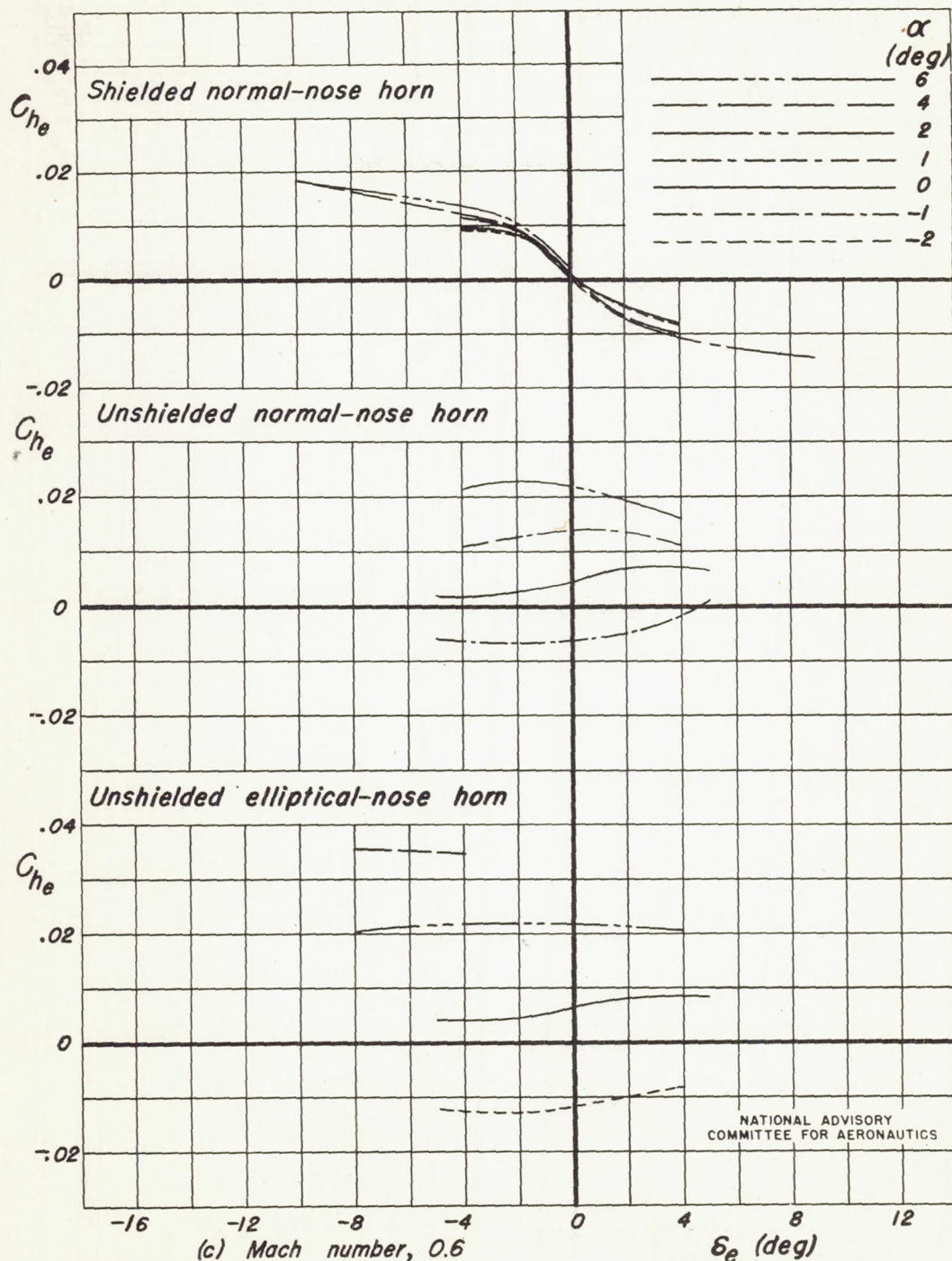


Figure 27. — Continued

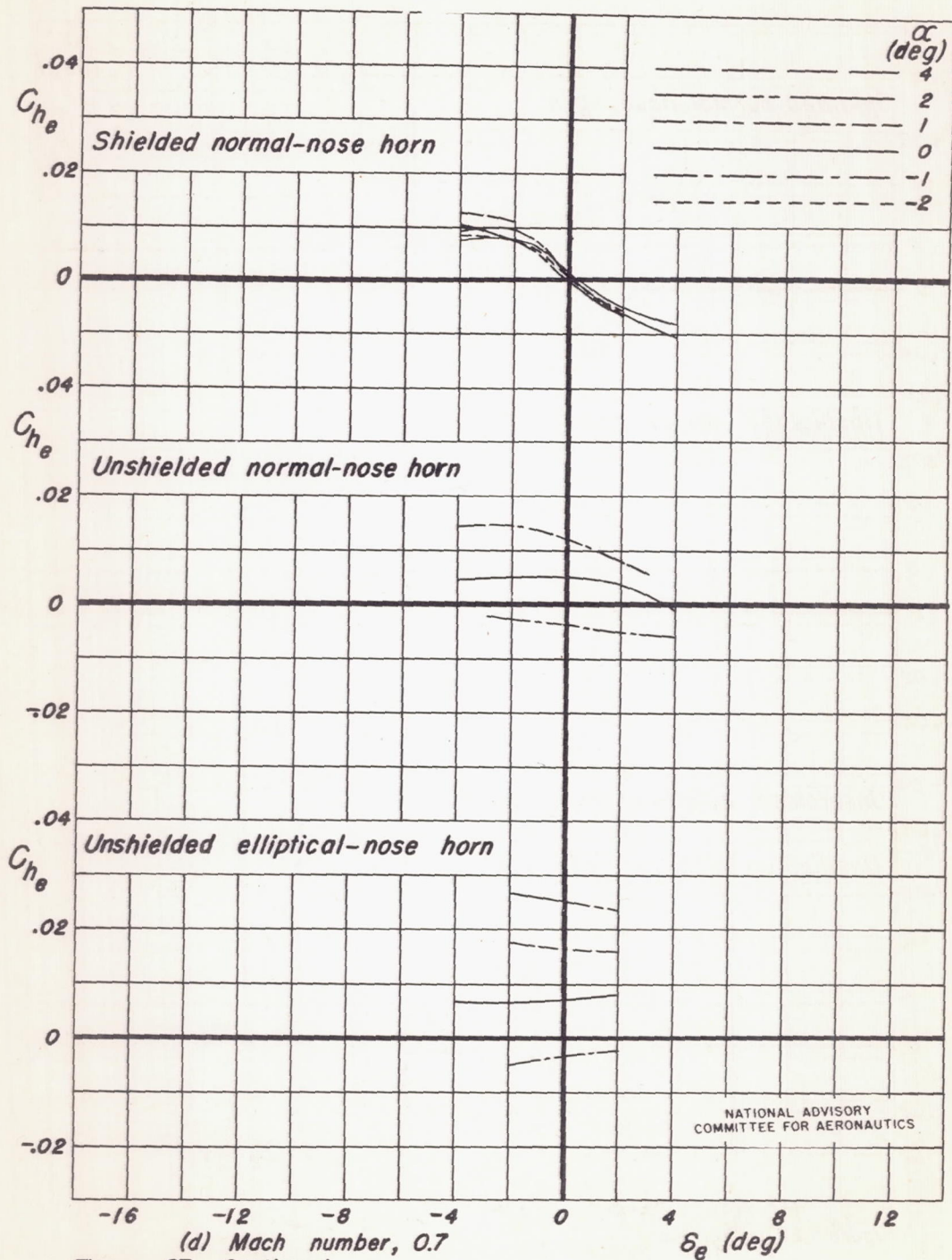
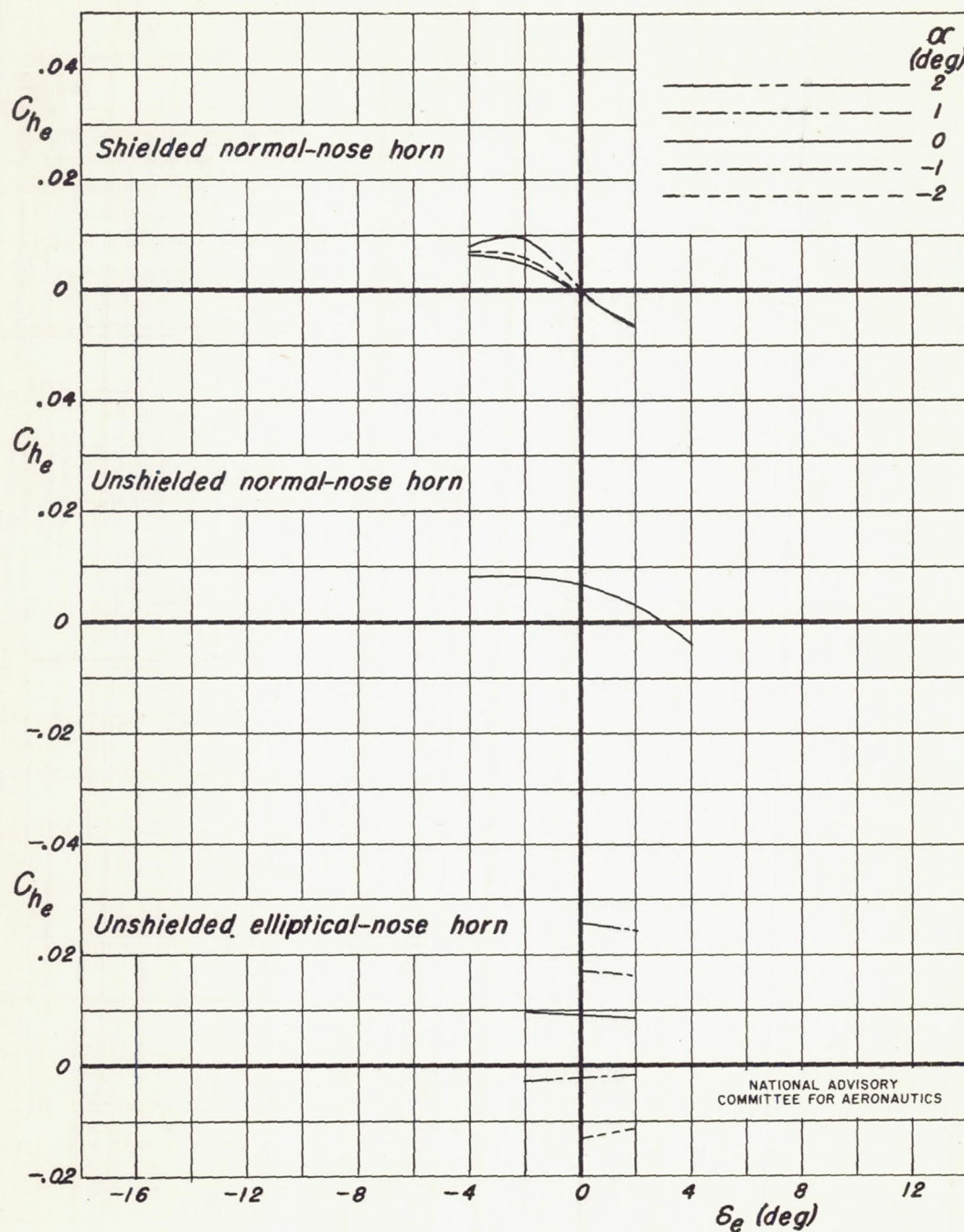
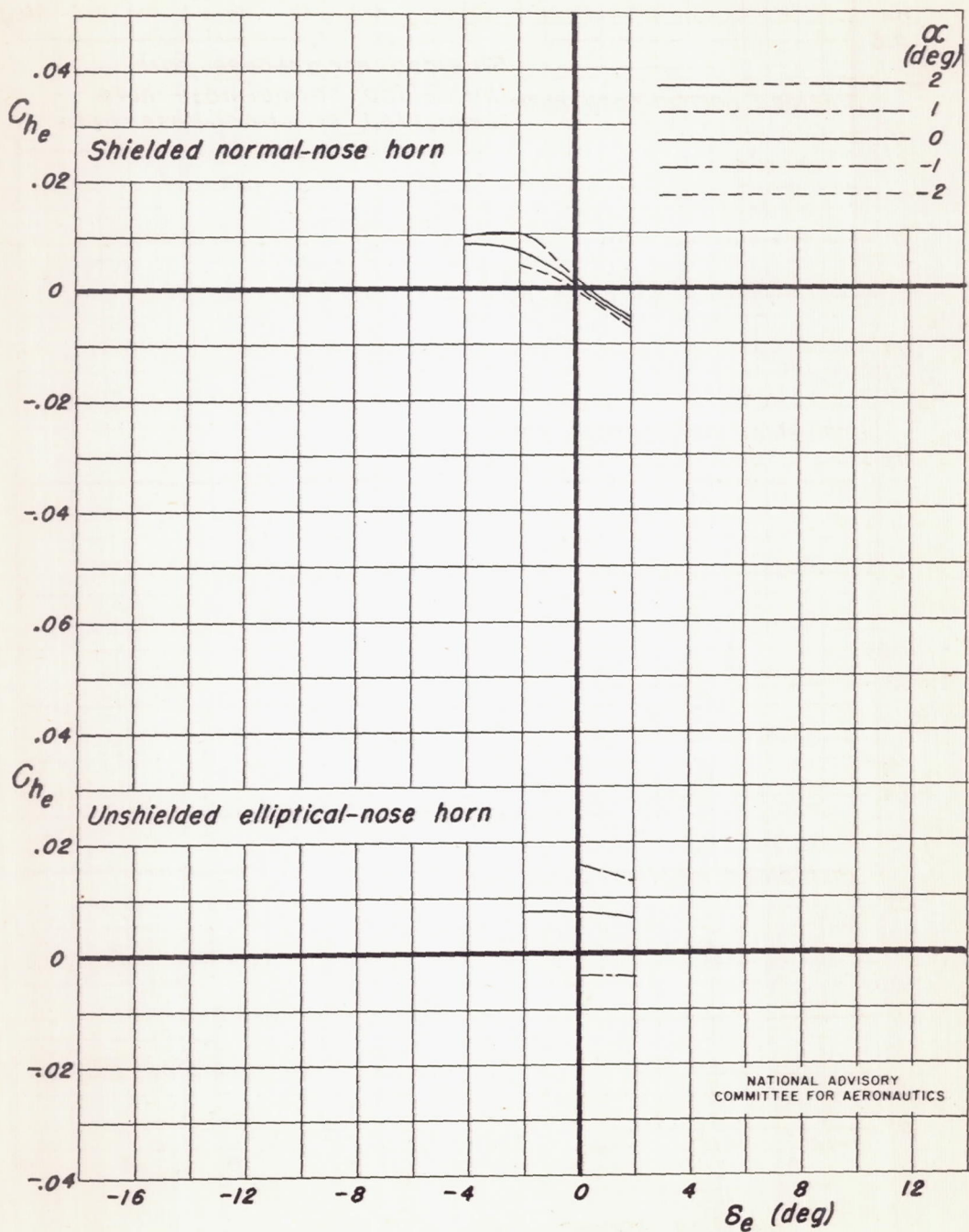


Figure 27.—Continued



(e) Mach number, 0.725  
Figure 27.—Continued



(f) Mach number, 0.75  
Figure 27.—Concluded

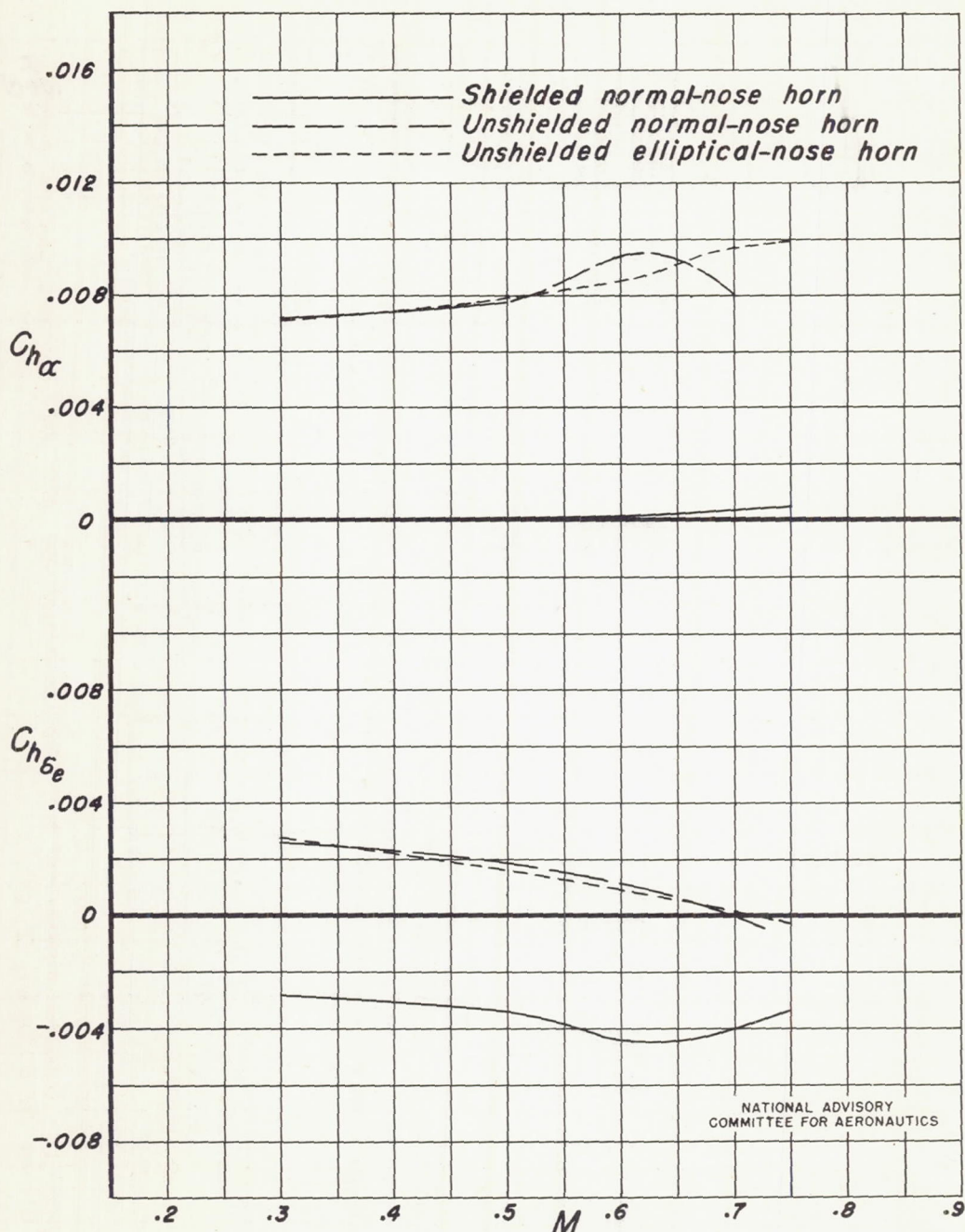
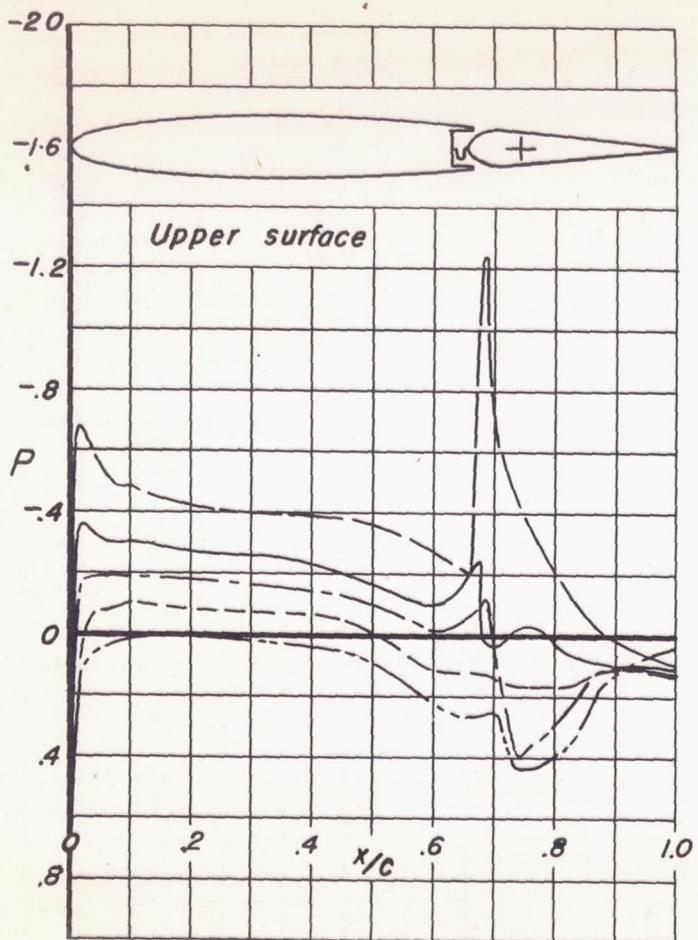
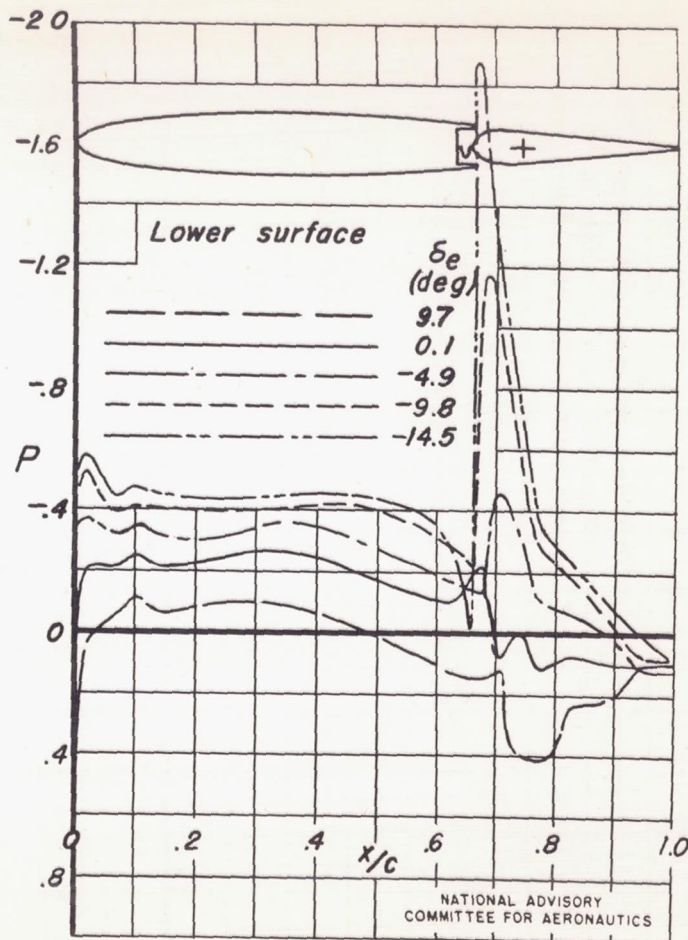


Figure 28.—Variation of elevator hinge-moment parameters with Mach number for the shielded and unshielded horn-balance elevators.

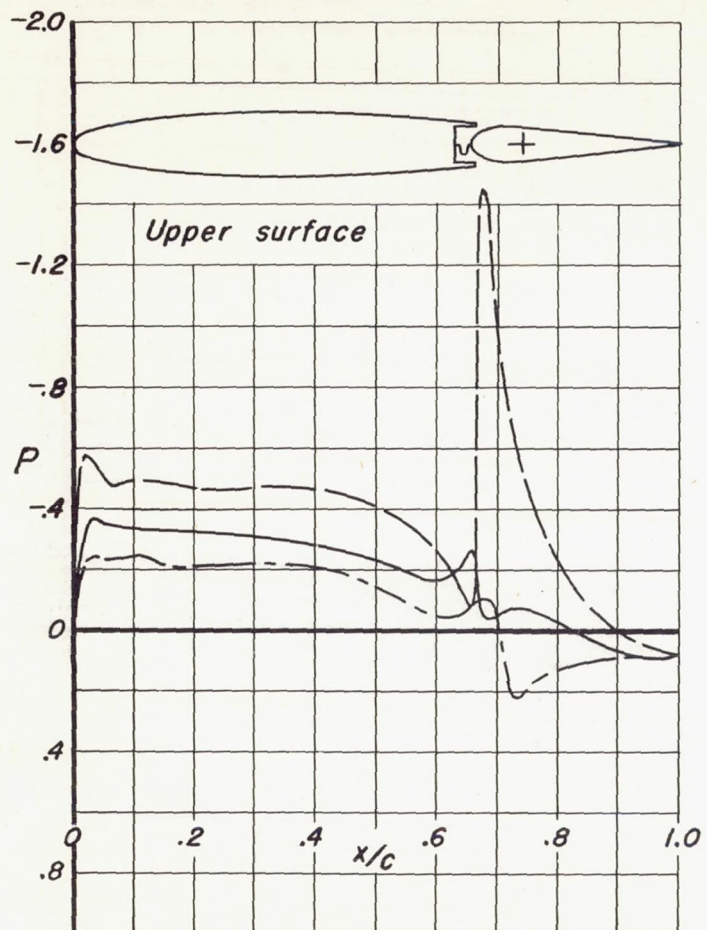


(a) Mach number, 0.30

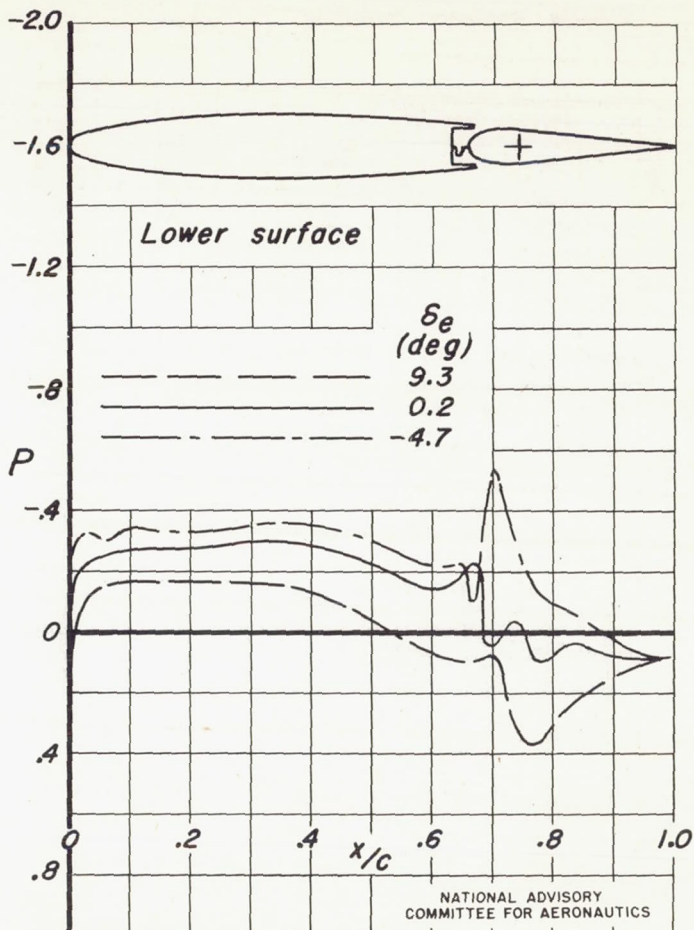
Figure 29.—Pressure distribution over the horizontal tail with the overhang-balance elevator.  
Station 52.6 inches;  $\alpha$ ,  $0^\circ$

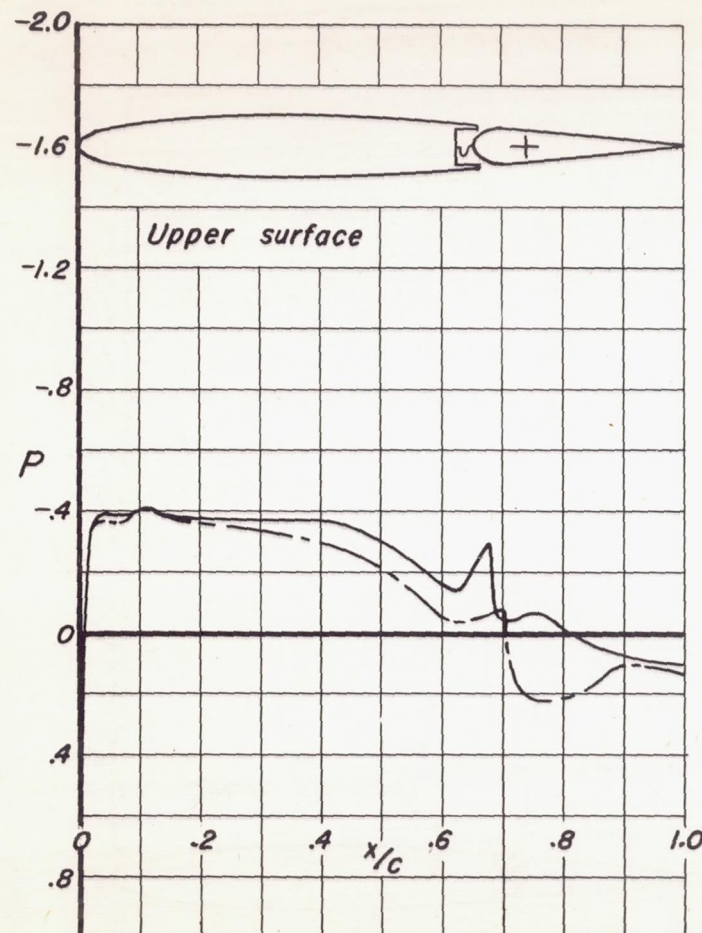


NATIONAL ADVISORY  
COMMITTEE FOR AERONAUTICS



(b) Mach number, 0.5  
Figure 29.-Continued





(c) Mach number, 0.7  
Figure 29.—Continued

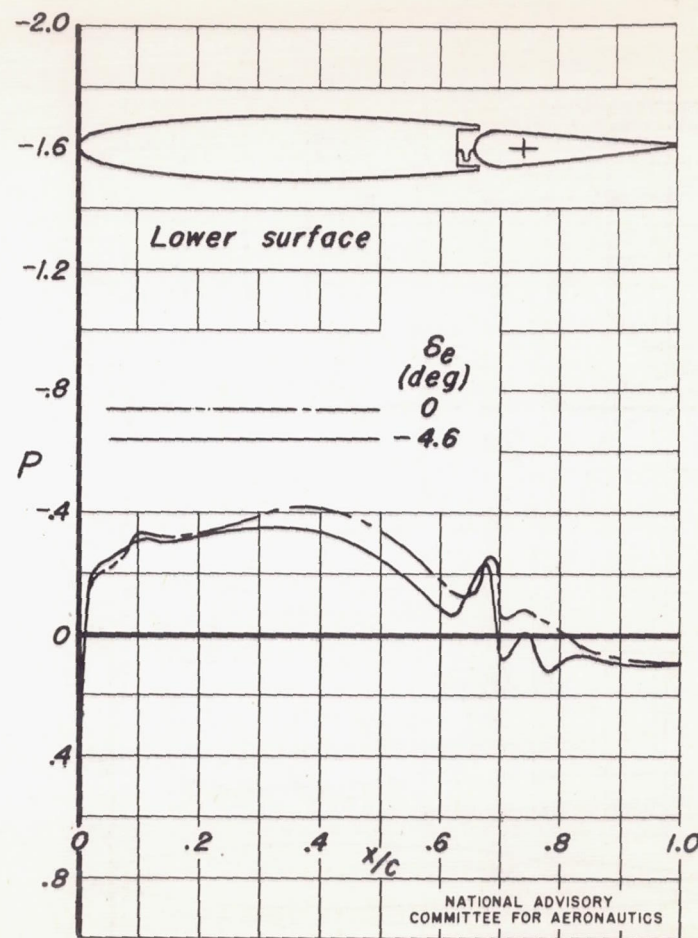
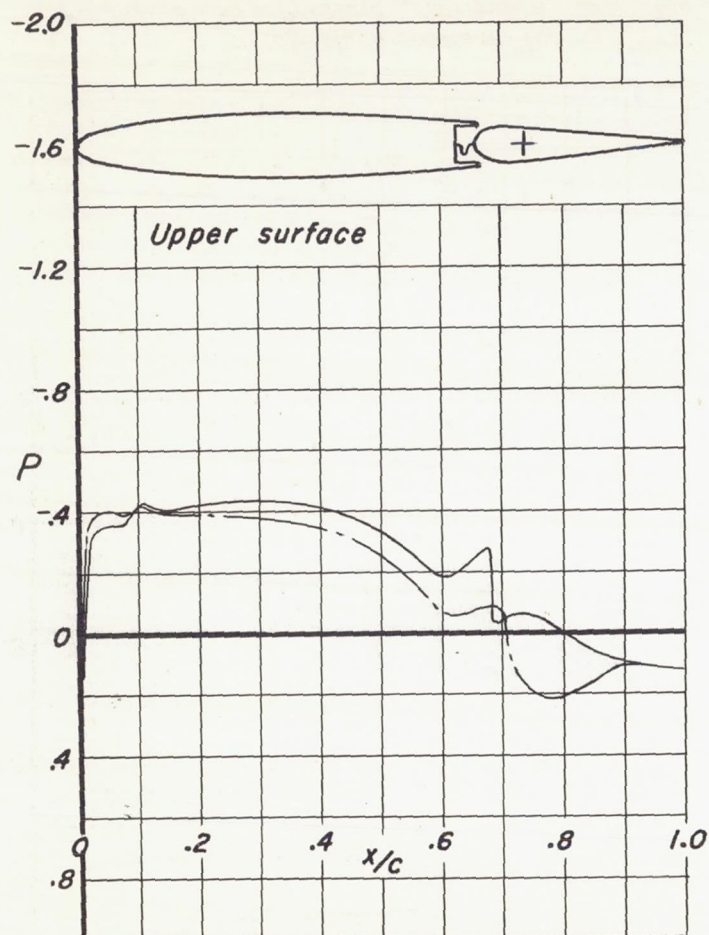
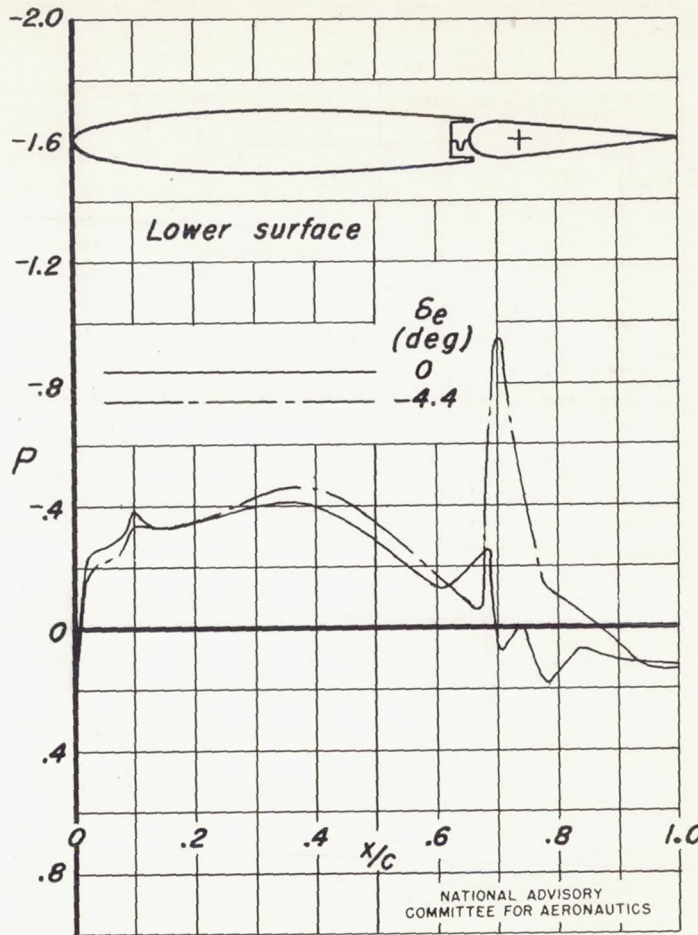


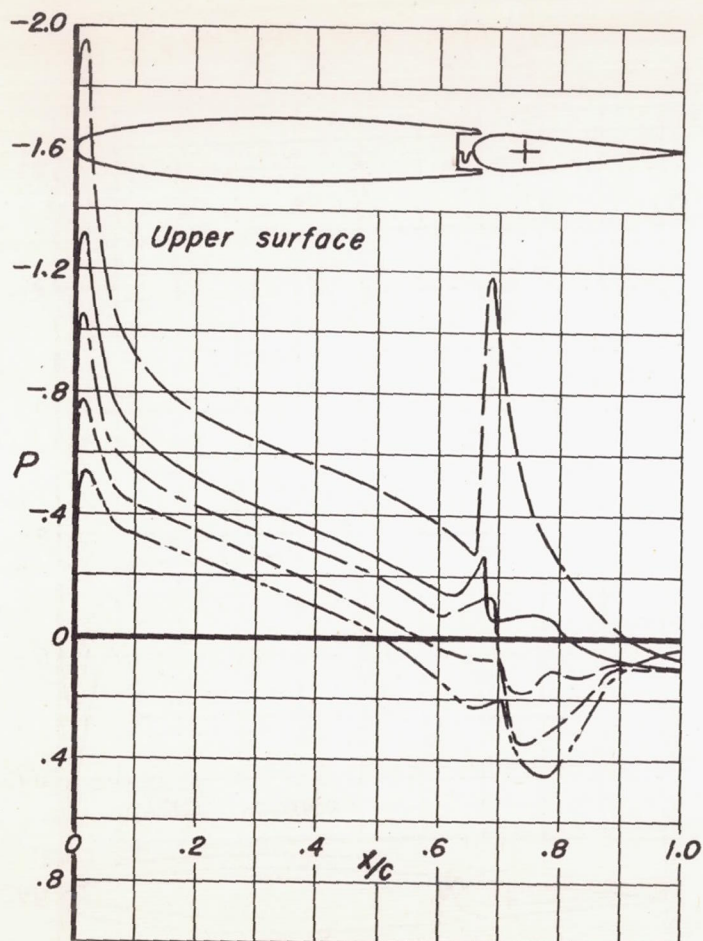
Fig. 29 d

NACA RM No. A7H29



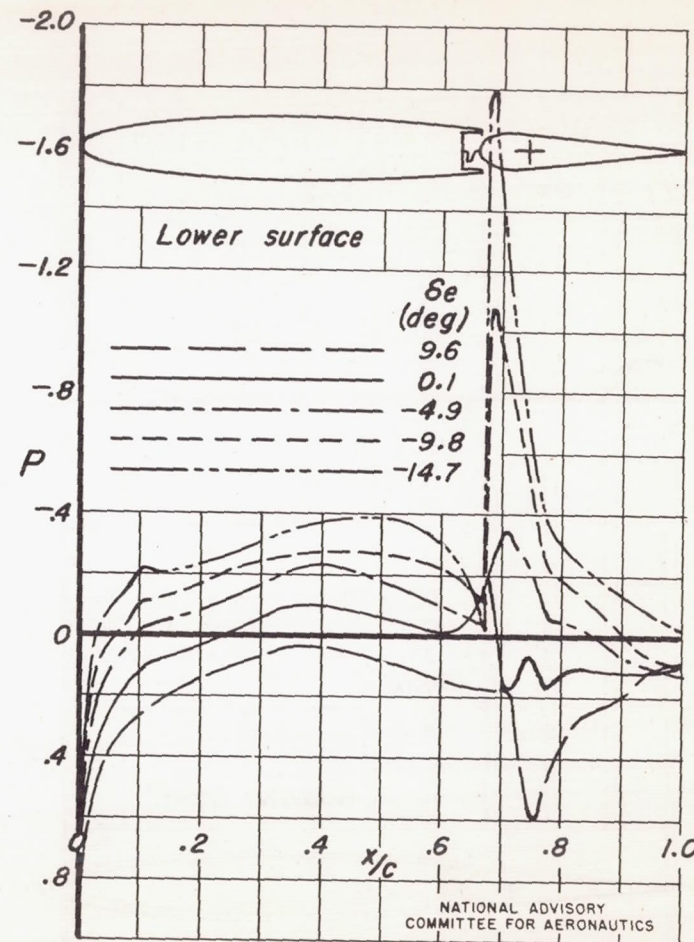
(d) Mach number, 0.75  
Figure 29.—Concluded





(a) Mach number, 0.3

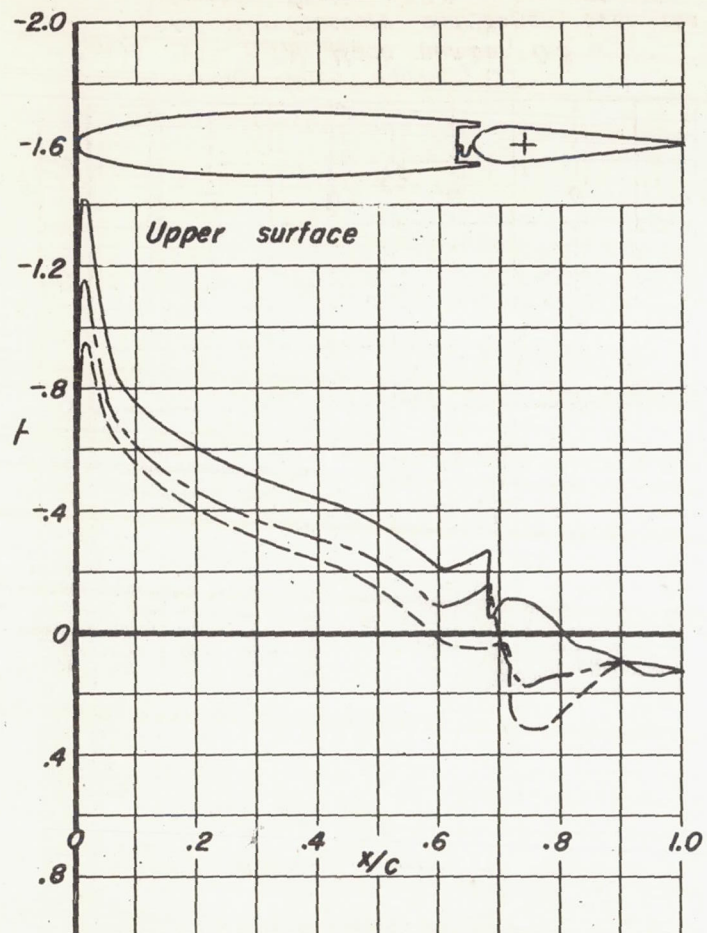
Figure 30.—Pressure distribution over the semispan horizontal tail with the overhang-balance elevator. Station 52.6; inches  $\alpha$ ,  $4^\circ$



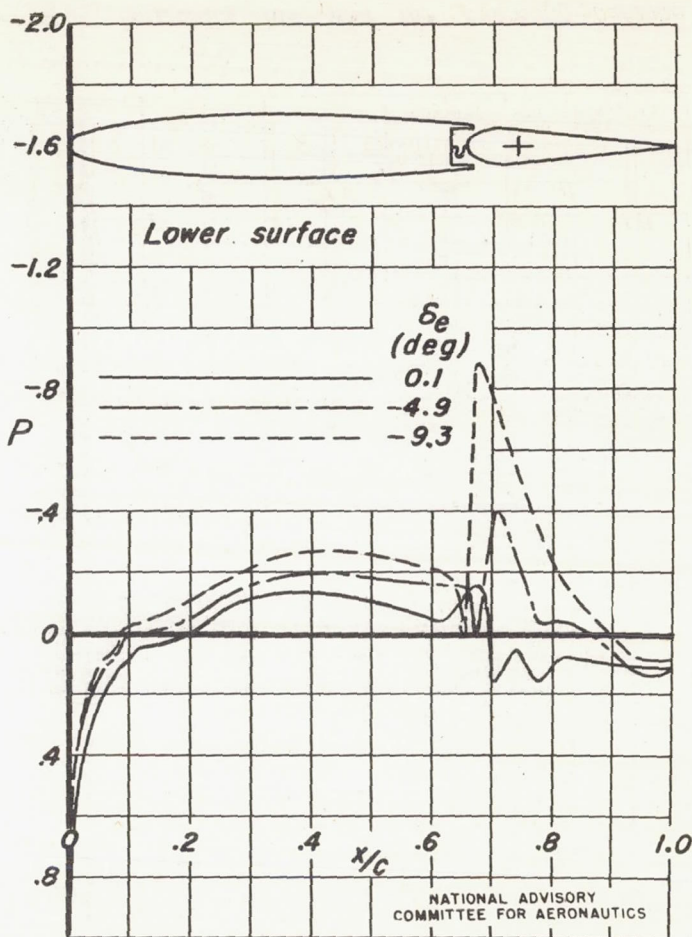
NATIONAL ADVISORY  
COMMITTEE FOR AERONAUTICS

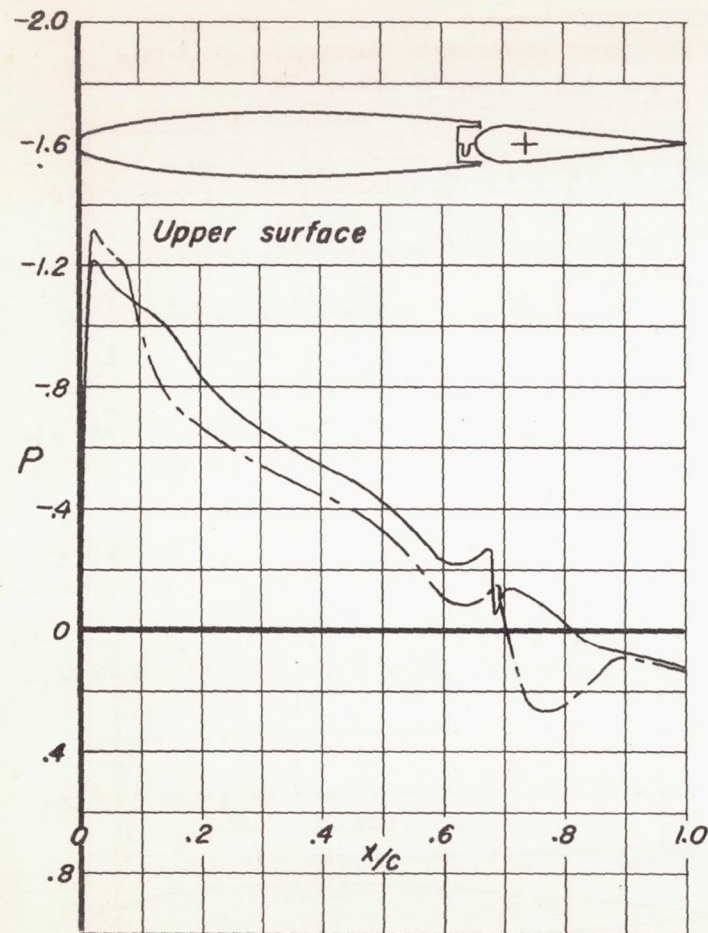
Fig. 30 b

NACA RM No. A7H29



(b) Mach number, 0.5  
Figure 30.—Continued





(c) Mach number, 0.7  
Figure 30.—Concluded

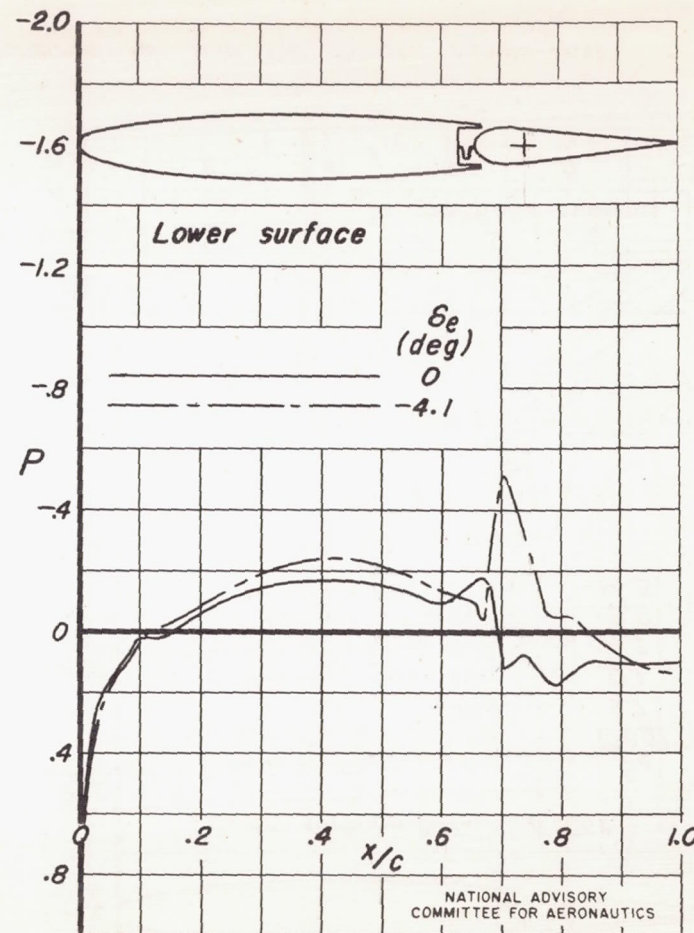
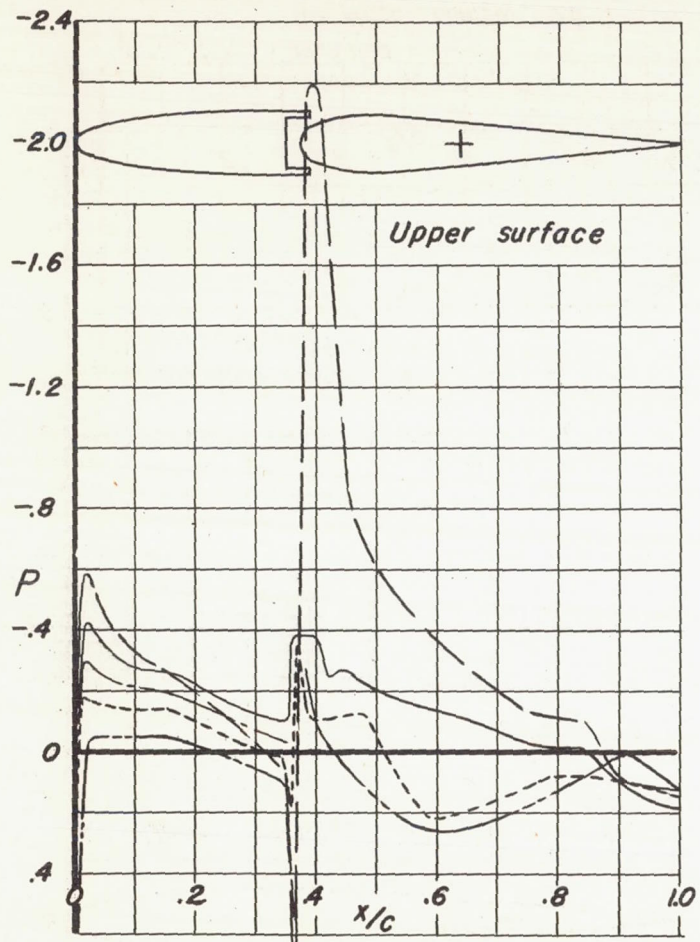


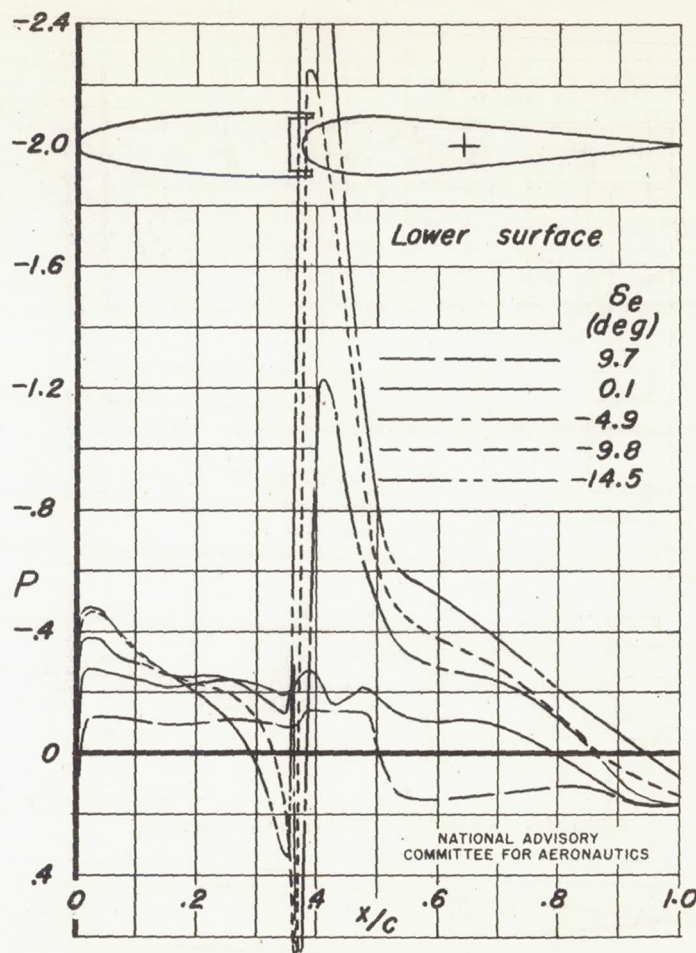
Fig. 31 a

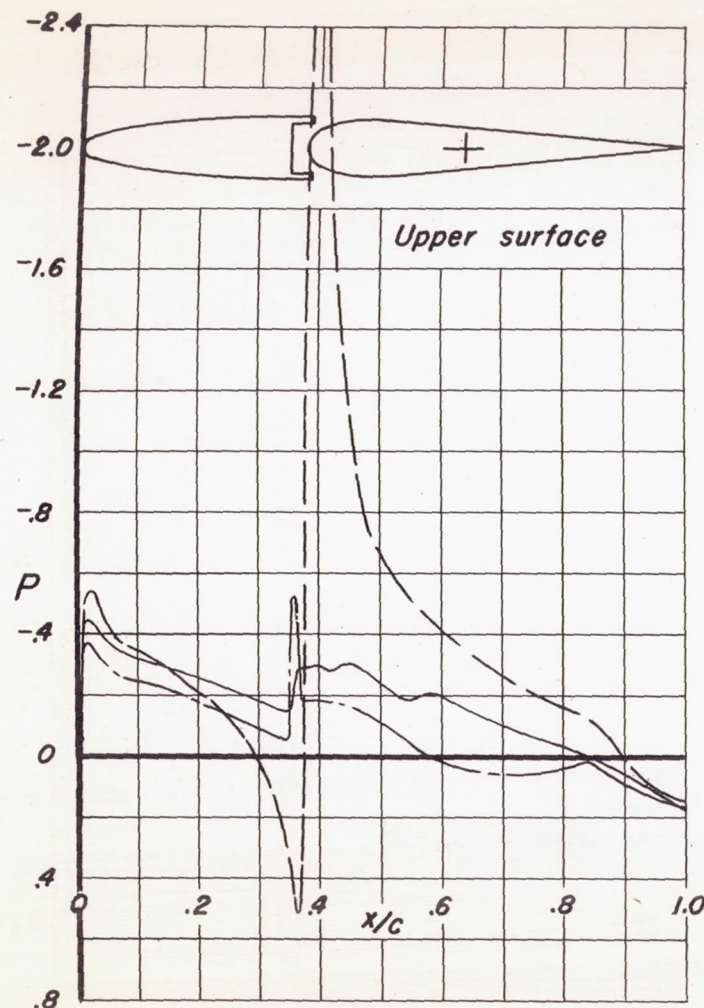
NACA RM No. A7H29



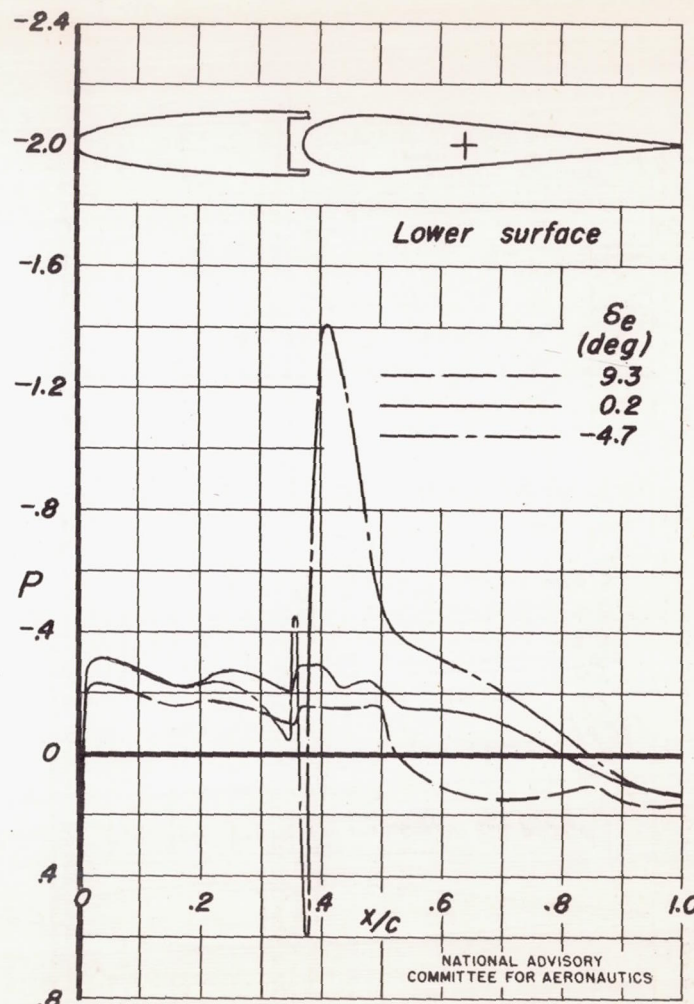
(a) Mach number, 0.3

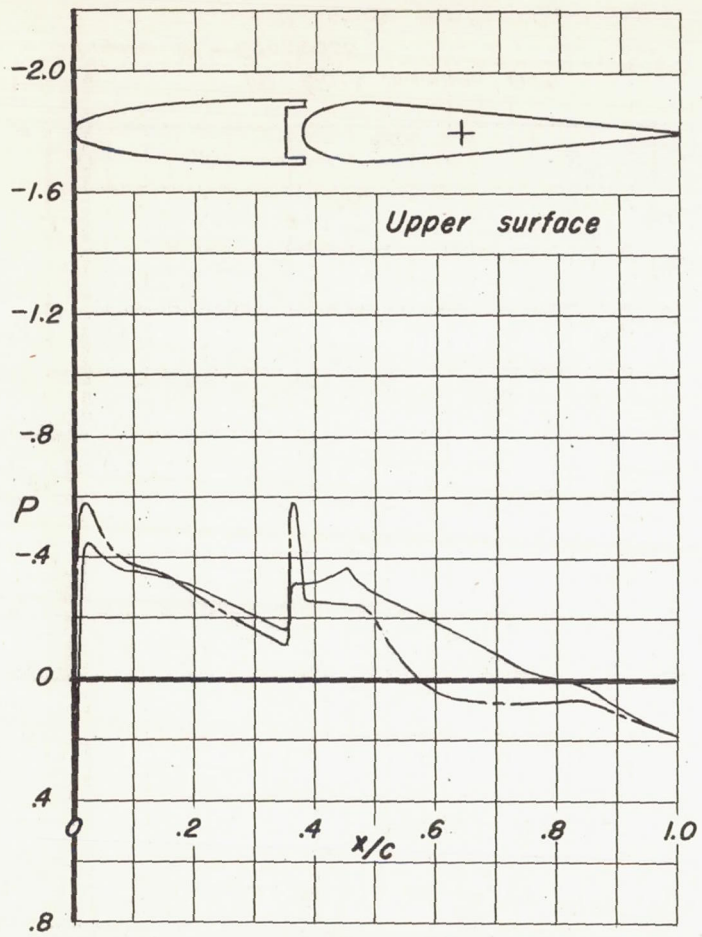
Figure 31.—Pressure distribution over the horizontal tail with the shielded normal-nose horn-balance elevator. Station 108.0 inches;  $\alpha$ ,  $0^\circ$



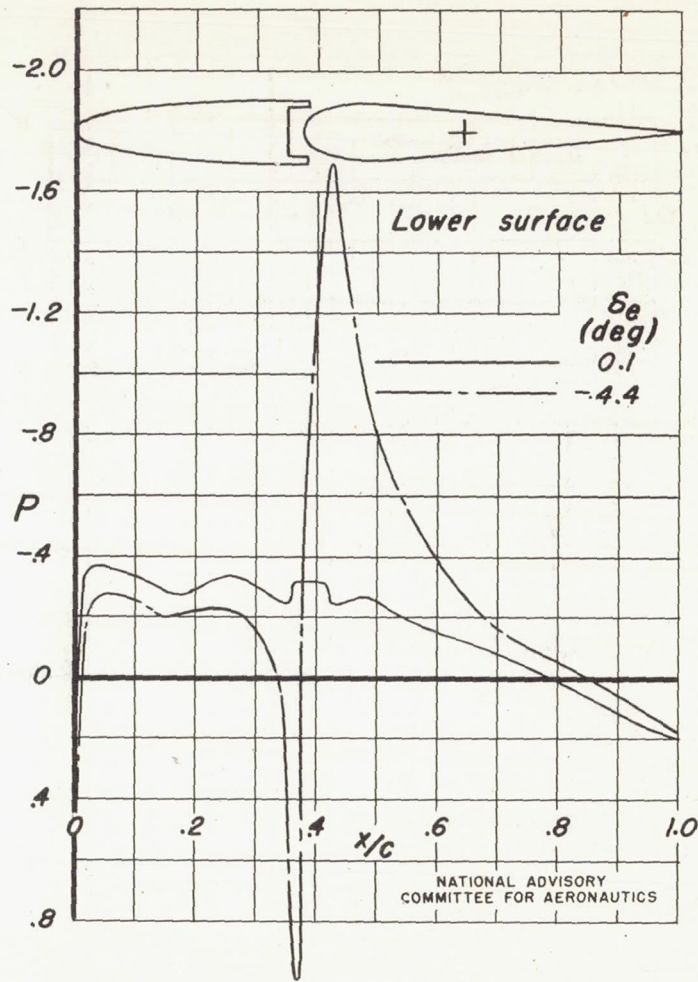


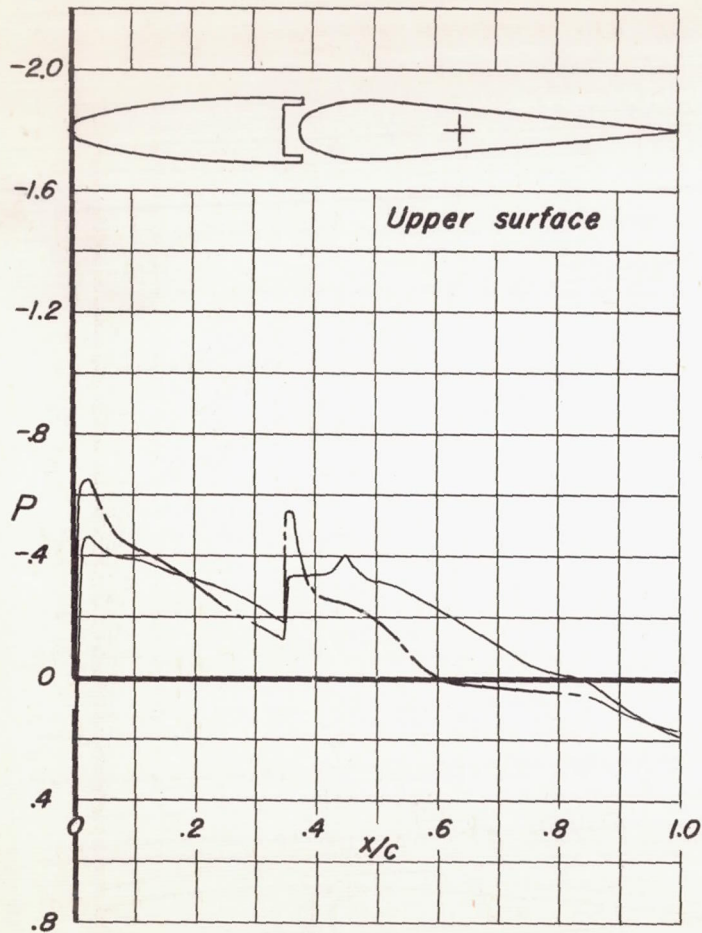
(b) Mach number, 0.5  
Figure 31.—Continued



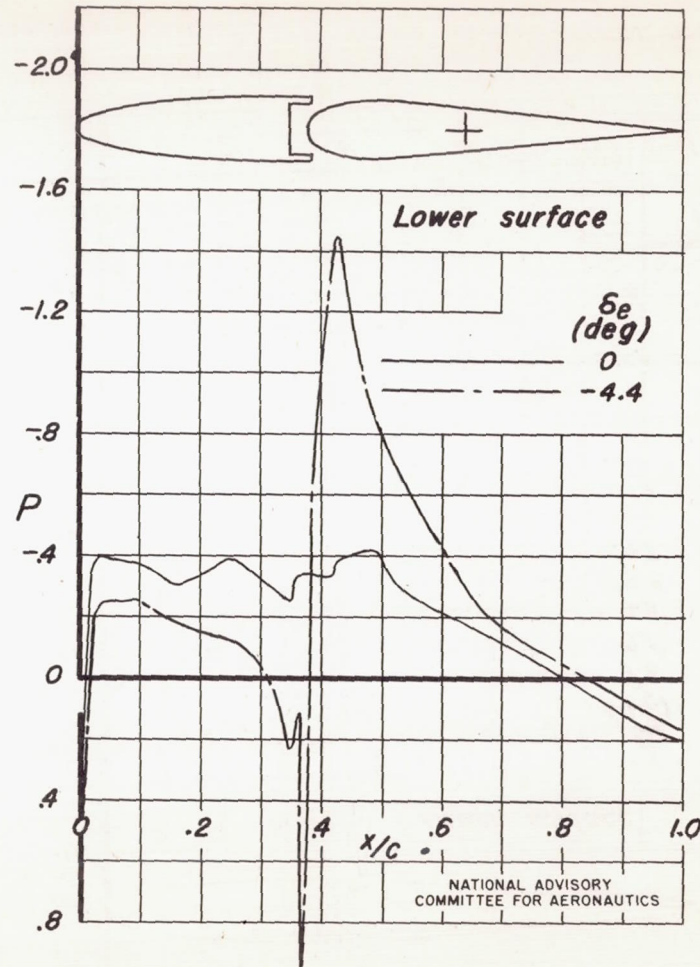


(c) Mach number, 0.7  
Figure 31.—Continued





(d) Mach number, 0.75  
Figure 31.—Concluded



NATIONAL ADVISORY  
COMMITTEE FOR AERONAUTICS

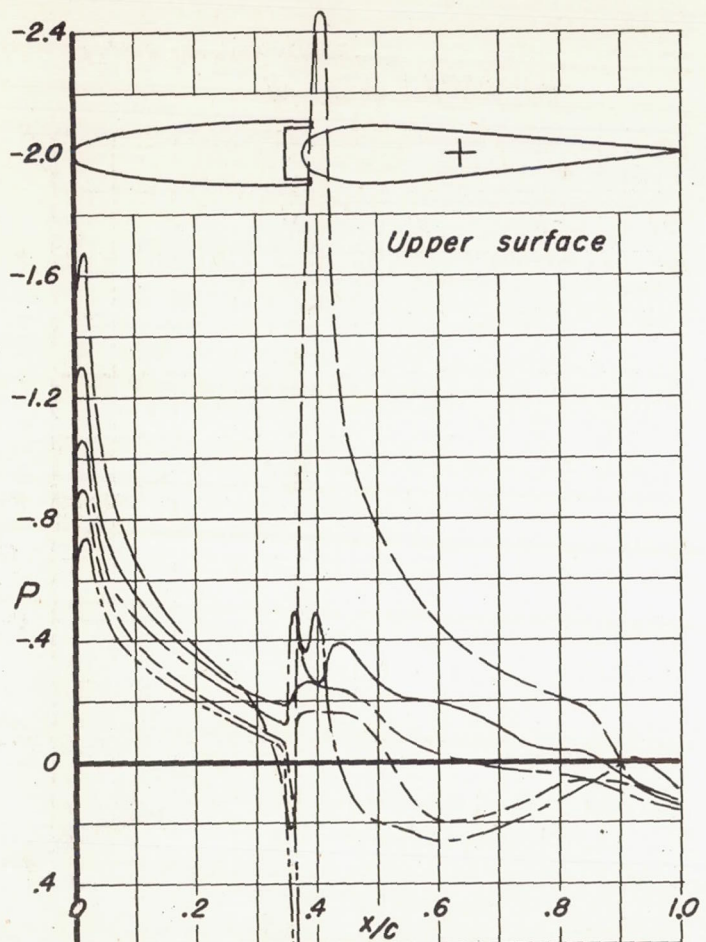
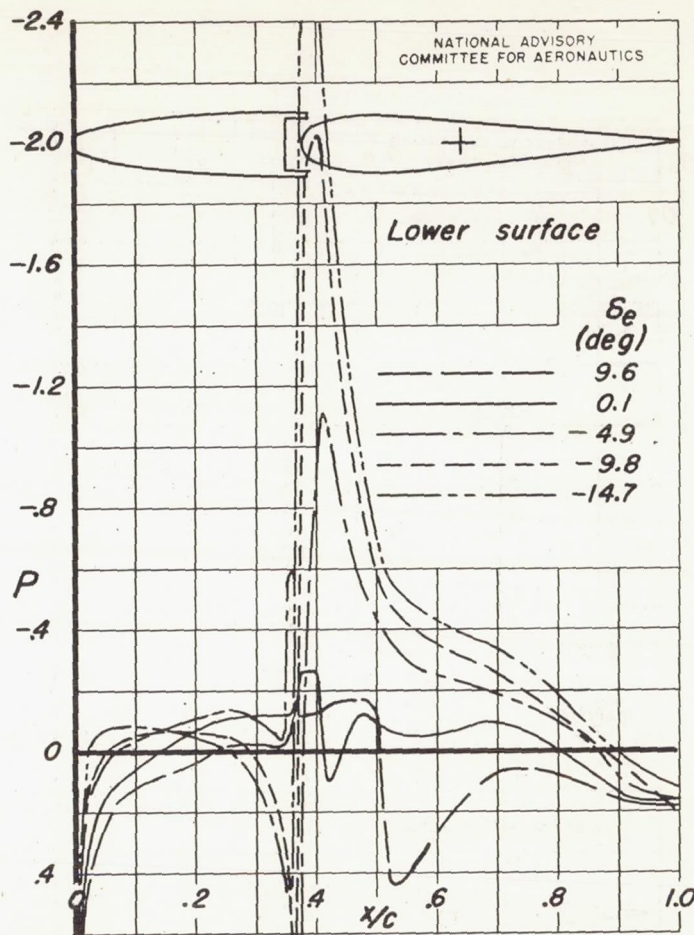
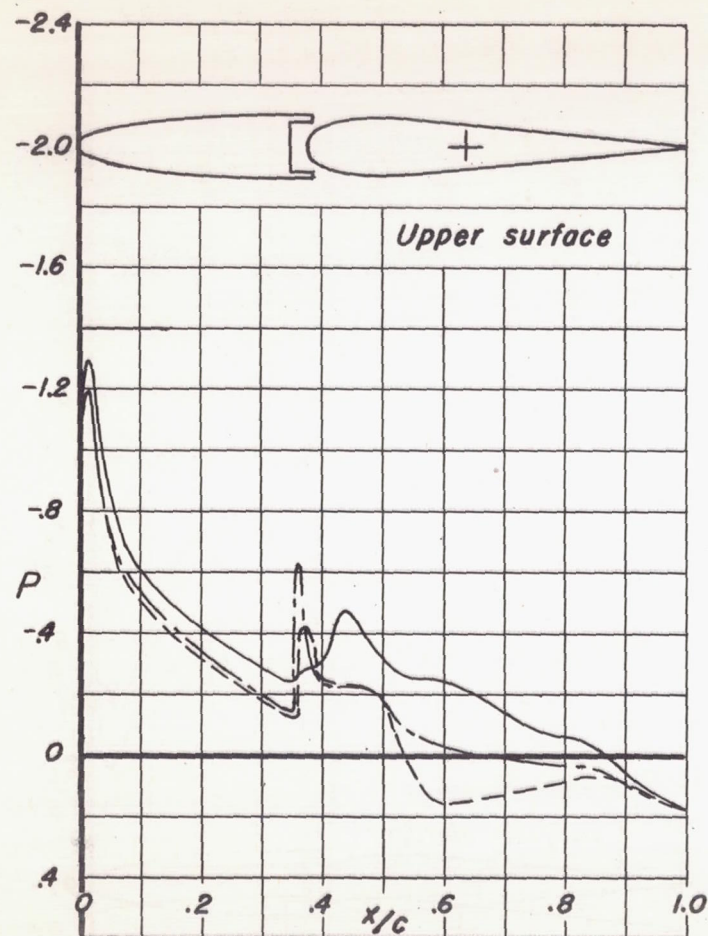


Figure 32.—Pressure distribution over the semispan horizontal tail of the shielded normal-nose horn-balance elevator. Station 108.0 inches;  $\alpha$ ,  $4^\circ$





(b) Mach number, 0.5  
Figure 32.—Continued

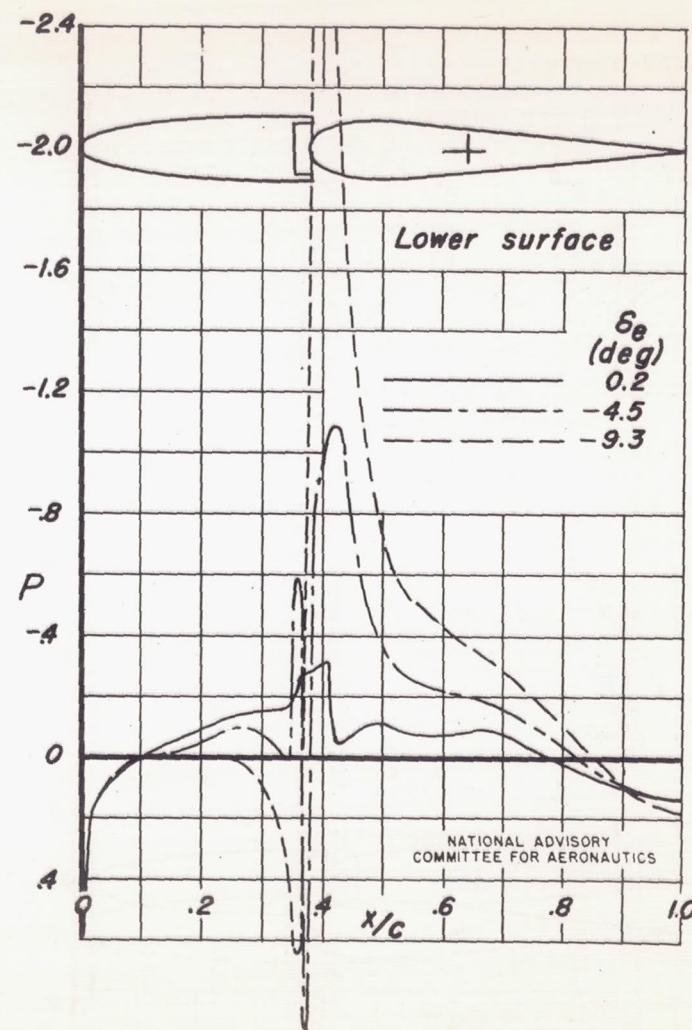
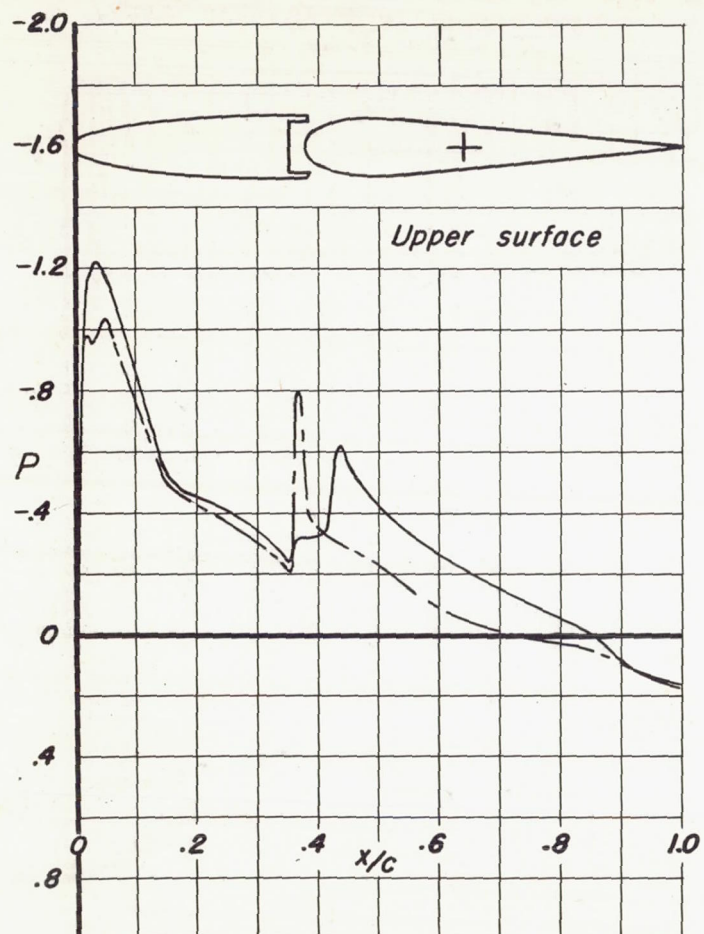
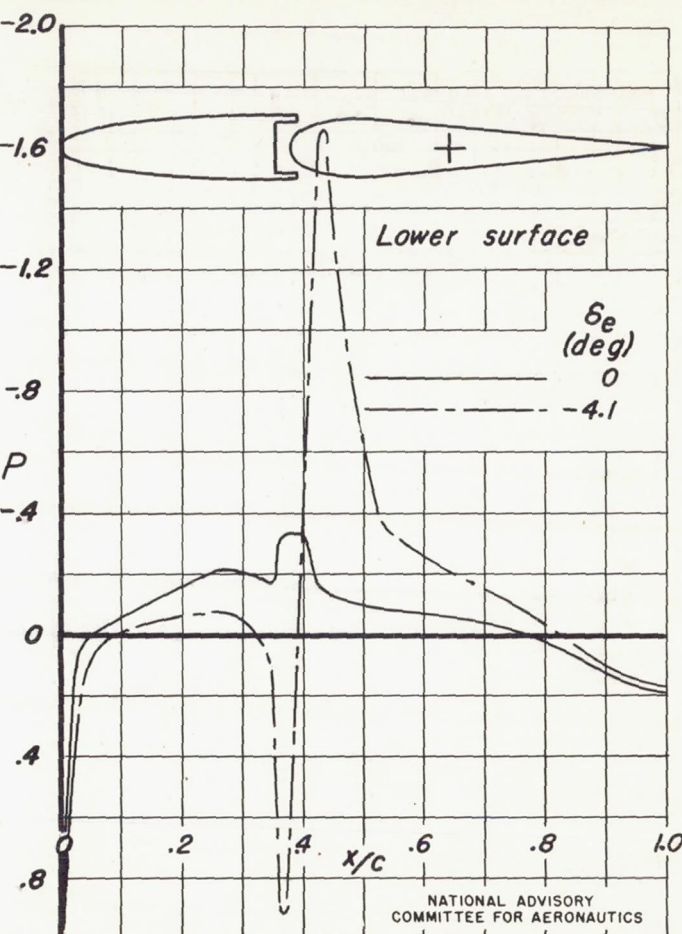


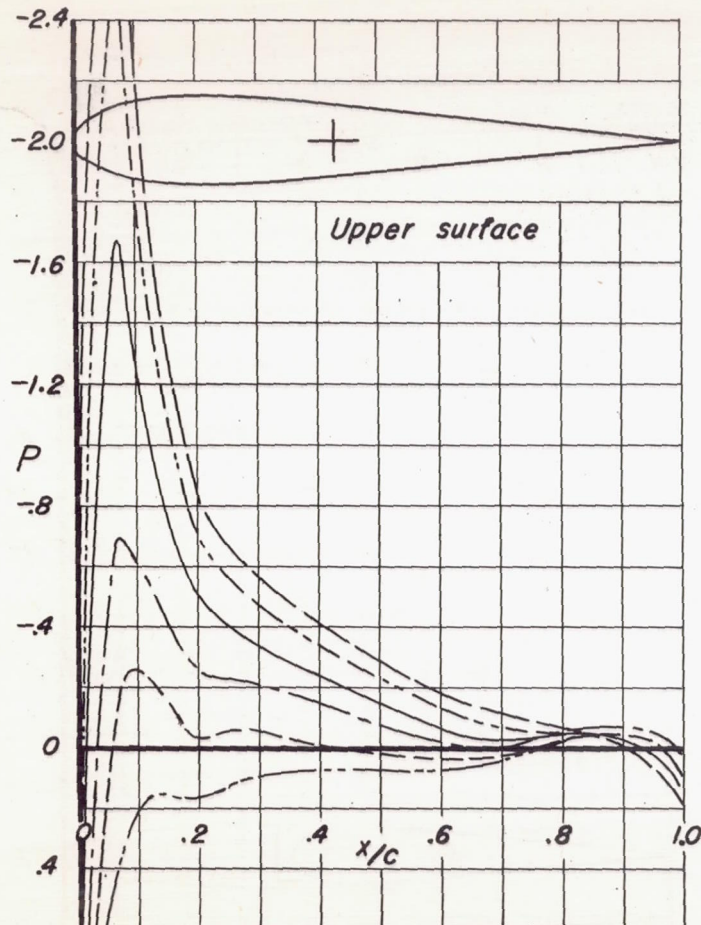
Fig. 32 c

NACA RM No. A7H29



(c) Mach number, 0.7  
Figure 32.—Concluded





(a) Mach number, 0.3

Figure 33.—Pressure distribution over the semispan horizontal tail with the unshielded normal-nose horn-balance elevator. Station 108.0 inches;  $\alpha_c$ ,  $0^\circ$

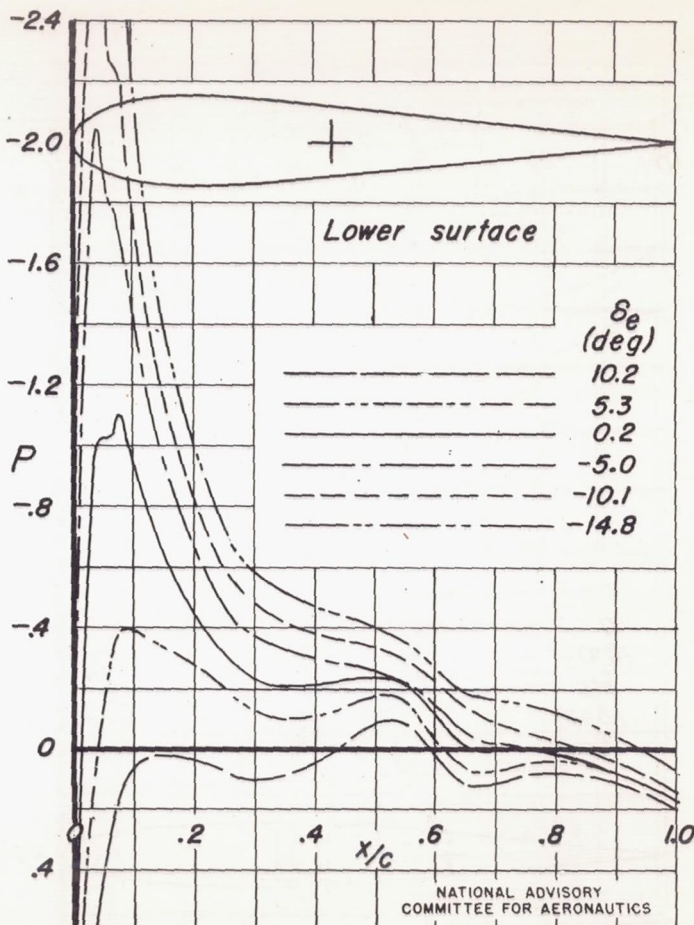
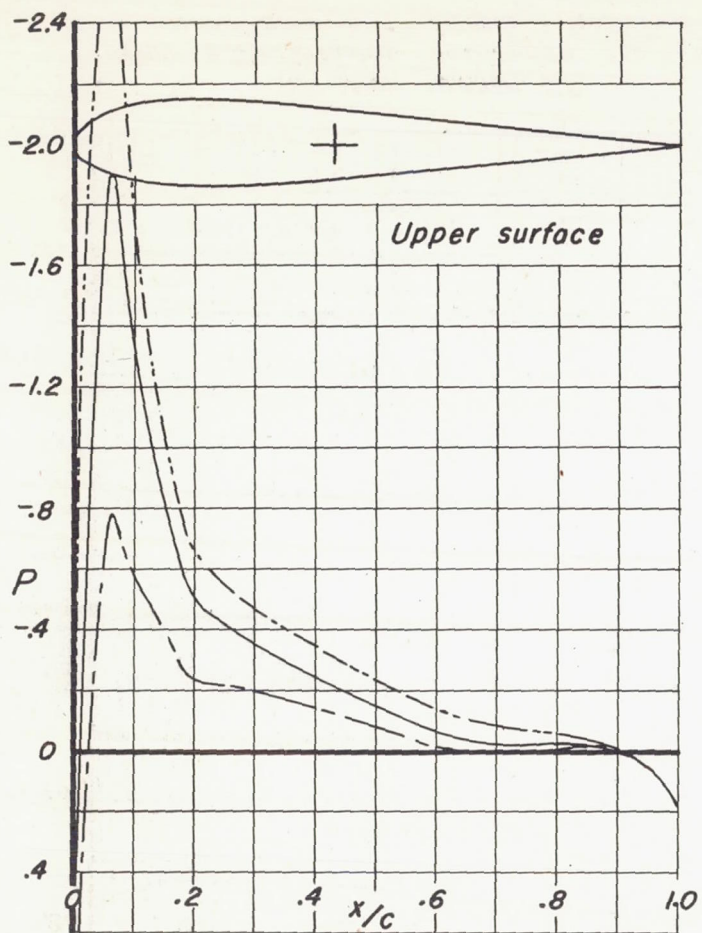
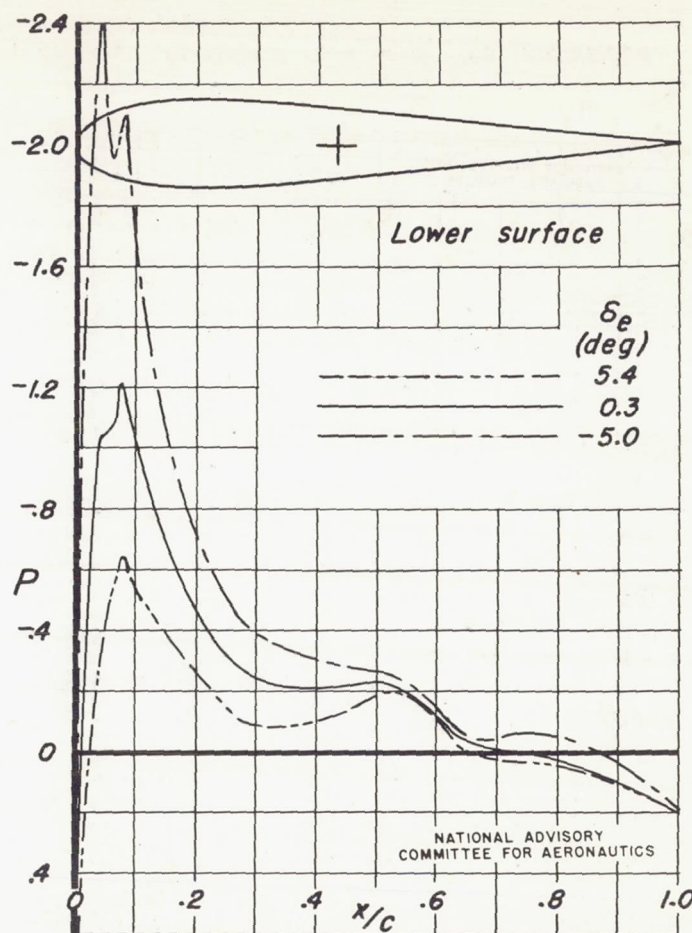


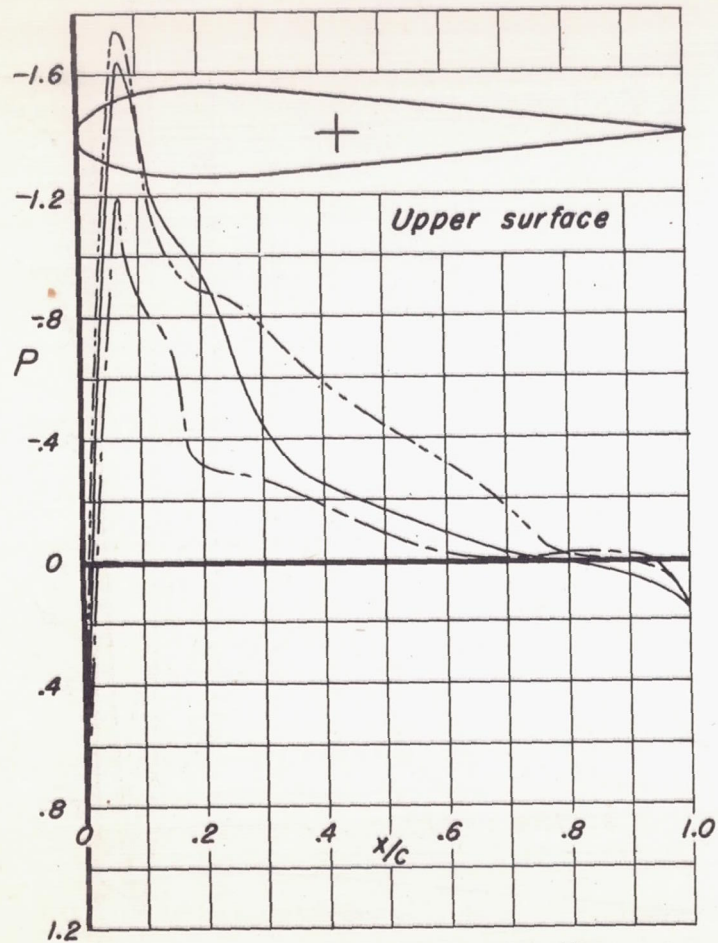
Fig. 33 b

NACA RM No. A7H29



(b) Mach number, 0.5  
Figure 33.—Continued





(c) Mach number, 0.7  
Figure 33.—Continued

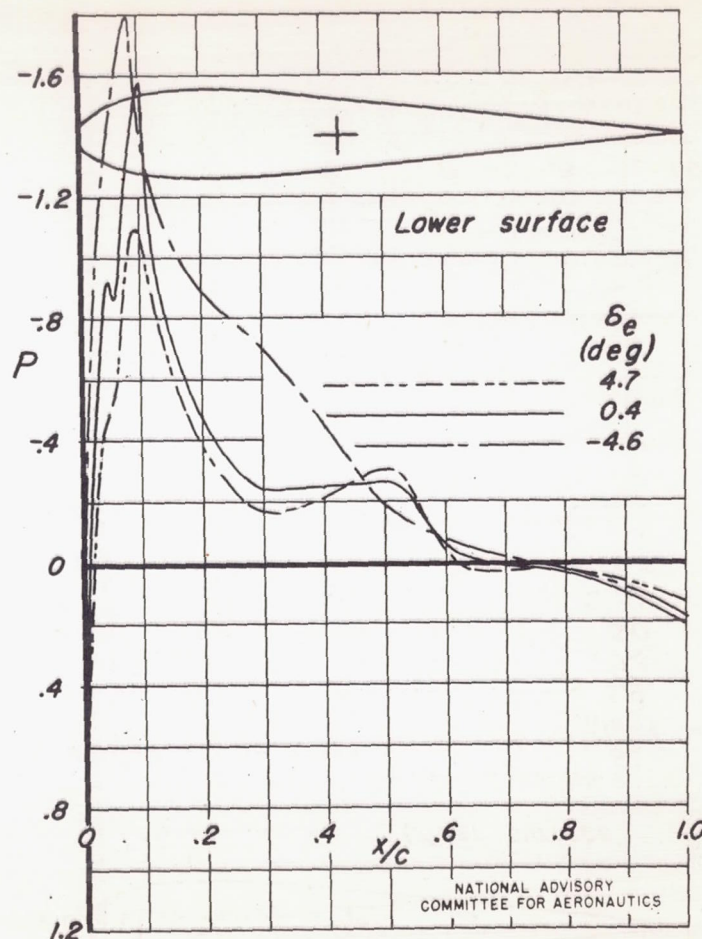
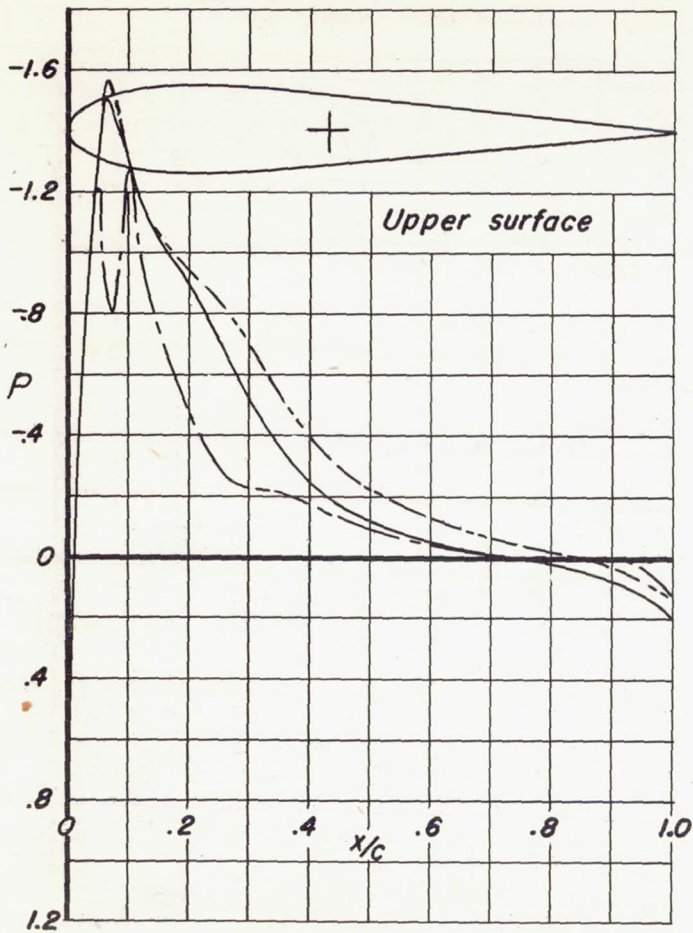
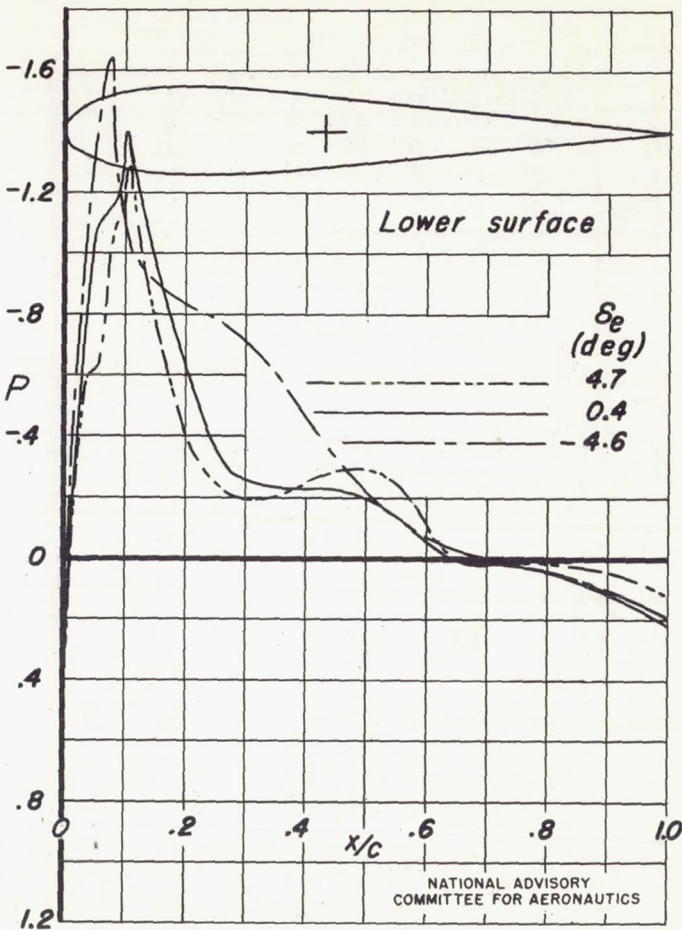


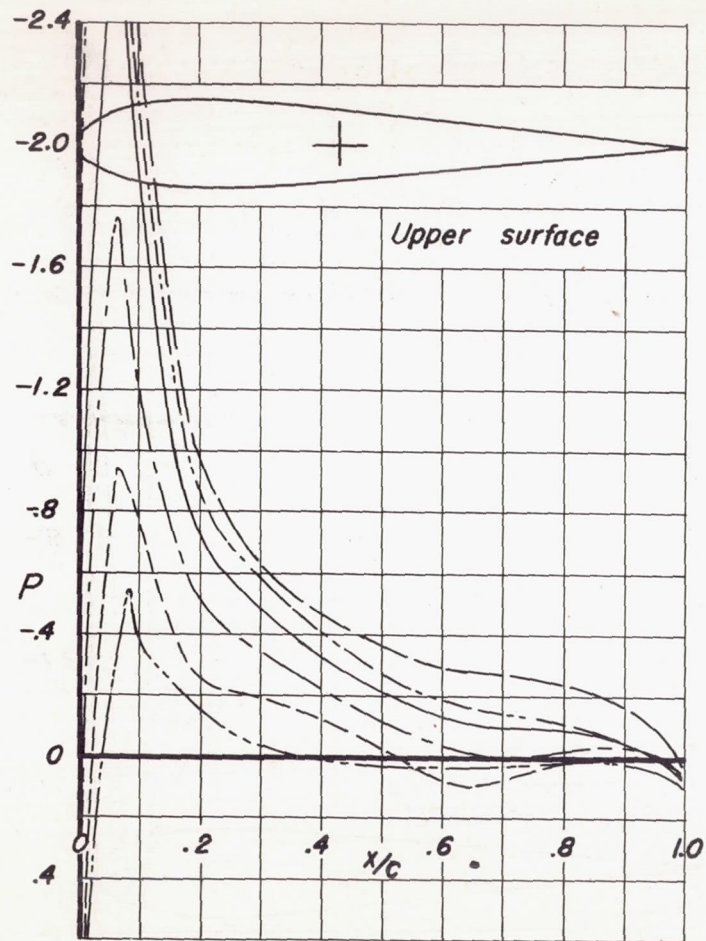
Fig. 33 d

NACA RM No. A7H29



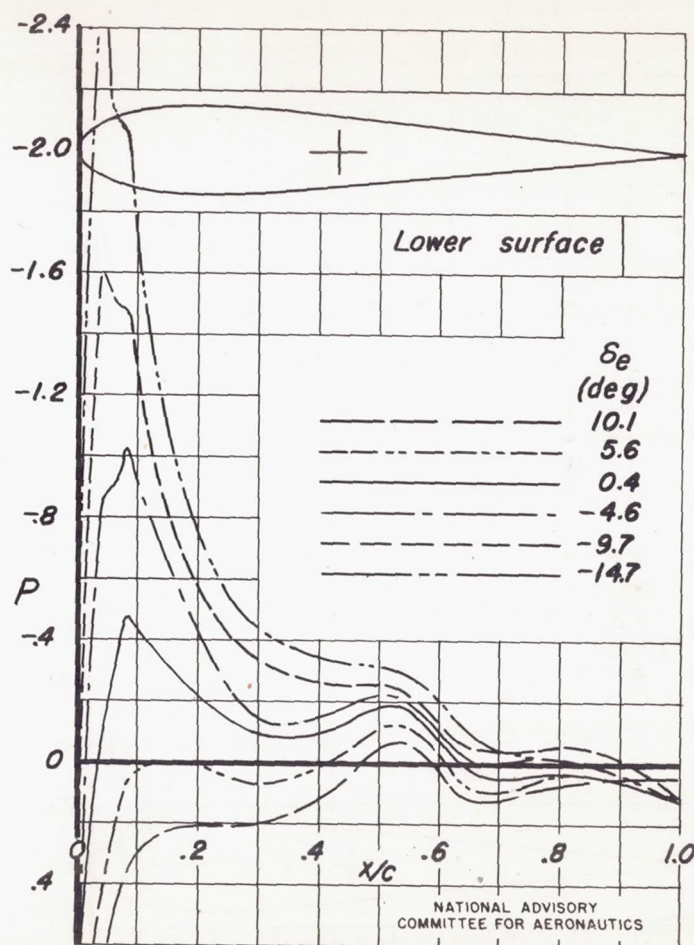
(d) Mach number, 0.725  
Figure 33.—Concluded





(a) Mach number, 0.3

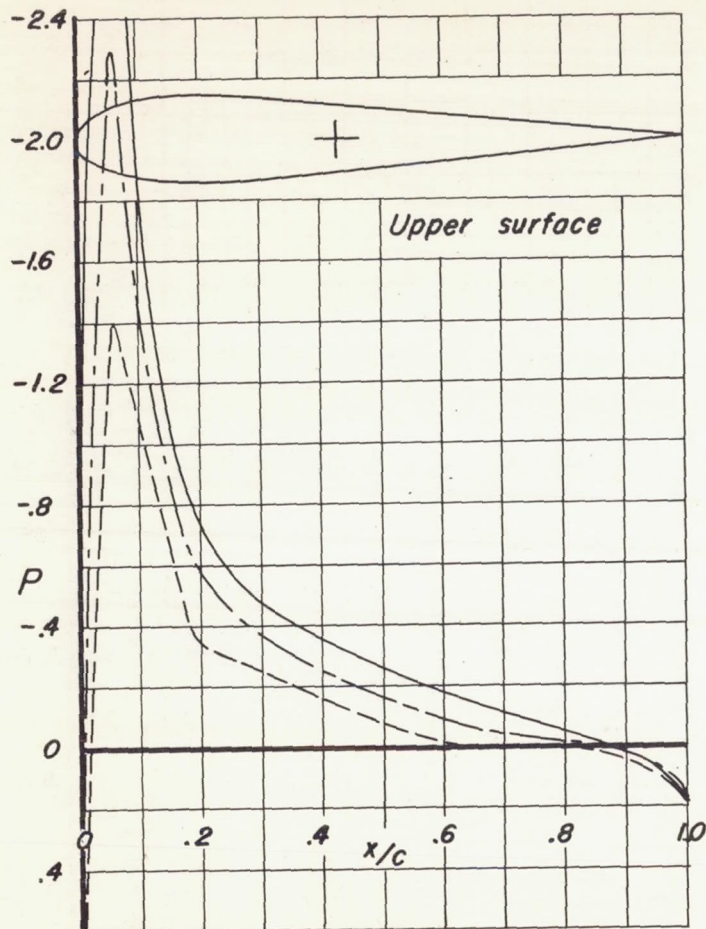
Figure 34.—Pressure distribution over the semispan horizontal tail with the unshielded normal-nose horn-balance elevator. Station 108.0 inches;  $\alpha$ ,  $4^\circ$



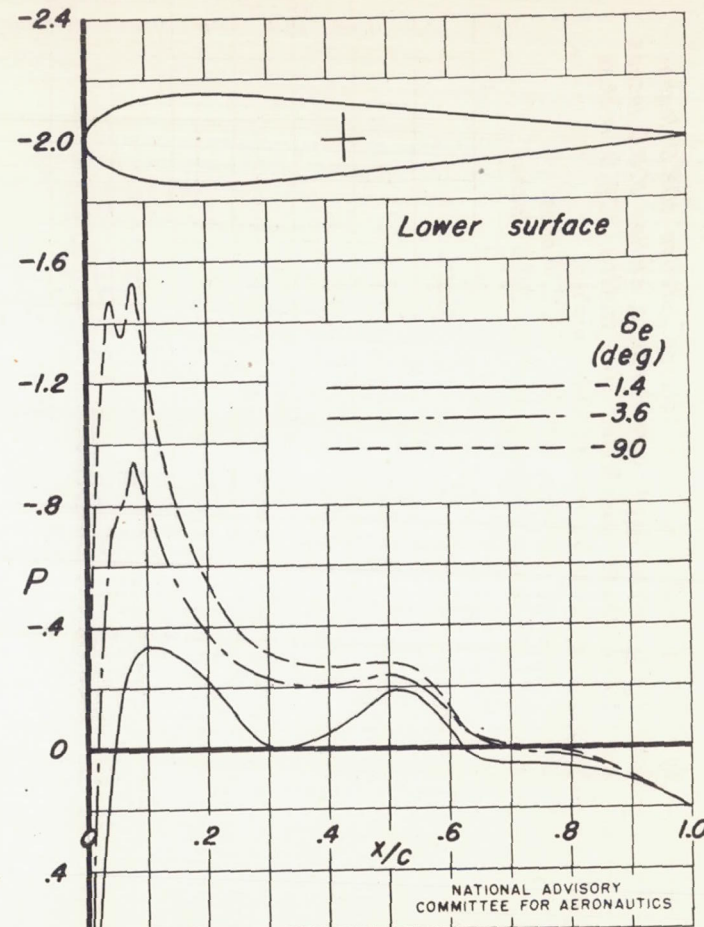
NATIONAL ADVISORY  
COMMITTEE FOR AERONAUTICS

Fig. 34 b

NACA RM No. A7H29



(b) Mach number, 0.5  
Figure 34.—Concluded



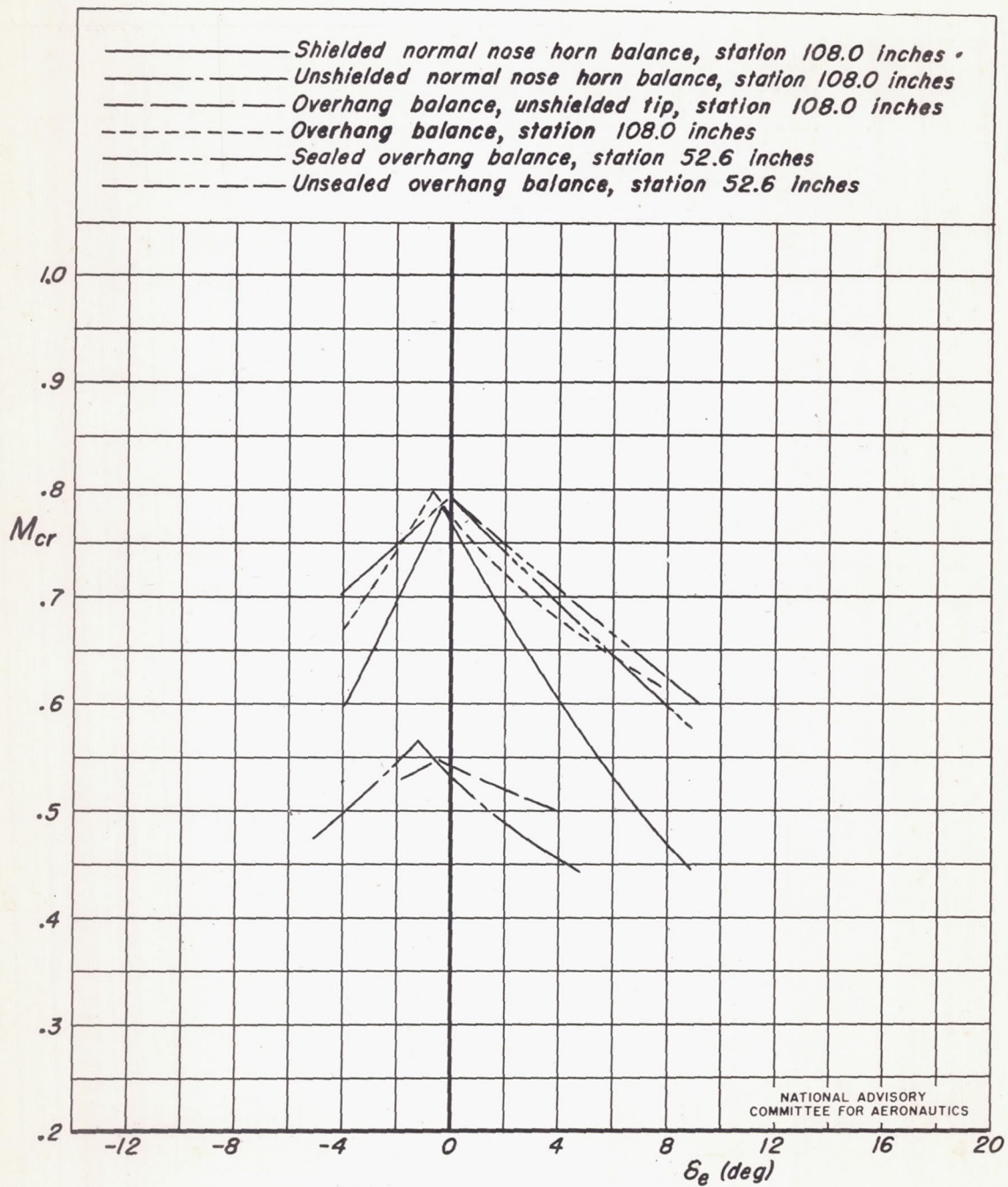


Figure 35.—Variation of critical Mach number with elevator angle for several elevator-balance configurations on the semispan horizontal tail.  $\alpha, 0^\circ$

